

CRANFIELD UNIVERSITY

GUILLAUME ROCOLLE

Simulation and Experimental Verification of the Flooding and
Draining Process of the Tidal Energy Converter “Deltastream” during
Deployment and Recovery

SCHOOL OF ENGINEERING

MSc BY RESEARCH THESIS
Academic Year: 2013 - 2014

Supervisor: Dr F. TRARIEUX
September 2014

CRANFIELD UNIVERSITY

SCHOOL OF ENGINEERING

MSc BY RESEARCH THESIS

Academic Year 2013 - 2014

GUILLAUME ROCOLLE

Simulation and Experimental Verification of the Flooding and
Draining Process of the Tidal Energy Converter “Deltastream” during
Deployment and Recovery

Supervisor: Dr F. TRARIEUX
September 2014

© Cranfield University 2014. All rights reserved. No part of this
publication may be reproduced without the written permission of the
copyright owner.

ABSTRACT

Deltastream is an on-going project carried by Tidal Energy Limited since almost twenty years. It is a tidal energy converter with a triangular shape and one turbine on each tower. It has gone through many evolutions of design but a first prototype will be installed in the end of 2014 at Ramsey Sound.

The deployment and recovery operations will be carried out with a single lift point through a heavy lift frame. Two issues have to be tackled during the operation: the rate of flooding of the ballasts and the tension on the lift crane cable. The most favourable sea state must be found in order to minimise the crane cable tension as well as the best inlets and outlets configuration for the ballasts system.

In order to tackle those issues, preliminary analytical work was conducted on the demonstrator to assess the stability during the flooding process. A scaled model was designed and built in order to be tested in a wave-towing tank.

The results from the tests highlight that the deployment and the recovery operations are safe for both the barge and Deltastream for the range of wave conditions tested in the tank. However, the sea state has an important impact on the proceeding of the operations, especially the period of the waves.

Keywords:

Tidal turbine, stability, flooding process, snatch load, wave-towing tank.

EXECUTIVE SUMMARY

The purpose of this project was to investigate experimentally the deployment and recovery scenarios of the tidal energy converter “Deltastream” in order to assess the behaviour during these two critical phases. For this purpose, a reduced scale model was designed and built based on a CAD design of the full scale demonstrator supplied by TEL.

The combined flooding and motion of the device at reduced scale requires particular attention as the physical phenomena involved must respect different scaling laws which can be difficult to re-create. The guide below presents the transformation of the relevant physical quantities from model scale to full scale. The similarity used is based on Froude due to the presence of inertial and gravitational forces acting on the device. The scaled values are multiplied by the formulas in the following table to obtain the full scale values:

Transformation from model to full scale		
Rig	1:20	Numerical value
Time	$x \sqrt{20}$	4.47
Length	$x 20$	20
Mass	$x 1.025 x 20^3$	8,200.00
Force	$x 1.025 x 20^3$	8,200.00

Table 1 Transformation from model to full scale

The model was fully built in the workshop of the Ocean laboratory as well as the test rig. The tests were carried out in the wave-towing tank at Cranfield. The first aim of those tests was to assess the impact of different sea states on the maximal tension experienced by the lift crane. The second aim was to assess the flooding process of the structure: duration of flooding and dynamic response of the structure during the process.

The first tests enabled to identify the different stages of the complete flooding (during deployment) and draining (during recovery) process which would then be the object of particular attention. The following graphs are detailing the different phases encountered during these two operations:

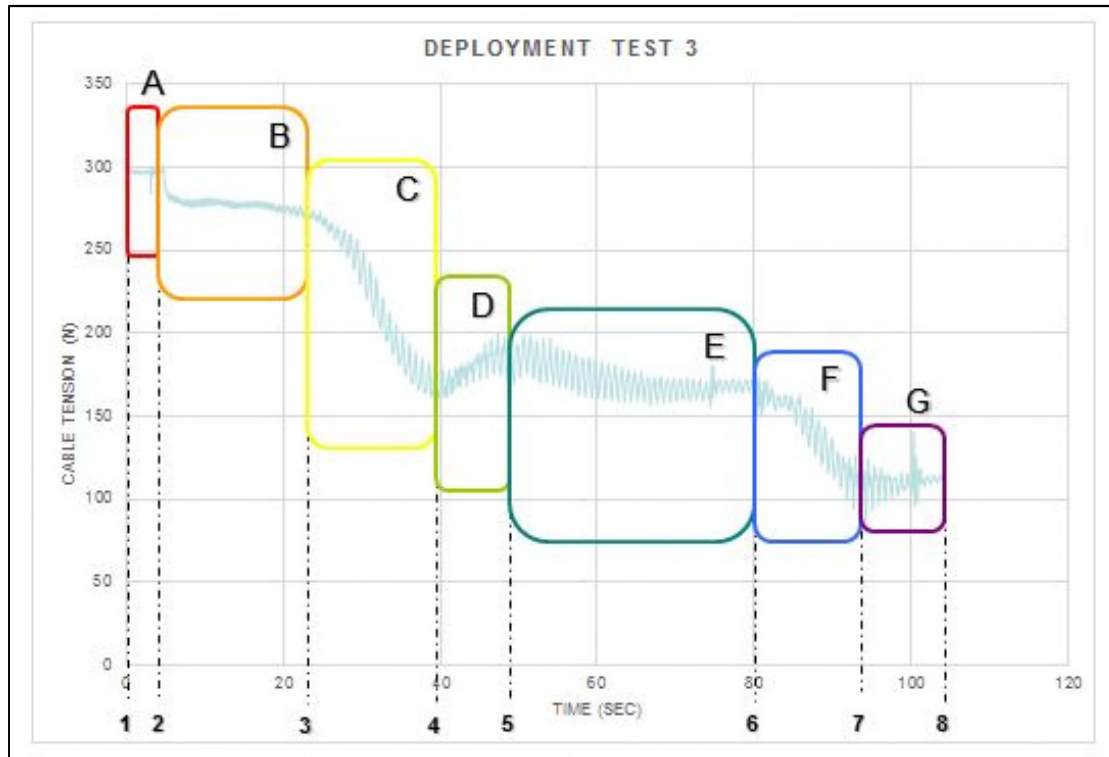


Figure 1 Time Slicing - Deployment operation

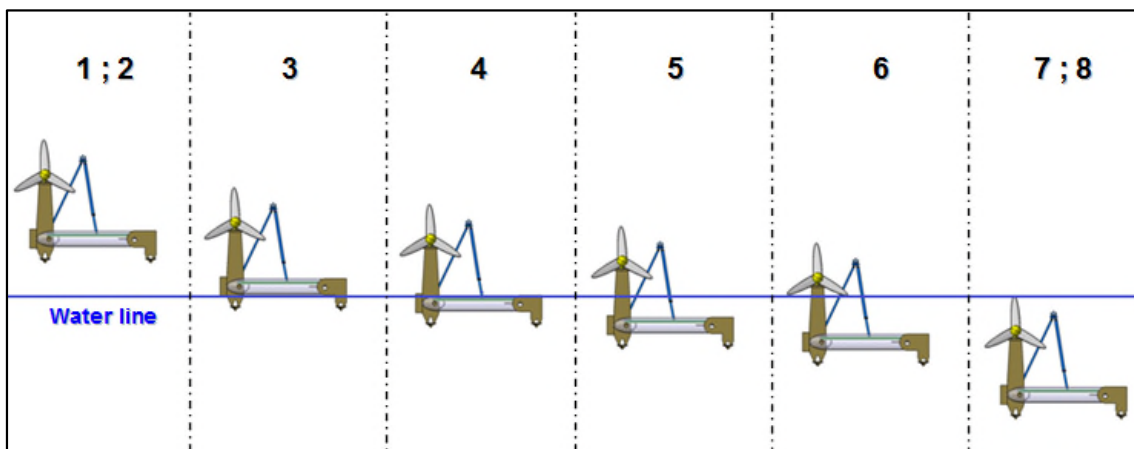


Figure 2 Position of the demonstrator given the time slicing

- Phase A (1:2): waiting phase between the beginning of the data acquisition and the launch of the actuators.
- Phase B (2:3): beginning of the descent of Deltastream towards the water surface.
- Phase C (3:4): first contact of the ballasts with the water line.
- Phase D (4:5): the ballasts are underwater but not completely filled.
- Phase E (5:6): the ballasts are flooded.
- Phase F (6:7): entrance of the turbine in the water.
- Phase G (7:8): DeltaStream is fully submerged.

The data acquisition was ended when the device was completely submerged and when no cable tension variation was no longer noticeable. This means the full descend until the tank bottom was not conducted.

During the deployment operation, the impact of the wave height, frequency and direction was assessed.

In total, twenty seven tests of deployment operation have been carried out. The same approach was adopted for the recovery operations with another thirty six tests.

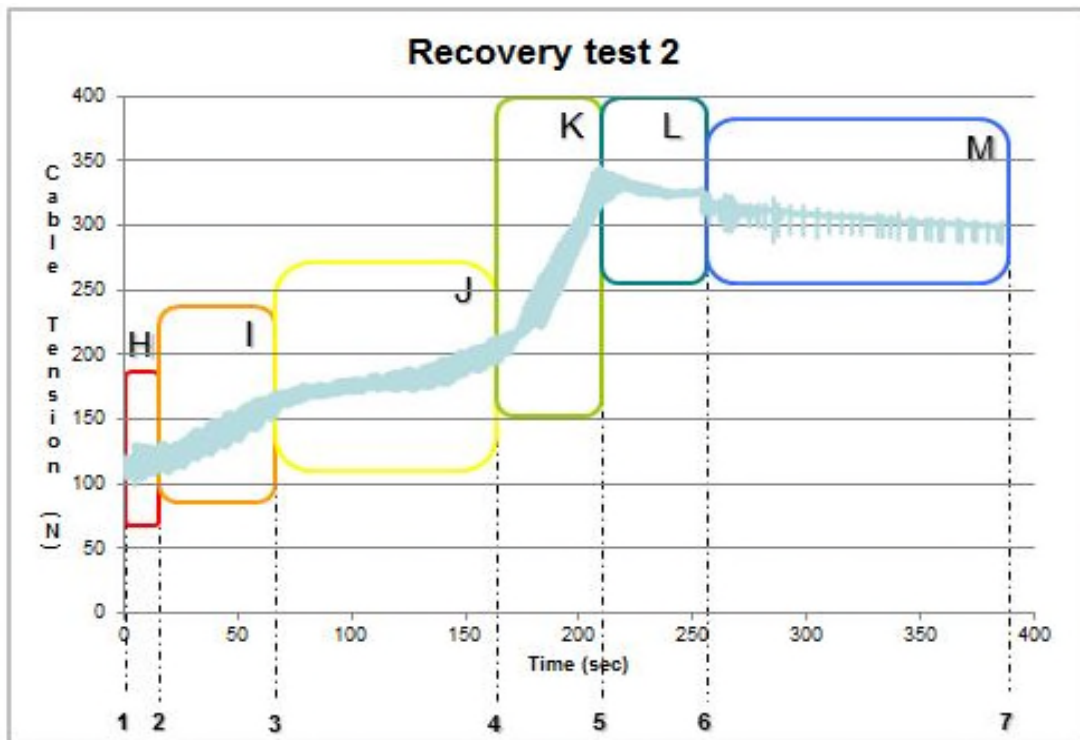


Figure 3 Time Slicing - Recovery operation

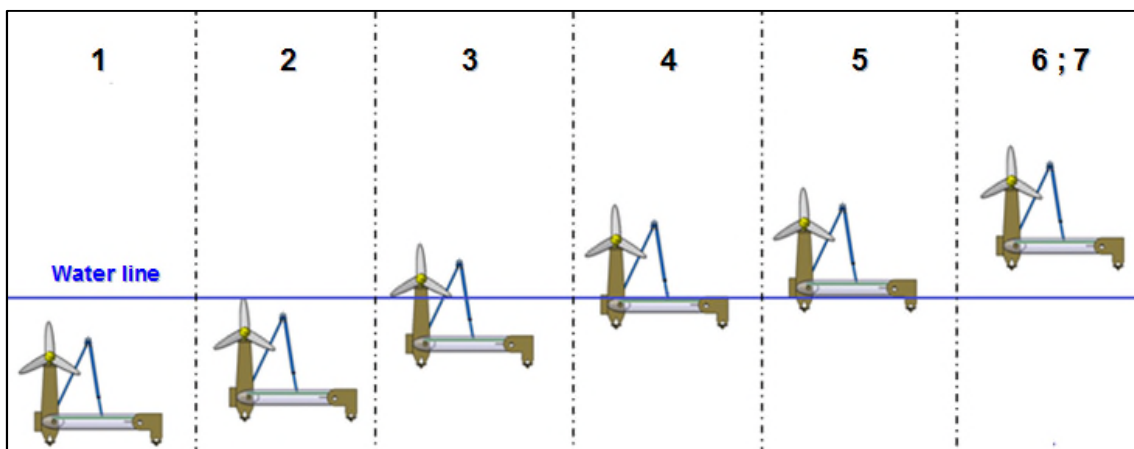


Figure 4 Position of the demonstrator given the time slicing

- Phase H: beginning of the ascending of Deltastream.
- Phase I: first part of the turbine off the water.
- Phase J: the turbine is completely out of the water.
- Phase K: the ballasts start to be drained.
- Phase L: 90% of the demonstrator is outside the water. Ballasts still drained.
- Phase M: the actuators are stopped in their initial position but the ballasts are not drain yet. The demonstrator is fully out of the water, the acquisition is stopped when the ballasts are drained.

The first series of test was carried out with an inlets and outlets configuration smaller than the one respecting the scale model. The following table is describing the two configurations tested:

Data	Configuration 1	Configuration 2
Number of inlet	6+4	6 + 4
Size of inlet	10 mm + 5mm Diameter	25 mm + 5 mm Diameter
Number of Vents	8	8
Size of Vents	5 mm Diameter	10 mm Diameter

Table 2 Test configuration data

The tables below are summarising all the sea state tested organised by configuration:

Configuration 1

Amplitude (m)	0	0.02	0.025	0.03	0.035
Frequency (Hz)					
0	Test 1				
0.5				Test 11	Test 12
1		Test 3	Test 4	Test 5	Test 6
1.2		Test 7	Test 8	Test 9	Test 10

Table 3 Test numeration and sea state - configuration 1

Configuration 2

Amplitude (m) \ Frequency (Hz)	Angle 0	Angle 45	Angle 90	Angle 135	Angle 180
	0.02	0.02	0.02	0.02	0.02
0.5	Test 13	Test 16	Test 19	Test 22	Test 25
1	Test 14	Test 17	Test 20	Test 23	Test 26
1.2	Test 15	Test 18	Test 21	Test 24	Test 27

Table 4 Test numeration and sea state - configuration 2

During the tests, multiple sea states have been tested. For convenience, the table below is summarising the inputs given to the wave maker and the corresponding full scale value:

Wave amplitude (m)		Wave frequency (Hz) and period (sec)		
Reduced scale	Full scale	Reduced scale frequency	Reduced scale period	Full scale period
0.02	0.4	0.5	2	8.94
0.025	0.5	1	1	4.47
0.03	0.6	1.2	0.83	3.73
0.035	0.7			

Table 5 Reduced Scale/Full scale values for the sea states

Two phenomena were assessed during the data processing: the maximum cable tension variation and the maximal cable tension. The first corresponds to the variation of tension around a mean value due to the wave impact on the device. The second corresponds to the maximal cable tension detected during the operations. The results collected during those multiple tests are displayed in the following table:

		MAXIMUM CABLE TENSION VARIATION		MAXIMUM CABLE TENSION	
		Worst Case	Best Case	Worst Case	Best Case
INPUTS	Wave Amplitude	0.7m	0.4m	0.7m	0.4m
	Wave Period	8.94 sec	4.47 sec	8.94 sec	4.47 sec
	Angle	180 degrees	45/90 degrees	0 degrees	135 degrees

Table 6 Summarised Results

Moreover, the results showed that the largest tension was during the recovery operation when Deltastream is piercing the water surface and the ballasts start to drain. It has to be pointed out that the limit mass of the lift crane (151 tonnes) is not reached within the range of sea states tested in the tank. It emerged that the period of the waves is the aspect which has the most impact on the demonstrator and especially on the snatch load experienced by the lift crane: a long period is the worst case scenario for the deployment and the recovery. Concerning the orientation angle of the device through the waves, a best position cannot be truly chosen. Even if the tendency indicates that the worst cases are either when the Turbine (in parked position) is facing the waves or when the waves are reaching first the back base of the device.

ACKNOWLEDGEMENTS

First, I would like to express my profound gratitude and my deep regards to my supervisor Dr Florent Trarieux who give me the opportunity to come to England to do my MSc by Research and guide me during the whole year.

My completion of this project could not have been accomplished without the help and the support of my colleague during those twelve months. I gratefully thank them for their support, ideas and help.

I would like to thank the Cranfield Handball Club, who allowed me to meet many great people from different countries and give me positive multicultural breaks during my research.

Finally, I would like to thank every person who participates to the accomplishment of this thesis by their presence, support and friendship.

TABLE OF CONTENTS

ABSTRACT	i
EXECUTIVE SUMMARY	iii
ACKNOWLEDGEMENTS.....	ix
LIST OF FIGURES.....	xiii
LIST OF TABLES.....	xviii
LIST OF EQUATIONS.....	xx
LIST OF ABBREVIATIONS.....	xxii
1 Introduction.....	24
1.1 Context	24
1.1.1 International Context	24
1.1.2 Deltastream Project.....	24
1.1.3 Cranfield University and TEL.....	27
1.1.4 Deployment Process	27
1.2 Objectives	30
1.3 Experimental Solutions	30
1.4 General methodology and thesis structure	34
2 Literature Review	35
2.1 Introduction	35
2.2 Analytical Stability Assessment	35
2.2.1 Stability of an offshore structure.....	35
2.2.2 Static floating stability.....	37
2.2.3 Static submerged stability	40
2.3 Flow inside a forced conduit – Analytical Study	41
2.3.1 Elementary Fluid Dynamics – The Bernoulli Equation.....	41
2.4 Scaling model and tests procedure.....	42
2.4.1 Ballast Filling Tests	42
2.4.2 Splash zone tests.....	45
2.5 Conclusion.....	46
3 Stability assessment on Deltastream 1	47
3.1 Floating Stability	47
3.1.1 Hypotheses	48
3.1.2 Problem-Solving Approach.....	49
3.2 Submerged Stability.....	64
3.2.1 Determination of the new Centre of Gravity	64
3.2.2 Determination of the Centre of Buoyancy.....	65
3.2.3 Lifting Point Position.....	65
3.3 Application to the demonstrator	68
4 Ballast Flooding Assessment on the Demonstrator.....	70
4.1 Principle of the Ballast	70
4.2 Simulation of the time of descent.....	71

4.2.1 Code Architecture	71
4.2.2 Deltastream 1 Calculation	73
5 Design of the Model and Test Preparation	77
5.1 CAD Model	77
5.1.1 Full Scaled Design	77
5.1.2 Scaled Model Design	85
5.2 Model Manufacturing	92
5.2.1 Manufacturing	92
5.2.2 Physical Data	96
5.3 Test Rig Design	99
5.3.1 Functional Analysis	99
5.3.2 Design	100
6 Test Program.....	105
6.1 Set-up in the Cranfield wave-towing tank.....	105
6.2 Instrumentation and data acquisition	106
6.3 Test runs.....	108
6.4 Data processing.....	110
6.4.1 Tests with the first configuration.....	110
6.4.2 Tests with the second configuration	125
6.5 Analysis and comparison with numerical predictions.....	136
6.5.1 Analysis and best scenarios.....	136
6.5.2 Comparison with numerical predictions.....	137
7 Conclusions.....	139
REFERENCES.....	141
APPENDICES	143
Appendix A Cranfield Wave-Towing tank.....	143
Appendix B Actuator Technical Data	144
Appendix C Tests Pictures.....	146

LIST OF FIGURES

Figure 1 Time Slicing - Deployment operation.....	iv
Figure 2 Position of the demonstrator given the time slicing	iv
Figure 3 Time Slicing - Recovery operation.....	v
Figure 4 Position of the demonstrator given the time slicing	v
Figure 1-1 Deltastream First Design.....	25
Figure 1-2 Deltastream Second Design	25
Figure 1-3 Deltastream Demonstrator Design	26
Figure 1-4 Deltastream unveiling.....	27
Figure 1-5 Deltastream under the barge - Test IFREMER March 2012	28
Figure 1-6 Mooring footprint in Ramsay Sound.....	29
Figure 1-7 Mooring Arrangement of the Deployment Barge.....	29
Figure 1-8 Deployment layout	32
Figure 2-1 Ship Motions in Six Degrees of Freedom.....	36
Figure 2-2 Heel and Trim rotations.....	37
Figure 2-3 Example of a GZ-curve	38
Figure 2-4 Submarine Stability - Stable State.....	40
Figure 2-5 Submarine Stability - Unstable State.....	40
Figure 2-6 Example of an OWC	43
Figure 2-7 Scale Model OWC -- Cranfield Test 2008.....	44
Figure 2-8 Examples of Subsea structure in the splash zone	45
Figure 2-9 Model of a subsea structure in the phase 1 of the test.....	46
Figure 3-1 Display of the Righting Arm.....	47
Figure 3-2 Origin and axes	48
Figure 3-3 Simplified Structure	49
Figure 3-4 Volume of a partially filled horizontal cylinder	51
Figure 3-5 Draft in unballasted condition.....	53
Figure 3-6 Volume Division	54
Figure 3-7 Z Coordinate for the side tubes.....	55

Figure 3-8 Determination of the Centre of Buoyancy	57
Figure 3-9 Determination of the Centre of Flotation	58
Figure 3-10 Floating Structure.....	58
Figure 3-11 Origin for the GZy Calculation.....	59
Figure 3-12 Transversal Stability Curve – GZy.....	60
Figure 3-13 Floating Structure - Inclination 130°	61
Figure 3-14 Transversal Stability Curves – Righting Stability Moment.....	62
Figure 3-15 Righting Stability Moment curve and its Trend Line	63
Figure 3-16 Points of Application of the different forces	67
Figure 3-17 Principal Dimensions of the demonstrator.....	68
Figure 3-18 Origin of the demonstrator	69
Figure 4-1 Streamline.....	70
Figure 4-2 Numerical Predictions	72
Figure 4-3 Loop For – Cube calculation	72
Figure 4-4 Matrix Result.....	72
Figure 4-5 Deltastream landed on the Seabed.....	74
Figure 4-6 CoG.Z over time.....	74
Figure 5-1 Turbine Tower of Deltastream 2.....	77
Figure 5-2 KML Document Picture Deployment 1	78
Figure 5-3 KML Document Picture Deployment 2	78
Figure 5-4 CAD of the Nacelle.....	79
Figure 5-5 Turbine Diameter	80
Figure 5-6 Triangular Shaped Frame - Ballast Location.....	80
Figure 5-7 Vents Localisation	81
Figure 5-8 Isometric view of the Lift Frame – Full scale	82
Figure 5-9 Origin and axes for the Inertia Tensor.....	82
Figure 5-10 Front (a) and rear (b) view	83
Figure 5-11 Side View	84
Figure 5-12 Demonstrator with Lift Frame.....	84

Figure 5-13 Scaled Model Drawing	86
Figure 5-14 Side view - Openings Location.....	87
Figure 5-15 Bottom View - Openings location	87
Figure 5-16 Isometric view of the Lift Head - Model Size	89
Figure 5-17 Isometric view of the Lift Frame – Model size	89
Figure 5-18 Isometric view of the scaled model	91
Figure 5-19 Deltastream Model before assembly and painting	92
Figure 5-20 Rear of the demonstrator assembly	93
Figure 5-21 Tower Turbine & Tubes.....	93
Figure 5-22 Assembly of the principal tower.....	94
Figure 5-23 Lift Frame linked to the demonstrator.....	95
Figure 5-24 Final Assembled Model.....	95
Figure 5-25 Added Masses location	96
Figure 5-26 Functional diagram interaction test rig	99
Figure 5-27 Actuator ROBO Cylinder RCP2-SA7C	100
Figure 5-28 Configuration of the movement transmission system.....	101
Figure 5-29 Final Test Rig.....	103
Figure 6-1 Drawing of the complete set-up	105
Figure 6-2 Set-up on the carriage.....	105
Figure 6-3 Set up on the desk.....	106
Figure 6-4 Labview Interface of the data acquisition	107
Figure 6-5 Deltastream orientations	108
Figure 6-6 Inlets/Outlets Position	109
Figure 6-7 Deployment curve with time-slicing.....	110
Figure 6-8 Recovery curve with time-slicing.....	111
Figure 6-9 Deployment Test 2 - Graph Shape.....	113
Figure 6-10 Recovery Test 2 - Graph Shape.....	113
Figure 6-11 Deployment Test 3 - Configuration 1.....	114
Figure 6-12 Deployment Test 6 with zoom-in– Configuration 1.....	115

Figure 6-13 Influence of the wave amplitude on the amplitude of the oscillations of tension – deployment tests 3/4/5/6	115
Figure 6-14 Influence of the wave amplitude on the maximal tension – Recovery test 7/8/9/10.....	117
Figure 6-15 Deployment test 10 - Configuration 1.....	118
Figure 6-16 Deployment test 12 with zoom-in - Configuration 1.....	118
Figure 6-17 Influence of the frequency on the amplitude of the oscillations of tension – deployment test 12/6/10.....	119
Figure 6-18 Influence of the frequency on the amplitude of the oscillations of tension – deployment test 11/5/9.....	120
Figure 6-19 Influence of frequency on the maximal tension – recovery test 11/5/9.....	121
Figure 6-20 Influence of frequency on the maximal tension – recovery tests 12/6/10.....	122
Figure 6-21 Deployment Test 12 – Configuration 1	123
Figure 6-22 Zoom-in from 15 to 47 seconds.....	124
Figure 6-23 Zoom-in from 100 to 128 seconds.....	124
Figure 6-24 Deployment curve with time-slicing	125
Figure 6-25 Deltastream position during deployment operation	126
Figure 6-26 Recovery curve with time-slicing.....	127
Figure 6-27 Deltastream position during recovery operations	128
Figure 6-28 Influence of the angle of the demonstrator on the maximal tension – recovery tests 1/4/7/10/13	129
Figure 6-29 Influence of the angle of the demonstrator on the maximal tension – recovery tests 2/5/8/11/14	130
Figure 6-30 Influence of the frequency on the angle of the oscillations of tension – deployment test 1/4/7/10/13	131
Figure 6-31 Influence of the angle on the amplitude of the oscillations of tension – deployment test 2/5/8/11/14	131
Figure 6-32 Time of Deployment - Configuration one and two	132
Figure 6-33 Time of Recovery - Configuration one and two	133
Figure 6-34 Comparison Graph – Deployment tests	134
Figure 6-35 Comparison Graph - Recovery	135

Figure 6-36 Floating Deltastream with a trim angle	138
Figure_Apx A-1 Wave maker	143
Figure_Apx A-2 Towing carriage	143
Figure_Apx C-1 Underwater Picture – On-going operation	146
Figure_Apx C-2 Underwater Picture – Landed.....	146
Figure_Apx C-3 Test operation - Deltastream lifted above the water	147
Figure_Apx C-4 Test operation - Deltastream entering into the water.....	147

LIST OF TABLES

Table 1 Transformation from model to full scale.....	iii
Table 2 Test configuration data.....	vi
Table 3 Test numeration and sea state - configuration 1	vi
Table 4 Test numeration and sea state - configuration 2	vii
Table 5 Reduced Scale/Full scale values for the sea states	vii
Table 6 Summarised Results	viii
Table 1-1 Functional specification of the test model.....	31
Table 1-2 Tests procedure summary.....	33
Table 3-1 Centre of Gravity Coordinates.....	48
Table 3-2 Structure Data	49
Table 3-3 Submerged Volume between 3.4 and 3.415m	53
Table 3-4 Partial Volumes and Weighting	54
Table 3-5 Coordinates of the Centre of Gravity for the Stand Cylinder	55
Table 3-6 Coordinates of the CoG of the Transversal Tube.....	55
Table 3-7 Coordinates of the CoB.....	56
Table 3-8 Centre of Buoyancy Coordinates	57
Table 3-9 Final coordinates of the Centre of Buoyancy.....	57
Table 3-10 Coordinates of the Centre of Flotation.....	58
Table 3-11 Coordinates of the initial Centre of Gravity.....	59
Table 3-12 GZ_y according to the angle of inclination	60
Table 3-13 Value of the particular angles of the stability	61
Table 3-14 Energy absorbed by Deltastream.....	63
Table 3-15 CoG of the ballasts system	64
Table 3-16 System Information	64
Table 3-17 Final CoG Coordinates – Ballasted Deltastream.....	65
Table 3-18 CoB coordinates – Fully Submerged Structure	65
Table 3-19 Application points of the forces	66
Table 5-1 Prototype Data	78

Table 5-2 Nacelle Data.....	79
Table 5-3 Ballast information.....	81
Table 5-4 CoG Coordinates.....	83
Table 5-5 Scale Factor with the Froude's Similarity.....	85
Table 5-6 Scaled Model Geometrical Data.....	85
Table 5-7 Colour Legend of the Scaled Model	86
Table 5-8 Ballasts volume of the scale model	88
Table 5-9 Desired and CAD coordinates of the CoG for the scaled model	90
Table 5-10 General Dimensions of the manufactured model	96
Table 5-11 CoG coordinates of the manufactured model with relative error	97
Table 5-12 Functional Specifications of the test rig	100
Table 6-1 Two configurations data	109
Table 6-2 Actuator phases and Deltastream estate during tests.....	112
Table 6-3 Wave Data for the first configuration	114
Table 6-4 Summarised Results and percentage – deployment test 3/4/5/6 ...	116
Table 6-5 Summarised Results and percentage – deployment test 7/8/9/10 .	116
Table 6-6 Summarised Results and percentage – deployment test 12/6/10 ..	119
Table 6-7 Sea state of the test 12	122
Table 6-8 Wave Data and angle for the second configuration.....	128
Table 6-9 Comparative results of volume flow rate	138

LIST OF EQUATIONS

(2-1).....	36
(2-2).....	36
(2-3).....	38
(2-4).....	38
(2-5).....	39
(2-6).....	39
(2-7).....	39
(2-8).....	41
(2-9).....	41
(2-10).....	42
(2-11).....	42
(2-12).....	42
(2-13).....	42
(2-14).....	43
(2-14).....	45
(3-1).....	50
(3-2).....	50
(3-3).....	50
(3-4).....	51
(3-5).....	51
(3-6).....	51
(3-7).....	51
(3-8).....	52
(3-9).....	52
(3-10).....	52
(3-11).....	52
(3-12).....	56
(3-13).....	56

(3-14).....	56
(3-15).....	59
(3-16).....	66
(4-1).....	70
(4-2).....	71
(4-3).....	73
(5-1).....	83
(5-2).....	90
(5-3).....	90
(5-4).....	97
(5-5).....	98
(5-6).....	98
(5-7).....	98
(5-8).....	98

LIST OF ABBREVIATIONS

Acronym

AUV	Autonomous Underwater Vehicle
CAD	Computer-Aided Design
CoB	Centre of Buoyancy
CoB.x	x coordinate of the Centre of Buoyancy
CoB.y	y coordinate of the Centre of Buoyancy
CoB.z	z coordinate of the Centre of Buoyancy
CoF	Centre of Flotation
CoF.x	x coordinate of the Centre of Flotation
CoF.y	y coordinate of the Centre of Flotation
CoF.z	z coordinate of the Centre of Flotation
CoG	Centre of Gravity
CoG.x	x coordinate of the Centre of Gravity
CoG.y	y coordinate of the Centre of Gravity
CoG.z	z coordinate of the Centre of Gravity
F.x	x coordinate of the Lifting force application point
F.y	y coordinate of the Lifting force application point
F.z	z coordinate of the Lifting force application point
KML	Keynvor Morlift Limited
M_{ϕ}	Metacentre for an heel rotation
M_{θ}	Metacentre for an trim rotation
OWC	Oscillating Water Column
PF	Principal Function
RF	Requirement Function
TEL	Tidal Energy Limited
Tta	Transversal Tube Area
Vta	Vertical Tube Area

Physical Constants

g The Gravitational Acceleration

Physical Quantities

D Draft

F Lifting Force

F_{∇} Buoyancy Force/Displacement

GZ Righting Stability Lever Arm

\dot{m} Mass Flow rate

M_H Heeling Moment

M_S Righting Stability Moment

M_T Trimming Moment

W_a Weight

Q Volume Flow rate

W_w Weight in Water

Physical Quantities – Greek Letter

Θ_0 Limited Angle of Static Stability

Θ_s Angle of Vanishing Stability

ρ_{water} Sea Water Density

∇ Submerged Volume

Units

deg Degree

g gram

Hz Hertz

m Meter

N Newton

Pa Pascal

s Second

W Watt

1 Introduction

1.1 Context

1.1.1 International Context

In 2012, the first commitment of the Kyoto Protocol ended with a decrease of 4.2% of the collective greenhouse gas emissions between 2008 and 2012. The aim of the Protocol, which was signed and ratified by 191 states, was to reduce the gas emissions by 5.2% in comparison with the 1990 level. During this four-year period, the United Kingdom managed to reduce their emissions by 12.5%.

On the 8th of December, 2012 in Doha, Qatar, the “*Doha Amendment to the Kyoto Protocol*” was adopted. The objective of this amendment is to undertake a second commitment of the Kyoto Protocol by reducing the greenhouse gas emissions by 18% below the 1990 level between 2013 and 2020.

In this context, the European Union decided to adopt a new contract in 2009. This contract has multiple objectives to achieve before 2020. Those objectives are focused on emissions cuts, energy efficiency and increase of the renewable resources. More precisely, the targets are to reduce the greenhouse gas emissions by 20% compared to the 1990 level, increase the energy efficiency by 20% and raise the weight of the renewable energies in the energy production by 20%.

1.1.2 Deltastream Project

Tidal Energy Limited is the company behind the development of the Tidal Energy Converter called Deltastream. The purpose of this device is to convert tidal currents into electricity with horizontal axis turbines. The first prototype of the Deltastream will be installed between the Welsh coast and Ramsey Island before the end of this year. The further objective of the company is to develop farms in a short time.

The original idea of Deltastream was born in 1997. At that stage, the structure was composed of three horizontal marine current turbines installed on a triangular frame; the diameter of the turbines was going to be 15m. The device would be lying on the seabed without any concrete foundations linking it to the seabed, as seen in Figure 1-1. The generation capacity of the device was planned to be up to 1.2 MW. This first geometry will be called Deltastream 1 in the thesis.

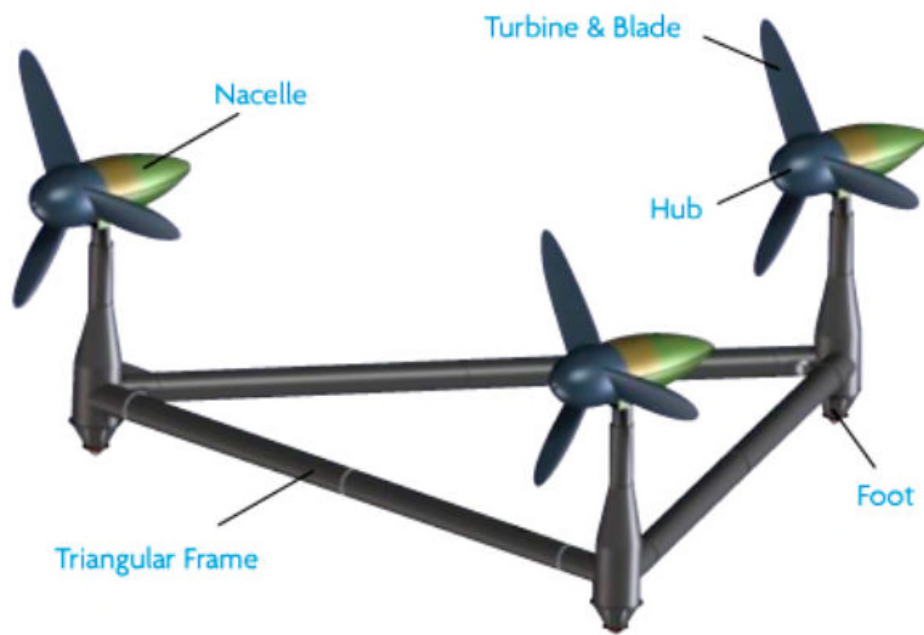


Figure 1-1 Deltastream First Design

As seen in Figure 1-2, the first concept was improved to a second slightly different structure. The geometry is basically the same with a small change for the towers and the nacelles. The diameter of the turbines was still 15 m with the same output power of 1.2 MW (3 x 400 kW). This second geometry will be called Deltastream 2 in the thesis.

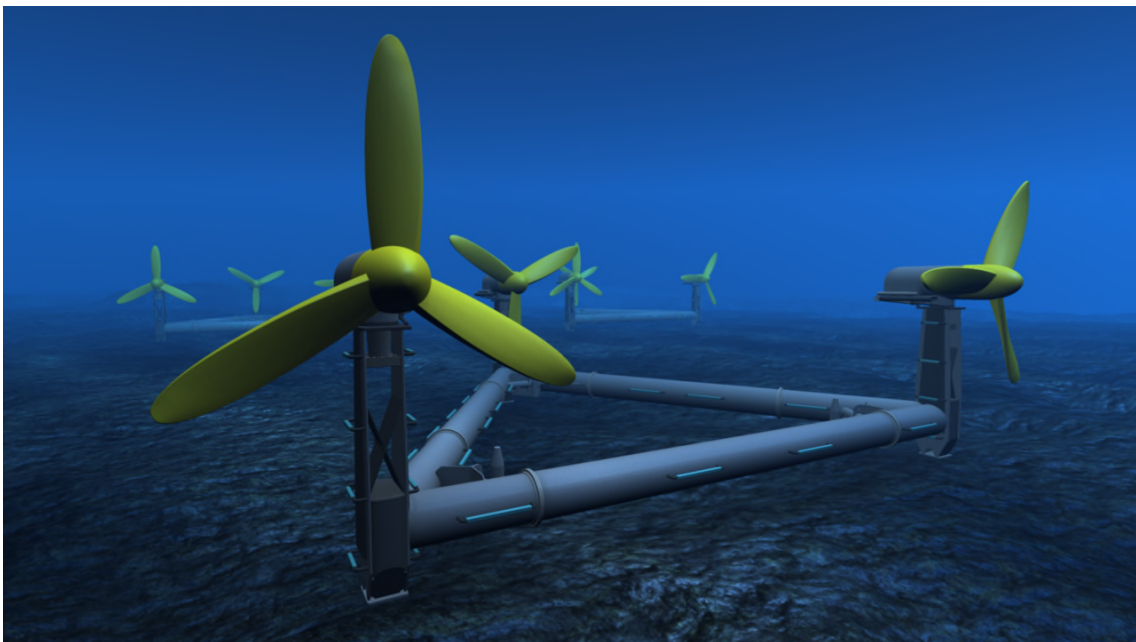


Figure 1-2 Deltastream Second Design

As seen in Figure 1-3 **Error! Reference source not found.**, a third structure has been designed in 2013 for the manufacturing of a prototype in order to be tested for 12 months. This structure keeps a triangular shape but it is smaller and with only one turbine installed. Moreover, the turbine is a 12 m diameter turbine, smaller compared to the 15 m diameter used in the previous versions of the structure. For Deltastream 1, three turbines are installed on the three towers of the triangle, creating equilibrium for the structure. In the case of Deltastream, installing only one turbine on one summit creates a loss of the equilibrium. The triangle is also much smaller in the third structure. This third geometry will be called Demonstrator in the thesis.

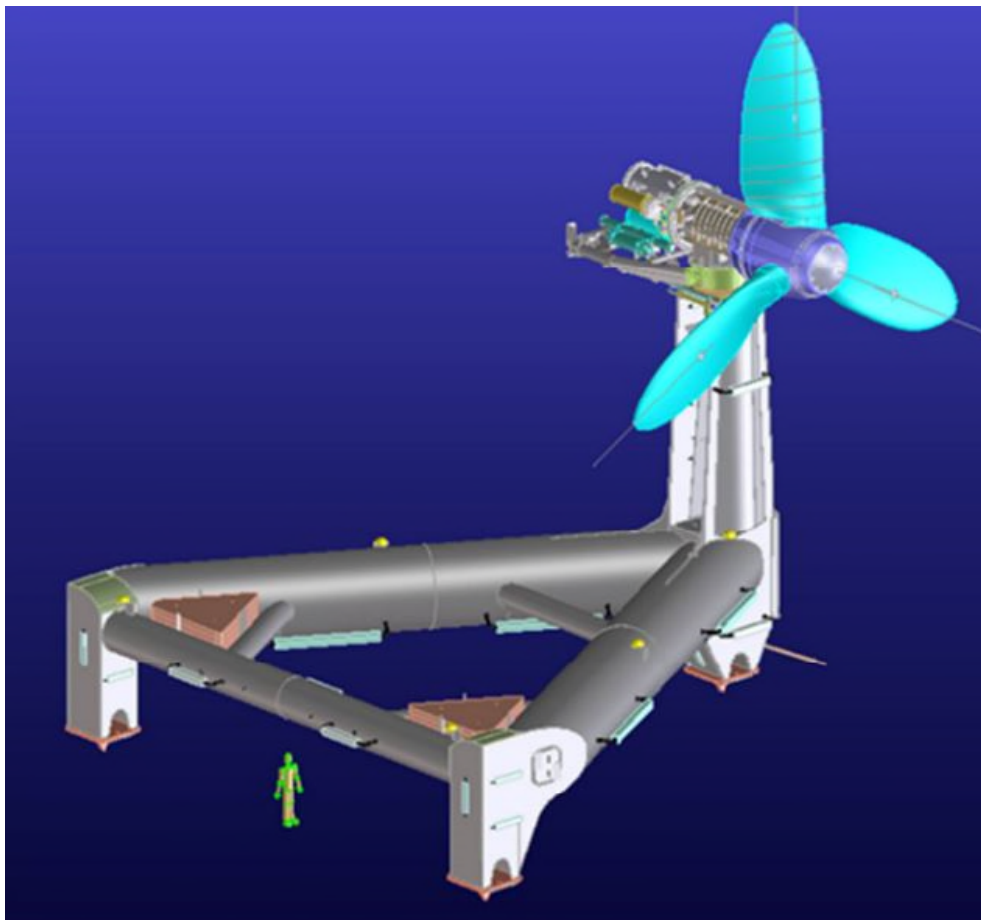


Figure 1-3 Deltastream Demonstrator Design

The official unveiling of the demonstrator was on Thursday 7th of August and took place in Pembrokeshire.



Figure 1-4 Deltastream unveiling on 07-Aug-2014

1.1.3 Cranfield University and TEL

Since 2007, Cranfield University has been involved in the Deltastream project working through structural and experimental work phases in turbine performance and turbine-structure interaction, structural design and deployment process. The experimental work has been undertaken in the Towing Tank of the Ocean Systems Laboratory at Cranfield and in the water circulation channel facility at IFREMER-Boulogne. During those seven years of collaboration, experimental tests have been conducted on the three different designs through multiple reduced scale models.

1.1.4 Deployment Process

As the design evolved, the deployment process evolved too. The first idea was a deployment under a barge to transport the structure to the area of installation. As shown on Figure 1-5, Deltastream is installed under the barge Wilcarry 1750 before the deployment. In the case of this deployment method, a crane is not needed to lift the structure. This one is attached under the barge by three different points and is going to the seabed due to its own weight. In this case, Deltastream is already flooded.

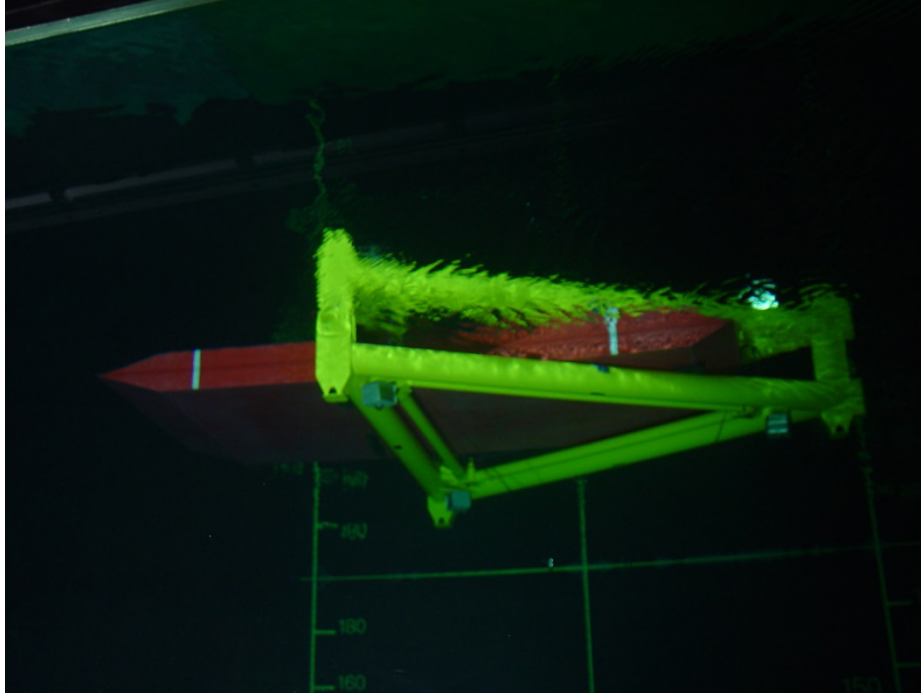


Figure 1-5 Deltastream under the barge - Test IFREMER March 2012

Considering the change in the Deltastream design, the process of the deployment has been modified. With the one-turbine structure, the deployment is a more classic one. Deltastream is transported to the location of the deployment using a barge but this time, the prototype is on the barge deck and not under the hull. The barge is equipped with a heavy lift crane which will handle Deltastream in/out of the water. Before the deployment, the barge must be moored to the seabed.

This process will be used for the prototype which has been built this year and will be installed during the autumn 2014. TEL has engaged an external company: Keynvor Morlift Limited (KML) which is specialised in heavy offshore structure deployment. As indicated in Figure 1-6, Deltastream will be installed in Ramsay Sound, an area between Wales and Ramsey Island. KML has surveyed the wave, wind and current conditions of Ramsey Sound and has provided TEL with a procedure for the Deployment and Recovery operations, as detailed in the document [5]. The mooring footprint is detailed in Figure 1-6 and in Figure 1-7.



Figure 1-6 Mooring footprint in Ramsay Sound

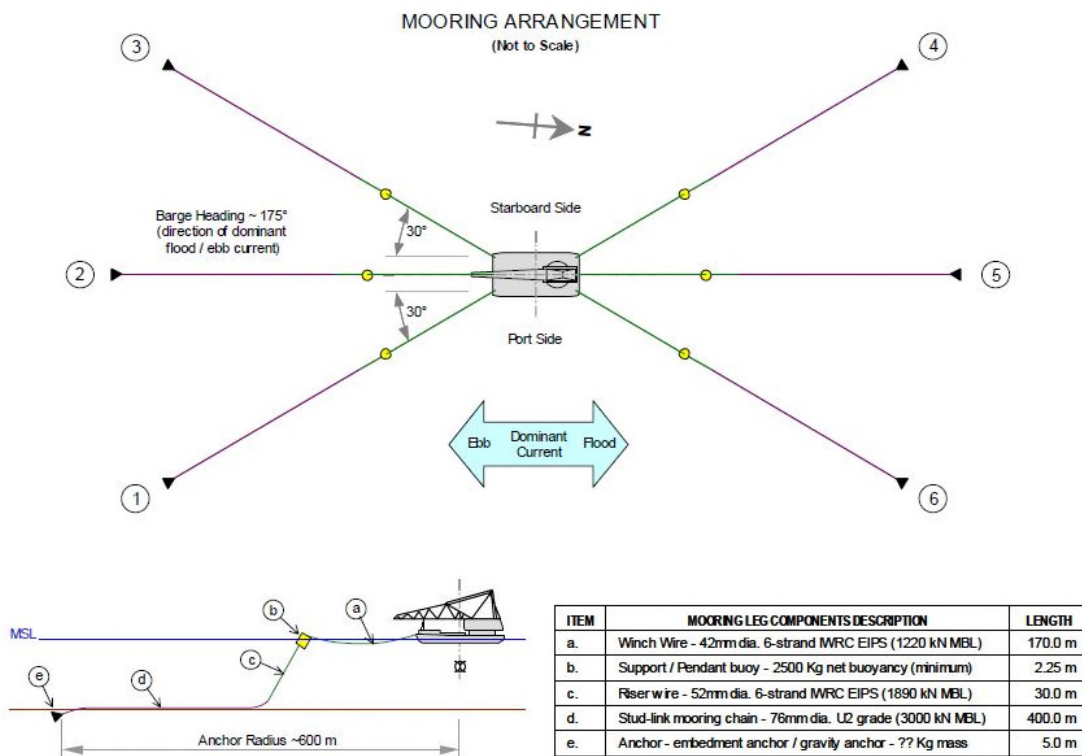


Figure 1-7 Mooring Arrangement of the Deployment Barge

Once the structure is lifted to the waterline, the ballasts are filled by seawater and are adding weight to the structure. This weight will allow the structure to be submerged and to start the descent toward the seabed. In order to counterbalance the lack of weight at the rear of this asymmetrical structure, two 40 tonnes weight ballasts are placed at the rear corners of the structure once this one is resting on the seabed.

1.2 Objectives

The objectives of this work were to model some relevant deployment and recovery scenarios of Deltastream. The main part of the work was focused on the flooding process via the ballast system. During the deployment, the structure was going through a phase called the splash zone which refers to the phase in-between full flotation and complete submergence.

The rate of submergence of the structure is important and it is directly linked to the rate of flooding of the ballast. Therefore, it was one of the most important parameters which needed to be scaled accurately. This parameter is related to the atmospheric pressure. The higher the atmospheric pressure is; the more difficult it is to fill the ballast. Thus, it takes more time. To conclude, one way to scale the rate of flooding was to scale the atmospheric pressure. However, this parameter cannot be scaled in the Cranfield wave and towing tank. Therefore, an analytical model was established for the flooding process.

1.3 Experimental Solutions

The aim of the tests consists in approaching as much as possible the reality of the deployment within known limitations. Multiple criteria are needed in order to fulfil the aim as best as possible:

- The first one is the model itself. In other words, the scale factor which defines the geometry of the model.
- The second one is the tank size and operations (wave, current, depressurised atmosphere).
- The last one is the price of the whole operation (design, manufacturing, tests, post-processing)

Those criteria are resumed in the following table with a flexibility given for the three of them. F0 means no flexibility and F1, F2 or F3 mean a variable flexibility.

Criteria	Criteria Features	
	Definition	Flexibility
Model design and layout	Scale factor ($\geq 1:40$)	F2
Tank facilities	Cranfield or IFREMER Boulogne	F1
Price	$\leq \text{£}1,000$	F0

Table 1-1 Functional specification of the test model

Concerning the test facilities, the Ocean System Laboratory is a wave and towing tank of 30 m long, 1.5 m wide and 1.5 m deep. The one in IFREMER Boulogne is a water circulation channel of 18 m long, 4 m wide and 2 m deep. The maximum scale factor is fixed at 1:40 as the model becomes very small.

The maximum price for parts and consumables was set at £1,000.

Using Table 1-1, it is clear that the parameter which can be modified easily is the model design and layout. Thus, three different operations can be arranged for the tests:

- Complete system with barge, mooring line and demonstrator.
- Partial system with barge and demonstrator.
- Demonstrator only under a fixed crane

For the complete system, the mooring system displayed in Figure 1-7 must be scaled. The footprint is a rectangle approximately 1,200 m long and 600 m wide. Scaled with the smallest scale factor (here 1:40), the footprint becomes a rectangle 30 m long and 15 m wide. It is larger with a larger scale factor (1:20 or 1:30). To accommodate this footprint, a large tank is necessary. Both Cranfield and Boulogne-sur-mer are not large enough to set up the complete footprint. Note the depth of the mooring system is not taken into account here. Furthermore, the smaller the scale factor is, the lesser the accuracy of the model is; and given the size of the demonstrator, a scale factor of 1:20 or 1:30 is advised. However, it is possible to reduce the size of the footprint by taking into account only part a and b of the mooring line (Figure 1-7). In that case, the rectangle is 9.5 m long and 4.25 m wide in the worst case (scale 1:40). With this simplification, the test can be carried out in IFREMER Boulogne. The only availability at IFREMER is in November-December 2014, so a deployment test there is not possible. Therefore, the complete system is not possible to achieve.

The partial system consists in scaling the barge along with the demonstrator. The mooring system is not taken into account here. These tests are practical to see the response of the demonstrator coupled with the response of the barge. The key parameter here is to have a non-fixed crane during the operation. Considering the size of the barge and the fact that the demonstrator will be deployed next to it (Figure 1-8), a scaled width of approximately 1 m is needed

for a scale of 1:40. The length needed is the length of the barge, 1 m as well. This footprint for the operation can be installed in the Ocean System Laboratory but with a risk of contact with the frame with the motion of the model in waves. Furthermore, the scale is small which means the tests will not be as accurate as possible. Moreover, the price to build a barge with an operating crane is too high for the budget allowed for those tests. The way it is, this system cannot be achieved this year.

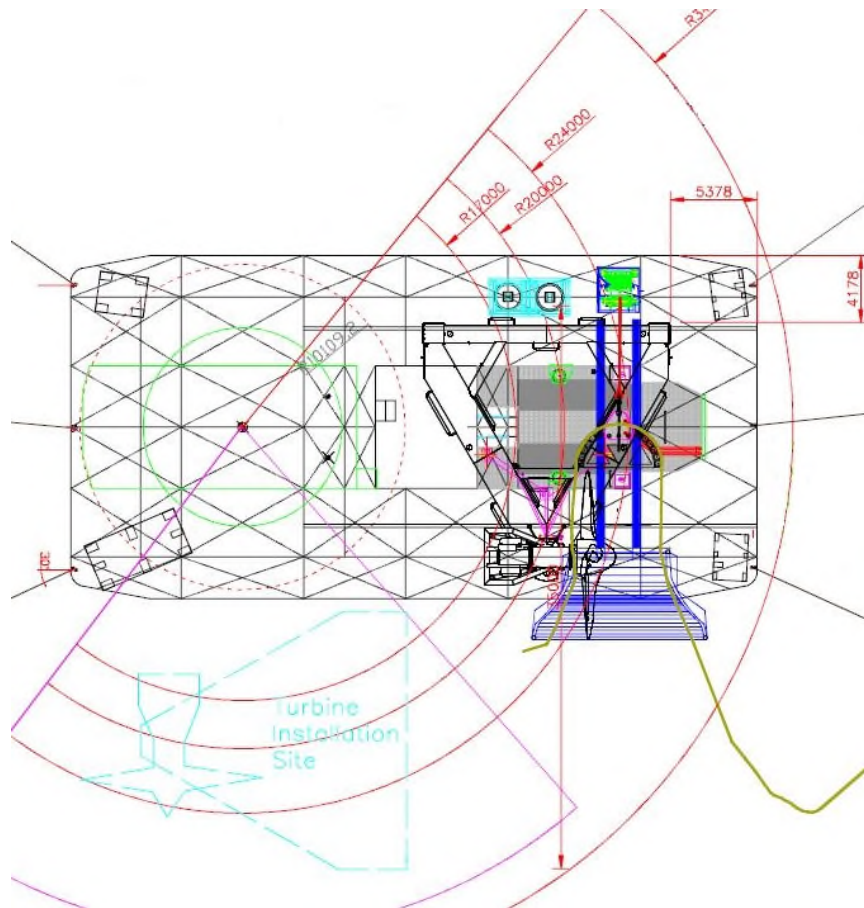


Figure 1-8 Deployment layout

The final solution consists in a fixed crane installed on the carriage of the tank in Cranfield with only the demonstrator scaled. With the size of the demonstrator, a larger scale is accessible. Indeed, a 1:20 scaled model is fitting in the tank. This system is reducing the amount of data accessible by the tests because it is reducing the deployment to its minimum. But considering the budget allowed and the availability of the testing facilities, it is the more accessible system available this year.

The following table is presenting the pros and cons of each option:

Testing possibility	Features	Benefits	Limitations
Complete System with Demonstrator, Barge and Mooring System	1:40 scale factor	<ul style="list-style-type: none"> - Multiple possibilities of test procedure - Accuracy with the real deployment process 	<ul style="list-style-type: none"> - Price (too expensive) - Size of the entire system (too large) - Size of the scaled demonstrator (too small) - Not in Cranfield Laboratory
	Scaled moving Barge + Scaled Demonstrator		
	30 m long / 15 m wide		
	IFREMER Boulogne		
Partial System with Demonstrator and Barge	1:40 scale factor	<ul style="list-style-type: none"> - Multiple possibilities of test procedure - Accuracy with the real deployment process - Possible in Cranfield Laboratory 	<ul style="list-style-type: none"> - Price (too expensive) - Size of the scaled demonstrator (too small)
	Scaled moving Barge + Scaled Demonstrator		
	1 m long / 1 m wide		
	Possible in Cranfield Laboratory but better in IFREMER Boulogne (less blockage ratio)		
Simplified System with only the Demonstrator	1:20 scale factor	<ul style="list-style-type: none"> - Large scale so more accurate - Possible in Cranfield Laboratory - Price 	<ul style="list-style-type: none"> - Simplification important of the deployment process
	Fixed Crane + Scaled Demonstrator		
	1 m long / 1 m wide		
	Cranfield Laboratory		

Table 1-2 Tests procedure summary

1.4 General methodology and thesis structure

The methodology followed during this project is summarised as below:

- Preliminary analytical study of the stability of Deltastream 1
 - Floating stability
 - Submerged stability
 - Extension to the Demonstrator
- Analytical study of the ballast flooding process of the Demonstrator
 - Creation of a code with Deltastream 1
 - Extension to the Demonstrator
- Scaled Model Design
- Model Manufacture
- Tests
- Comparison with numerical predictions

In order to follow this methodology, the thesis is organised as follows:

Chapter 1 introduces the context of the Deltastream project and presents the evolutions of the project in the past few years.

Chapter 2 reviews procedures of stability and ballast flooding then experimental procedure for deployment operations.

Chapter 3 presents the stability work undertaken analytically on Deltastream 1

Chapter 4 describes the analytical model for the ballasts flooding

Chapter 5 outlines the design process and data of the full scale model, the scaled model and the test rig.

Chapter 6 is about the tests session carried out in July 2014.

Chapter 7 is a conclusion with a discussion of the result and a presentation of the further work.

2 Literature Review

2.1 Introduction

By its nature, the Deltastream project is using multiple areas of hydrodynamics engineering during its deployment, operation and recovery. First, as an offshore structure, its stability must be investigated. Second, as the device is fitted with a ballast system, an assessment of those ballasts has to be undertaken. This will be the analytical points undertaken in the thesis. One of the aims of the literature review is to establish a method to study the two points summarised above.

The second aim of the literature review concerns the testing procedure on subsea structures. It will be focused on the splash zone and the scale factor for a ballasting test. It will also describe a testing method which will be the basis for the method used during the tests in the Ocean Laboratory.

2.2 Analytical Stability Assessment

2.2.1 Stability of an offshore structure

An offshore structure is first defined by its Centre of Gravity, Centre of Buoyancy and its draft. An axis system is used to define the six motions of the structure in six degrees of freedom:

- Three translations of the Centre of Gravity in the direction of the three axes:
 - Surge in the longitudinal direction (the x -axis)
 - Sway in the lateral direction (the y -axis)
 - Heave in the vertical direction (the z -axis)
- Three rotations around these axes:
 - Roll around the x -axis (ϕ angle)
 - Pitch around the y -axis (θ angle)
 - Yaw around the z -axis (ψ angle)

These motions are displayed in Figure 2-1.

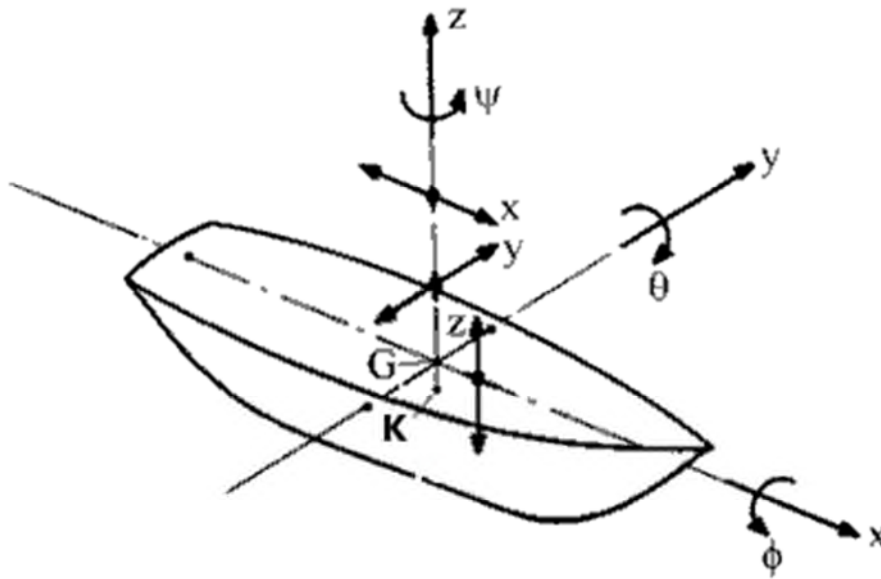


Figure 2-1 Ship Motions in Six Degrees of Freedom

An offshore structure is encountering loads during its floating or flooding phase. These loads are interacting with the structure and are creating a loss of stability. In the case of a study of the static stability, two forces are taken into account:

- The Weight of the structure, which corresponds to the vertical down-thrust force due to the mass of the structure and the gravitational acceleration. Its point of application is the Centre of Gravity (CoG) and its intensity is defined by the following equation:

$$Wa = gm \quad (2-1)$$

In which:

m: masse of the device (kg)

g: gravitational acceleration (m/sec²)

- The Buoyancy Force. It is the force generated by the volume of fluid displaced by the structure. This so-called buoyancy is the vertical up-thrust applied on the structure due to this displaced volume. Its point of application is the Centre of Buoyancy (CoB) which corresponds to the CoG of the submerged volume of the structure. Its intensity is defined by the following equation:

$$F_{\nabla} = \rho g \nabla \quad (2-2)$$

Where:

ρ: density of the displaced fluid (kg/m³)

∇: submerged volume (m³)

Those two forces lead to a state of equilibrium of the structure. This phase is either a floating balance of the structure (ship, buoy...) or a submerged balance (submarine, AUV...). In general, a submerged device is achieved through a ballast system.

2.2.2 Static floating stability

2.2.2.1 Definitions and calculations

The static floating stability of a ship is here to enforce the structure in an equilibrium position when external forces or moments are bringing it out of balance. Those disturbances can be manifested as a translation or a rotation about the CoG. Usually, a ship has only one plan of symmetry called the middle line plane, a vertical plan which is considered the principal plan of reference. The symmetry of the offshore structure ensures that the CoG is on this plan. As for the CoB, it depends on the symmetry of the submerged part of the structure. In order to undertake a study of a floating stability, the forces are considered only to act in the plan of symmetry. Therefore, the CoB and the CoG are assumed to belong to this plan of symmetry. If the longitudinal horizontal axis is included in the plan of symmetry, the rotation is called heel. If the transversal axis is included in the plan of symmetry, then the rotation is defined as trim (Figure 2-2). If the fluid displaced during those rotations is constant, the centre of those rotations is called the Centre of Flotation (CoF). The CoF is defined as the centroid of the area of the structure in the waterline level (water plan area). In some case, the CoG and the CoF can be the same point.

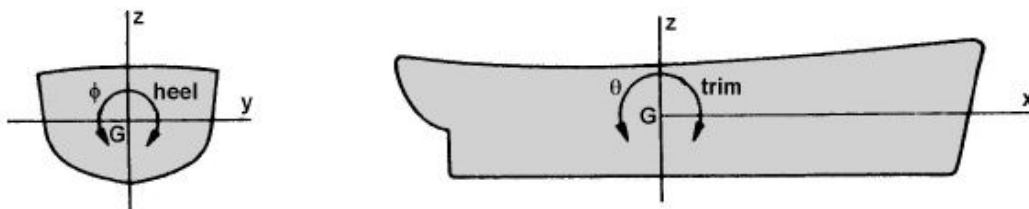


Figure 2-2 Heel and Trim rotations

When the structure is balanced, its CoG and CoB are in the same vertical line. If it is not the case, the structure will trim or heel until those two points are once again in the same vertical line. An external heeling or trimming moment M_H is forcing the structure to rotate around the Centre of Flotation of the structure, thus creating a gap between the horizontal position of the CoG and the CoB. This gap is called the righting stability lever arm \overline{GZ} and it develops a moment defined as the righting stability moment M_S . A balance is found again when:

$$M_H = M_S \quad (2-3)$$

With M_S defined by:

$$M_S = \rho g \nabla * \overline{GZ} \quad (2-4)$$

The value \overline{GZ} is very useful because it determines the magnitude of the stability moment. The stability of a structure can be very conveniently presented with the righting moments or lever arms about the CoG considering the different angle of heeling or trimming. A function is then expressed and the corresponding curve is called the GZ-curve or the static stability curve.

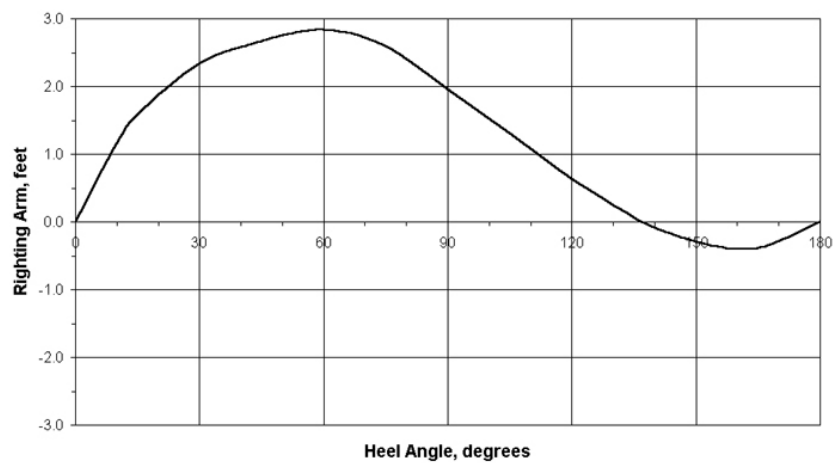


Figure 2-3 Example of a GZ-curve

An aspect interesting in the study of the stability is the Metacentre point M_Φ for a heel rotation and M_Θ for a trim rotation. It is the point of intersection of the lines through the vertical buoyant force at a zero angle and at an angle of heel/trim. With the \overline{GM} the stability of the equilibrium can be assessed very easily. Indeed, if this value is negative, the equilibrium is unstable. In the contrary, if this value is positive, the equilibrium is stable.

2.2.2.2 Stability curve characteristics and interpretations

A curve like the one displayed in Figure 2-3 is suitable to assess the stability of an offshore structure. Four characteristics can be assessed from a GZ-curve:

- The slope at the origin is interesting because for small angle of heel or trim, the righting level arm is proportional to the curve slope and the metacentre is a fixed point. It can be deduced from this that the tangent to the GZ curve at the origin is the metacentric height \overline{GM} .

- The maximum \overline{GZ} value is indicating the biggest heeling moment that the structure can resist without capsizing. Both the heeling/trimming angle and the \overline{GZ} are important.
- The Range of Stability is the range of angle for which the \overline{GZ} is positive. The angle where the stability becomes negative is known as the angle of vanishing stability (Θ_s). The area below this curve represents the maximum potential energy the structure can absorb via a roll motion.
- The area under the static stability curve corresponds to the work which has to be done in order to reach a chosen heel/trim angle. Thus this area defines the ability of the floating structure to absorb roll/yaw energy due to external effect (waves, wind...):

$$P_{\Theta^*} = \int_0^{\Theta^*} M_S \cdot d\theta \quad (2-5)$$

$$P_{\phi^*} = \int_0^{\phi^*} M_S \cdot d\phi \quad (2-6)$$

The first equation corresponds to the work for a trim angle of rotation when the second one corresponds to a heel angle.

2.2.2.3 The inclining experiment

Much of the data needed in stability calculations can be tackled by geometrical considerations. Knowing the submerged volume of the structure and some loading conditions, \overline{GM} can be assessed for an inclination angle smaller than ten degrees. This method is called the inclining experiment and it is using the following equation:

$$\overline{GM} = \frac{p \cdot c}{\rho \nabla \cdot \tan(\alpha_i - \alpha_0)} \quad (2-7)$$

In which:

α_i : given angle of heel or trim (degrees)

α_0 : angle of the upright position (degrees)

p: mass added to the structure in order to create an inclination (kg)

c: position of the mass added (m)

2.2.3 Static submerged stability

For a submerged stability study, a first assessment has to be done before any plots of the stability curves can be carried out. For a submerged structure (like a submarine) to be stable, the CoG must be below the CoB (Figure 2-4).



Figure 2-4 Submarine Stability - Stable State

Indeed when the CoG is below the CoB and the structure starts to roll, the forces applied on the system (Weight and Displacement) will force it to go back to its equilibrium position. In the contrary when the CoG is above the CoB, the forces acting on the structure in the case of a roll will make the loss of stability of the structure even worse, as displayed in Figure 2-5.

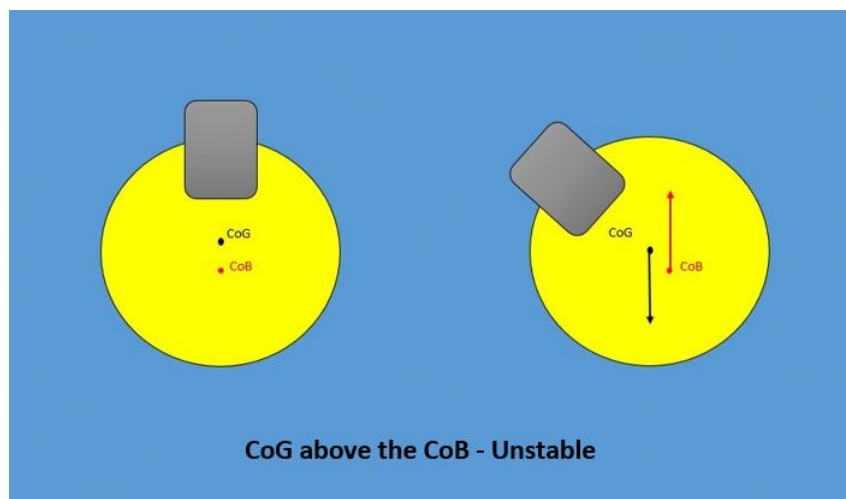


Figure 2-5 Submarine Stability - Unstable State

2.3 Flow inside a forced conduit – Analytical Study

2.3.1 Elementary Fluid Dynamics – The Bernoulli Equation

A flow can develop three different energies: kinetic energy, pressure energy and potential energy. Considering the no friction effect within the potential flows, energies are conserved along a streamline. When it is assumed that the density and the weight of the fluid are constant (in another words the flow is incompressible), the following equation is found:

$$\frac{v^2}{2g} + z + \frac{P}{\rho g} = \text{constant along streamline} \quad (2-8)$$

Where:

v: fluid flow speed at a point on a streamline (m^3)

g: gravitational acceleration (m/sec^2)

z: depth of the streamline (m)

P: pressure at the chosen point (Pa)

ρ : density of the fluid at all points in the fluid (kg/m^3)

This equation is called the Bernoulli Equation. It results from the Euler equations for a non-viscous and incompressible flow written in terms of the velocity potential of the fluid.

When the fluid is physically constrained within a device such as a ballast tank, the conservation of the mass ensued from the Bernoulli equation is used. Considering a steady flow in such a situation with one or multiple inlets and one or multiple outlets, the conservation of the mass implies that the rate at which the flow is going into the device must be identical to the rate at which the flow is going out of the device. The mass flow rate from an outlet or an inlet is given by the following equation:

$$\dot{m} = \rho Q \quad (2-9)$$

In which:

\dot{m} : mass flow rate in kg/s

ρ : density of the fluid (kg/m^3)

Q: volume flow rate in m^3/sec

Given the area of the outlet/inlet and the rate of the fluid going through it, an equation for the volume flow rate Q is determined:

$$Q = V \cdot A \quad (2-10)$$

Where:

V: rate of the fluid in the inlet/outlet (m/sec)

A: area of the inlet/outlet (m²)

As the mass is conserved, the final equation of the conservation of the mass flow rate is found:

$$\rho_{inlet} V_{inlet} A_{inlet} = \rho_{outlet} V_{outlet} A_{outlet} \quad (2-11)$$

With a constant density, $\rho_{inlet} = \rho_{outlet}$ thus the equation above becomes the continuity equation for incompressible flows, depending only on the velocity and the area.

2.4 Scaling model and tests procedure

2.4.1 Ballast Filling Tests

When a testing process is focused on the rate of filling of ballasts, two physical data must be taken into account: the volume of the ballast and the pressure of the air inside. Indeed, the Bernoulli equation depends, amongst other things, on the atmospheric pressure. Translation to full scale data with a reduced scale model cannot be applicable if the pressure has not been scaled.

As a ballast system is used to submerge Deltastream, it is interesting to wonder how the model can be properly scaled in volume and pressure. However, a specialised facility is needed to scale the pressure. The Maritime Research Institute Netherlands (MARIN) has a depressurised wave and towing tank. The atmospheric pressure can be decrease until 2.5% of its initial value:

$$[P'_{scaled}]_{min} = 0.025 [P'_{init}] \quad (2-12)$$

The maximal scale factor is issued from the formula above.

$$[\alpha]_{max} = \frac{[P'_{init}]}{[P'_{scaled}]_{min}} = 40 \quad (2-13)$$

The cost to use this facility is 20,000 Euros per day on a double shift basis.

Knowing that it is possible, at a certain cost, to scale the pressure, some tests can be carried out with a scaled volume and a scaled atmospheric pressure.

For this scaling method, the following scales are used:

$$V_{init} = \alpha^3 V_{scaled} \quad ; \quad P'_{init} = \alpha P'_{scaled} \quad (2-14)$$

Here the volume of water and air are scaled with the same scale factor α^3 . Using the Froude Similarity, this scaled model is ensured from the ratio of air forces which need to be equal to α^3 in order to maintain dynamic similarity.

Another scaling method consists in scaling the volume with a factor of α^2 and let the pressure unmodified. This method is a result of the scale factor of the pressure α and the perfect gas equation. Moreover when the pressure is not changed, the method is only available for gas, so for the air in the ballasts. Therefore, the volume of air must be scaled with the scale factor α^2 and the volume of water with a scale of α^3 . This scale method is difficult to achieve under certain conditions, when the volume of air and water is variable in the case of the filling of ballasts. A perfect example of this scaling method is the Oscillating Water Column (OWC). This device is an energy converter using the waves to create electricity. The motion of a wave creates a pressure effect which is creating a flow putting in motion a turbine which is going to create energy.

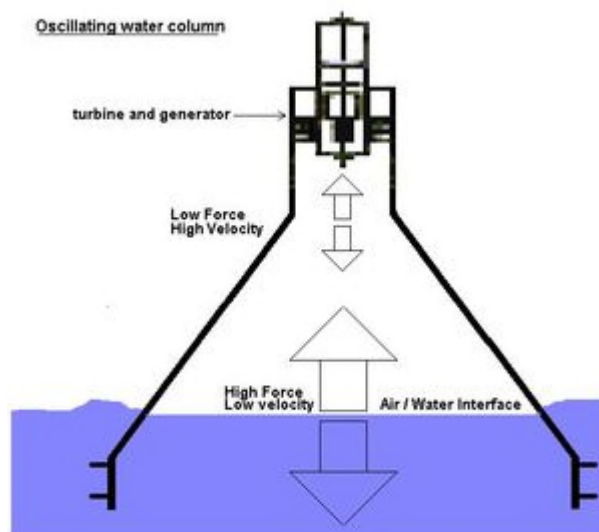


Figure 2-6 Example of an OWC

In that case, it is possible for the tests to scale the volume of air differently from the volume of water. The following figure shows the correct scaling undertaken during these tests.

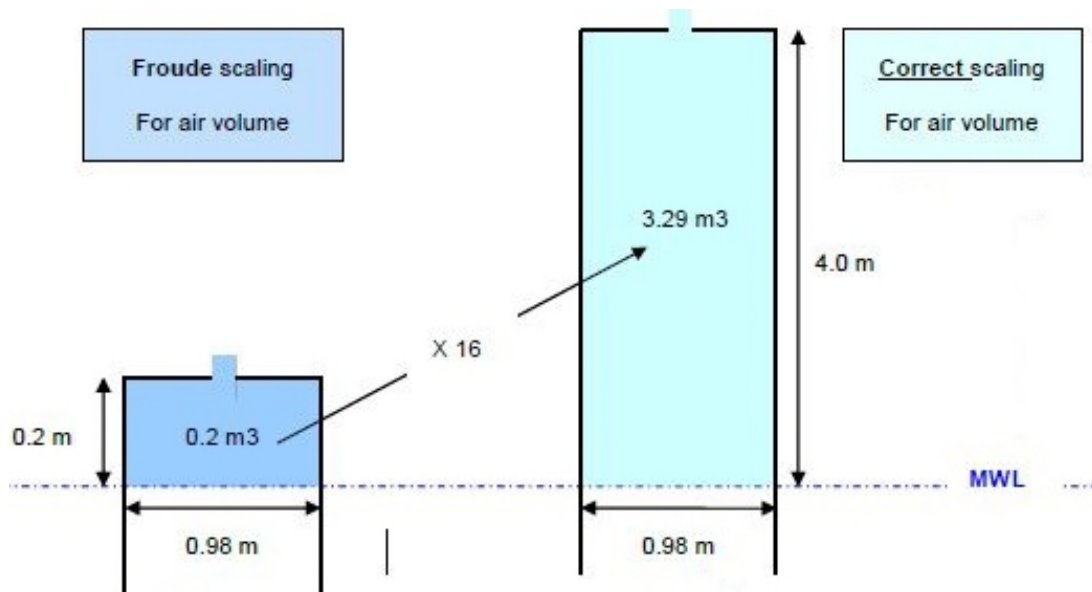


Figure 2-7 Scale Model OWC

The volume of the submerged part of the device is unchanged but the volume of the air chamber is enlarged (multiply by 16).

Moreover, it brings important modifications of the geometry of the device. And it is possible in a case of a device with a submerged volume changing through time (subsea structure being flooded).

Concerning the tests, scaling the pressure as well as the volume appears to be the most accurate solution. Nonetheless, it is really expensive to use a tank allowing a scale pressure. Therefore, it is worth it to look into another solution to compensate the unmodified pressure.

According to the continuity equation, the mass flow rate of the water going in is identical to the mass flow rate of the air going out. However, the mass flow rate depends on the velocity of the flow and this velocity depends on the atmospheric pressure. If this pressure is not scaled, the velocity will not be scaled properly because according to the Bernoulli equation, it depends on it. Indeed, the atmospheric pressure remains the same but the depth of the inlet of the ballast is smaller, so the velocity will be less important, implying a less important mass flow rate and therefore a rate of filling less important. The solution here is to scale the inlet and outlet area of the ballast in order to approximate as much as possible the reality of the full-scaled model. To determine suitable areas, it is the volume flow rate which is going to be scaled. Using the Froude's similitude to scale the model, the volume flow rate is scaled as follows:

$$Q_{init} = \mu \cdot \frac{\alpha^3}{\sqrt{\alpha}} \cdot Q_{scaled} \quad (2-14)$$

Where:

Q_{init} : mass flow rate for the full-scaled model (kg/sec)

Q_{scaled} : mass flow rate for the scale model (kg/sec)

α : scale factor

μ : ratio between sea salt water density and tank water density

2.4.2 Splash zone tests

The second interesting aspect while testing Deltastream is the splash zone. The splash zone is the area immediately above and below the mean water level. Going through this area for an offshore structure means that it goes from a floating phase to a submerged phase.



Figure 2-8 Examples of Subsea structure in the splash zone

This area has long been a major concern for the deployment of subsea structures because of the non-linearity of the wave load during the operation due amongst other things to varying buoyancy and first order wave loads. In the case of devices which are not experiencing a change of mass due to ballasts, an experimental methodology has been developed. It is divided in five phases where the structure is free-hanging in slings to a fixed point and kept in position:

1. Lower side of the structure just above the free surface
2. Structure half submerged (from start to completion of flooding)
3. Upper side of the structure just emerging at the free surface

4. Structure fully submerged and descending
5. Lower side of the structure just above the seabed



Figure 2-9 Model of a subsea structure in the phase 1 of the test

2.5 Conclusion

During the deployment phase, Deltastream is being submerged due to the filling of the ballasts. A qualitative approximation of the filling of the ballast can be carried out through a study of the floating stability. The device has at least three compartments and it is important to visualise in which order and at which rate those ballasts will be filled. The second point approached in the literature review concerns the rate of the flooding. The Bernoulli equation along with the continuity equation can be used to model the flooding of the ballast and then obtained the rate of the flooding. With this information, the rate of submersion of the device can be obtained. Finally, the model scale needs to be scaled accurately and it means that the atmospheric pressure needs to be scaled. But an alternative has been found to avoid the very large cost of a wave tank capable of lowering the atmospheric pressure.

3 Stability assessment on Deltastream 1

Whether for a subsea structure (submarine, subsea offshore structure...) or a floating structure (boat, offshore platform...), a study on the stability is a recommended task. In the case of Deltastream, the structure is going through multiple phases:

- **Floating phase:** the structure is floating; the ballasts are not being filled yet.
- **Splash-zone phase:** the ballasts start to be filled; the structure is being progressively submerged.
- **Submerged phase:** the structure is completely submerged; the ballasts are full and the weight of the structure drags it toward the seabed.

Depending on the phase Deltastream is going through, the stability analysis is different. Despite those differences, the method is the same. To complete a stability study, first the \overline{GZ} of the structure has to be found in the principal directions of it (Transversal and Longitudinal). Figure 3-1 illustrates the Righting Arm of a structure.

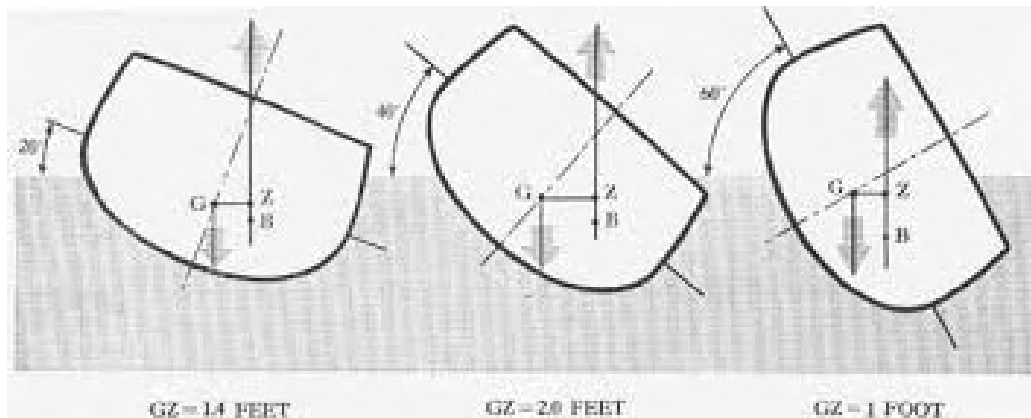


Figure 3-1 Display of the Righting Arm

3.1 Floating Stability

In this part, the stability of the floating structure is determined. Calculations with Excel and the Dassault System CAD Software Catia are used. Through this analysis, the draft of the floating structure is assessed, the Centre of Buoyancy is determined and a method is developed to determinate the different stability curves

3.1.1 Hypotheses

The following hypotheses have been used:

- The structure remains horizontal during the floating process.
- The origin of the structure is given in Figure 3-2.
- Only the Weight (W_a) and the Displacement (F_{∇}) are taken into account.
- In order to calculate the initial Centre of Buoyancy (CoB), the geometry is simplified according to Figure 3-3.
- In the calculation of the stability curves, the displaced volume of the blade is not taken into account.
- According to TEL, the coordinate of the Centre of Gravity from the origin are:

CoG.x (mm)	CoG.y (mm)	CoG.z (mm)
0.00	20,395.00	6,838.00

Table 3-1 Centre of Gravity Coordinates

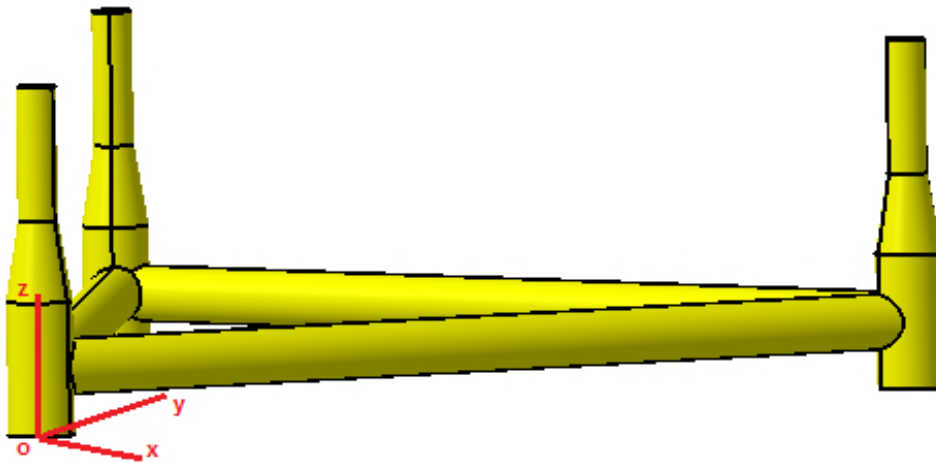


Figure 3-2 Origin and axes

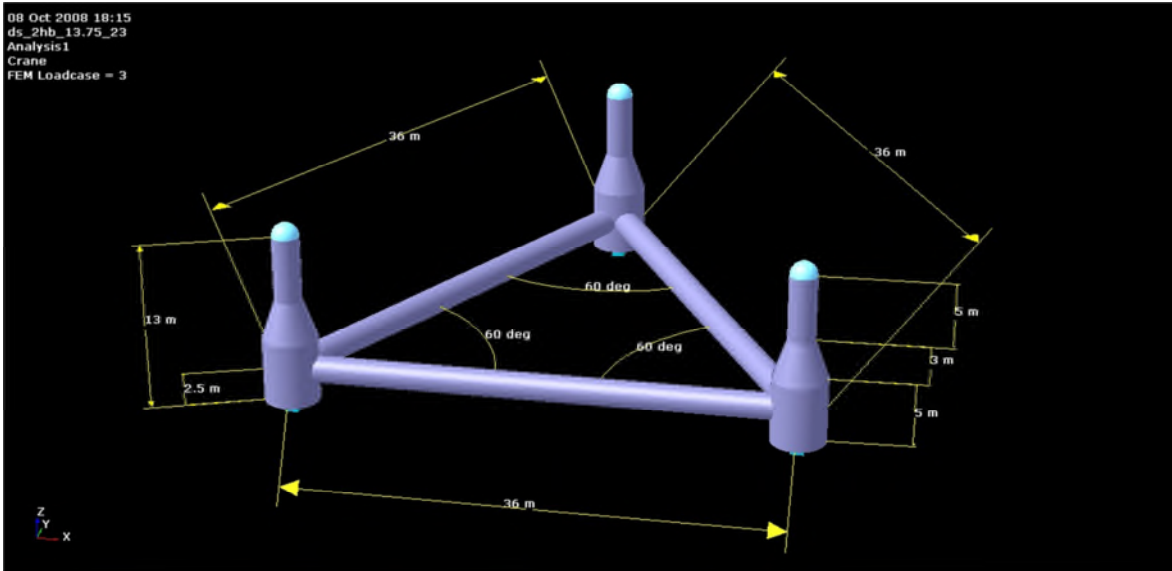


Figure 3-3 Simplified Structure

The following table summarises the important data of the structure:

Mass	379,000.00	kg
Weight	3,717,990.00	N
Transversal Tube Length	33.5	m
Transversal Tube Diameter	2.032	m
Height (Without turbine)	13	m
Vertical Tube Diameter	2.5	m
Vertical Tube Height	5	m
Top Tube Diameter	1.5	m
Top Tube Height	5	m
Cone Height	3	m
Sea Water Density	1,025	kg/m ³
Gravitational Acceleration	9.81	m/s ²

Table 3-2 Structure Data

3.1.2 Problem-Solving Approach

First of all, the CoB of the structure is determined. The submerged volume is first needed in order to determine the CoB. It is calculated with a simple Static Fundamental Principal with two forces applied: The Weight and the Displacement. Using Excel to calculate the Displacement with multiple possible drafts, the submerged volume corresponding to the displacement at equilibrium is found.

3.1.2.1 Determination of the Centre of Buoyancy

The first step followed for the determination of the Centre of Buoyancy is the calculation of the submerged volume of Deltastream. It is calculated using the two following formulas:

$$Wa + F_{\nabla} = 0 \quad (3-1)$$

$$F_{\nabla} = \rho_{water} * \nabla * g \quad (3-2)$$

Where

ρ_{water} : density of salt water (kg/m³)

g: gravitational acceleration (m/sec²)

∇ : volume of water displaced by the structure (m³)

The first formula corresponds to the Static Fundamental Principal applied on Deltastream and only on the z axis. The second one corresponds to the usual formula used to determine the Displacement of a solid in a fluid. Using those two formulas and knowing the value of Wa , the volume of displaced water determined is 369.76 m³ with the following equation:

$$\nabla = - \frac{Wa}{\rho_{water} * g} \quad (3-3)$$

The second step is to determinate the Draft (D) of the structure corresponding to this submerged volume. The method used was an iterative calculation of the submerged volume corresponding to a chosen draft until a submerged volume as close as possible to the one determined previously is found. The calculation was divided in three parts:

- First, when the water line has not reached the Transversal tubes of the structure (from 0 to 1.4 m).
 - Then when the water line has reached the Transversal tubes until the centre of those tubes (from 1.5 to 2.4 m).
 - Finally, when the water line is over the tubes centre (from 2.5 to 3.5 m).
-
- **From 0 to 1.4 m**

In this case, only three horizontal cylinders are submerged. The formula of the submerged volume is three times the formula of a cylinder, with the height of the cylinder corresponding to the draft. The latter is changed progressively (0.1 by 0.1 m) and the submerged volume is calculated for each value of the draft.

For a draft of 1.4 m, the value reached by the submerged volume is 20.62 m³ which is far from the total submerged volume. As a result, the draft needs to be increase again but after 1.4 m of draft, the tubes linking the three towers of Deltastream start to be submerged, and it brings a small change in the calculation.

- From 1.5 to 2.4m

In this interval of draft, the cylinders of the triangle structure start to be submerged. Therefore, this part must be taken into account in the calculation. Figure 3-4 displays all the data needed to calculate the volume of a partially filled horizontal cylinder.

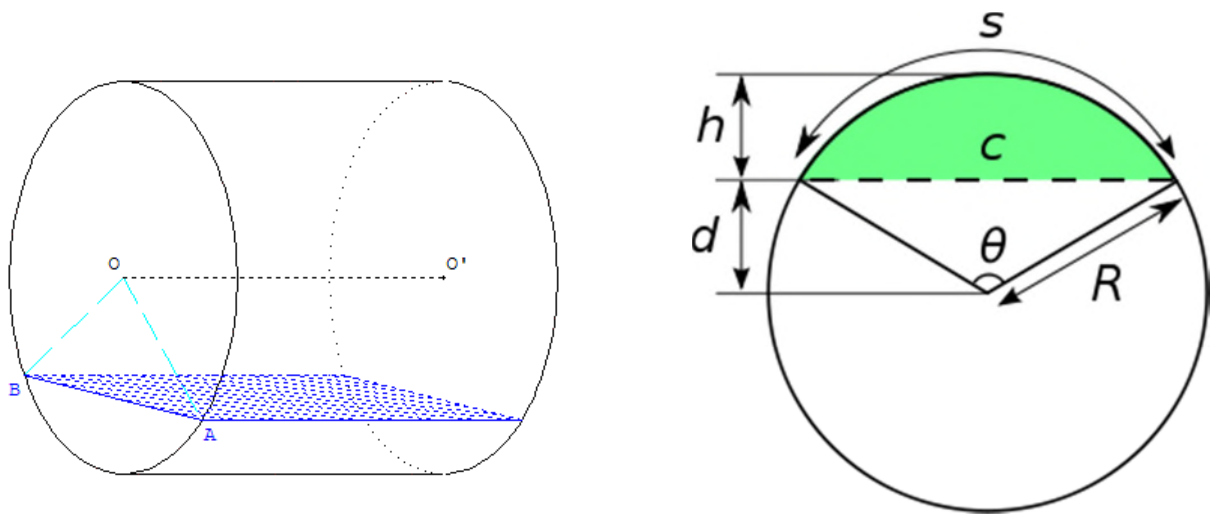


Figure 3-4 Volume of a partially filled horizontal cylinder

The volume which needs to be determined is the volume corresponding to the green area on the right picture (A_{green}). The formulas used to determine this volume are the following:

$$d = l - D \tag{3-4}$$

$$\theta = 2 * \arccos \frac{d}{R} \tag{3-5}$$

$$A_{green} = \frac{R^2}{2} * (\theta - \sin \theta) \tag{3-6}$$

$$V_{cylinder} = L * A_{green} \tag{3-7}$$

Where

R: radius of the cylinder (m)

D: draft of the structure (m)

l: length between the bottom of the structure and the centre of the cylinder (m)

L: length of the cylinder (m)

As soon as $V_{Cylinder}$ is determined, $V_{Displaced\ Water}$ is calculated as follow:

$$V_{Displaced\ Water} = 3 * (D * V_{ta} + V_{Cylinder}) \quad (3-8)$$

For a draft of 2.4 m, the value reached by the submerged volume is 177.91 m³. Once again, the volume is not reached. The draft still needs to be increased but this time a slight change in the previous equations is necessary. The modification is explained in the third part.

- From 2.5 to 3.5m

In-between those two values of draft, the white area on the right picture in Figure 3-4 is the one which needs to be calculated. A subtraction between the whole area and the green one is necessary:

$$A_{white} = A_{SiC} - A_{green} \quad (3-9)$$

$$V_{Cylinder} = L * A_{white} \quad (3-10)$$

$$\Delta = 3 * D * A_{StC} + 3 * V_{Cylinder} \quad (3-11)$$

Where

A_{SiC} : Complete area of the side cylinder (m²)

For a draft of 3.5 m, the value reached by the submerged volume is 377.07 m³. Through those results, it is clear that the submerged volume which needs to be reached is somewhere between 3.4 and 3.5 m. In order to be more accurate in the determination of the volume, the same calculation is done again but with a smaller change of draft each time (0.005 by 0.005 m first and then 0.001 by 0.001 m). The result must be close to 3.4 m as the submerged volume for this draft is closer to the required submerged volume.

Draft (m) – D	Submerged Volume (m ³) - ∇
3.4	368.57
3.405	369.11
3.41	369.64
3.411	369.75
3.412	369.85
3.413	369.96
3.414	370.06
3.415	370.17

Table 3-3 Submerged Volume between 3.4 and 3.415m

The exact value of the submerged volume determined in the first step of the calculation is not reached. But the difference is of the order of 0.01 m³ which corresponds of an error of $2.7045 \cdot 10^{-5}$ which can be neglected. To conclude, the draft corresponding to the submerged volume of the structure is 3.411 m.

Figure 3-5 shows the waterline which corresponds to the draft found earlier.

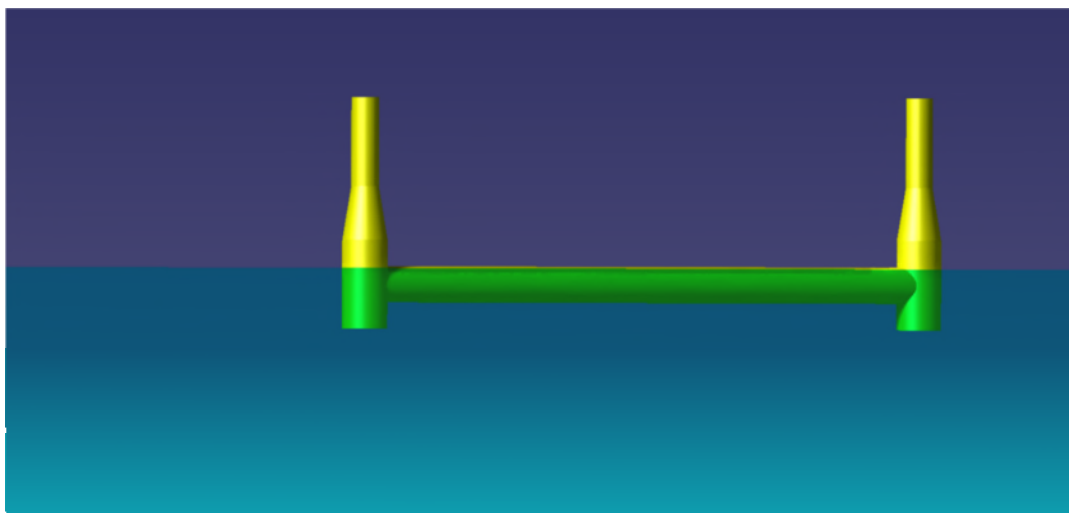


Figure 3-5 Draft in un-ballasted condition

The third and final step is the determination of the Centre of Buoyancy, knowing the draft of the structure. To achieve this objective, two methods were used. The first one involves a barycentre calculation when the second one is using a CAD software.

- Barycentre Calculation

The first step of this calculation is to divide the submerged volume of the structure in multiple smaller and simplified volumes, then attribute a weighting to each of them. Once this has been properly defined, the coordinates of each

volume Centre of Gravity and then the barycentre are calculated. From the Draft Calculation method on Excel undertaken previously, the volumes of the Stand and Side Parts are already known. Using those results, six different volumes with their values are provided, and so their weighting by dividing the partial volume by the Total Submerged Volume. The division of the Deltastream submerged volume is displayed in Figure 3-6.

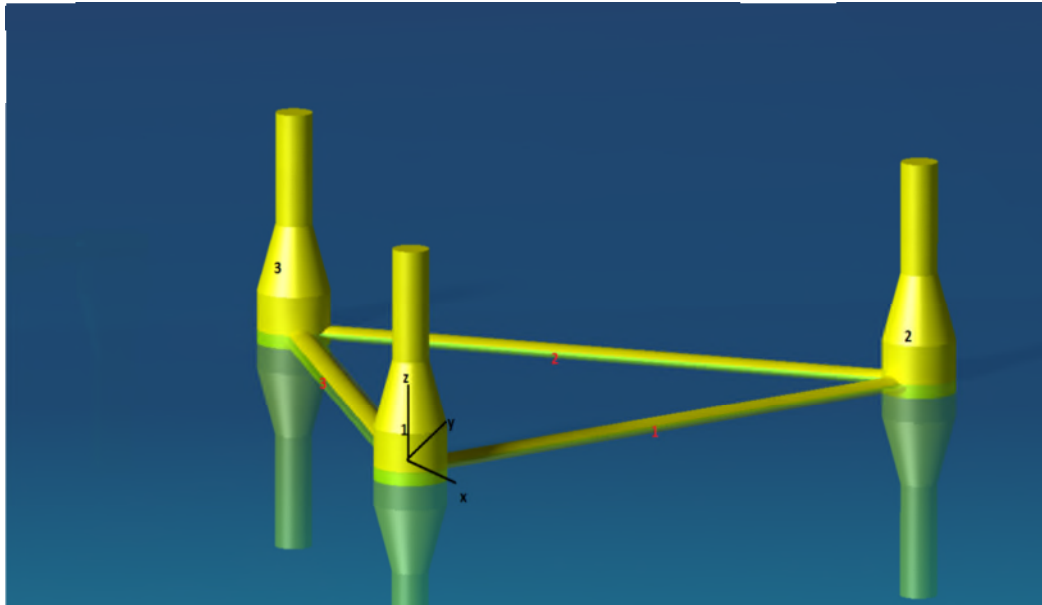


Figure 3-6 Volume Division

Even if this picture shows the complete volume of Deltastream, only the submerged parts of those volumes are taken into account. The following table displays the information of volume and weighting needed for the calculation.

Structure	Volume (m ³)	Total Volume (m ³)	Weighting (%)
Turbine Tower 1	16.74	369.75	4.53
Turbine Tower 2	16.74		4.53
Turbine Tower 3	16.74		4.53
Transversal Tube 1	106.51		28.81
Transversal Tube 2	106.51		28.81
Transversal Tube 3	106.51		28.81
		Total Weighting	100.02

Table 3-4 Partial Volumes and Weighting

Knowing the origin of the base from Figure 3-6, the coordinates of the centre of gravity of each Stand Cylinder are determined. As for the Z coordinate, the draft is divided by two. The coordinates are summarised in the following table.

	CoG.x (m)	CoG.y (m)	CoG.z (m)
Turbine Tower 1	18	31.177	1.7055
Turbine Tower 2	0	0	1.7055
Turbine Tower 3	-18	31.177	1.7055

Table 3-5 Coordinates of the Centre of Gravity for the Stand Cylinder

For the side tubes, the x and y coordinates are determined with geometry calculations on an equilateral triangle. The CAD software is required to determine the z coordinate. A section of the side's cylinder is drawn and the z coordinate is found using the inertia function of the software, as shown in Figure 3-7.

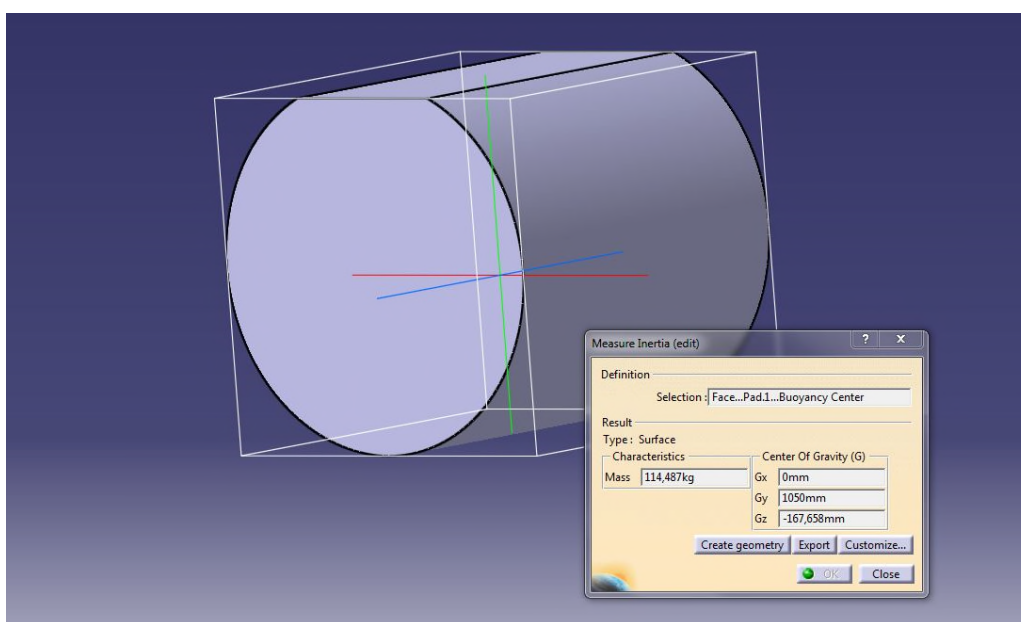


Figure 3-7 Z Coordinate for the side tubes

In this drawing, the origin of the base is the centre of the complete cylinder (without the extrusion at the top). The CoG is 167.658 mm below the CoG of the complete cylinder which is at 2.5 m from the bottom of the structure in the complete Deltastream structure. Therefore, the value of the CoG.z is 2.33m. The results are resuming in the Table 3-6.

	CoG.x (m)	CoG.y (m)	CoG.z (m)
Transversal Tube 1	9	15.59	2.33
Transversal Tube 2	-9	15.59	2.33
Transversal Tube 3	0	31.18	2.33

Table 3-6 Coordinates of the CoG of the Transversal Tube

Knowing the CoG for each one of the six volumes, the barycentre calculation can be done using the following equations.

$$x_g = \frac{\sum_{i=1}^6 m_i x_i}{\sum_{i=1}^6 m_i} \quad (3-12)$$

$$y_g = \frac{\sum_{i=1}^6 m_i y_i}{\sum_{i=1}^6 m_i} \quad (3-13)$$

$$z_g = \frac{\sum_{i=1}^6 m_i z_i}{\sum_{i=1}^6 m_i} \quad (3-14)$$

Where

x_g : x coordinate of the barycentre

y_g : y coordinate of the barycentre

z : z coordinate of the barycentre

(m_i, x_i) : Couple (weighting, x coordinate) of the i volume

(m_i, y_i) : Couple (weighting, y coordinate) of the i volume

(m_i, z_i) : Couple (weighting, z coordinate) of the i volume

With this formula, the following CoB coordinates are found:

CoB.x (mm)	CoB.y (mm)	CoB.z (mm)
0	20,784.53	2,247.17

Table 3-7 Coordinates of the CoB

This table is giving the results obtained with the calculation previously described. For those coordinates and the following from Catia, the origin of the base is the one represented in Figure 3-2.

- CAD Calculation

The second method consists in drawing only the submerged part of Deltastream and determining its centre of gravity with the inertia function of Catia. The drawing is showed in Figure 3-8 and the “measure inertia” window is displayed. The centre of gravity of this structure matches with the centre of buoyancy of Deltastream in floating stage.

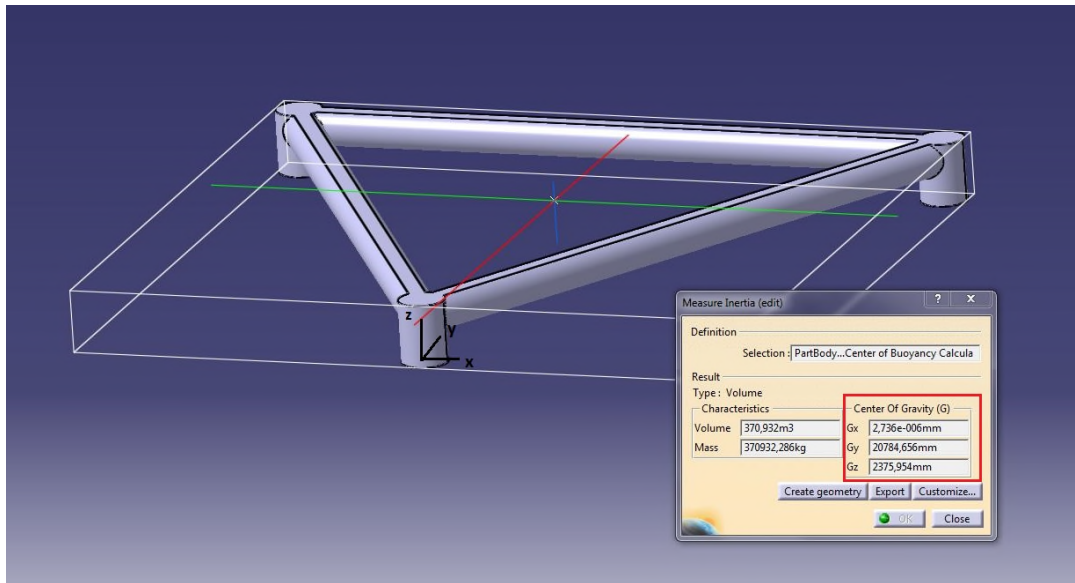


Figure 3-8 Determination of the Centre of Buoyancy

The following table resumes the results from calculation with Catia. A value of 0 is taken for CoB.x because Catia found a value 2.736e-006 mm, which can be neglected considering the size and the symmetry of the structure.

CoB.x (mm)	CoB.y (mm)	CoB.z (mm)
0	20,784.66	2,375.95

Table 3-8 Centre of Buoyancy Coordinates

The difference between the first CoB.y and the second one can be neglected because the difference is about a tenth of a millimetre. But for the CoB.z, the difference is about fifteen centimetres. The difference between the two values can be explained by the hypothesis used for the barycentre calculation. Indeed, the side tubes have been approximate by cylinder but each extremity of those tubes is not flat, some volumes are not taking into account. Those volumes are more on the top of the structure, which explains the raise of the CoB.z.

From now, the average of those two values is used, as shown in Table 3-9.

CoB.x (mm)	CoB.y (mm)	CoB.y (mm)
0	20,784.60	2,311.56

Table 3-9 Final coordinates of the Centre of Buoyancy

3.1.2.2 Determination of the Righting Arm for a trim angle

Deltastream is here experiencing a trim angle. The method to plot the Stability curve of Deltastream structure is described. With this graph, the inclination

taken by the structure when given a specific force like the forces developed by the waves or the current will be easily accessible. In order to plot this graph, the CoF is first necessary. It can be determined as the centre of the surface of flotation. The best way to obtain it is to use the Catia Software.

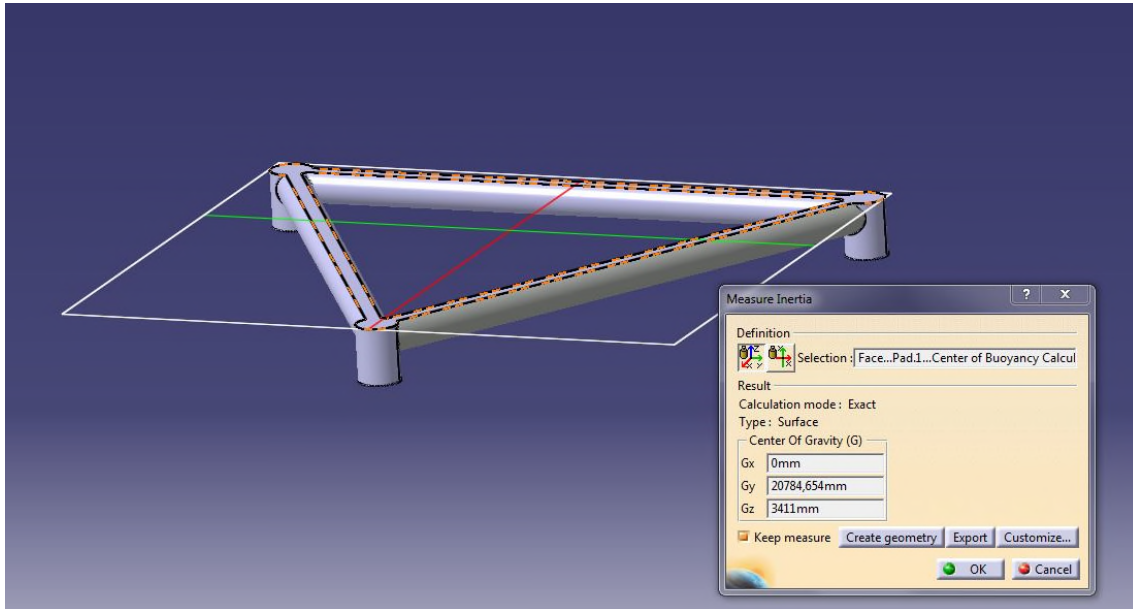


Figure 3-9 Determination of the Centre of Flotation

According to the software, the following coordinates are obtained:

CoF.x (mm)	CoF.y (mm)	CoF.z (mm)
0	20784.654	3411

Table 3-10 Coordinates of the Centre of Flotation

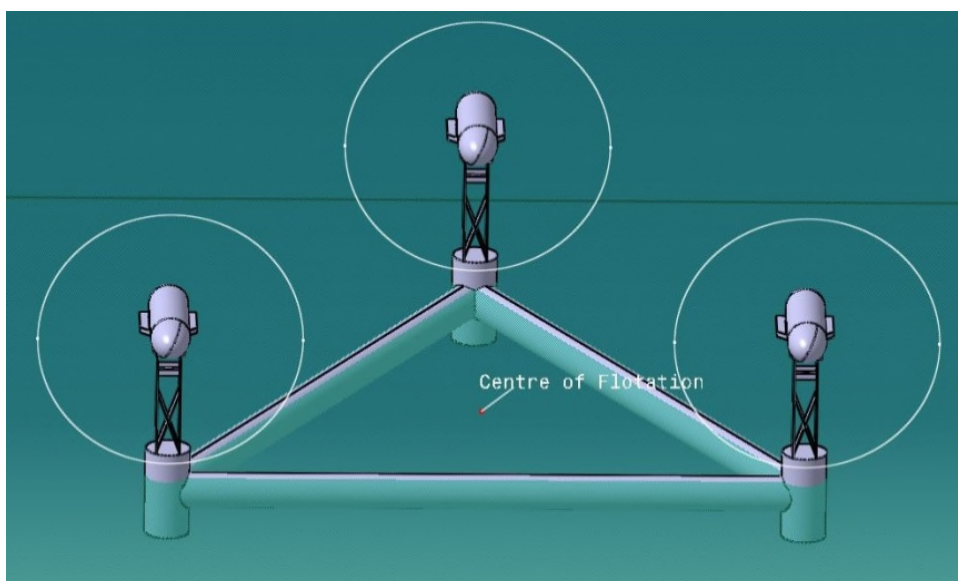


Figure 3-10 Floating Structure

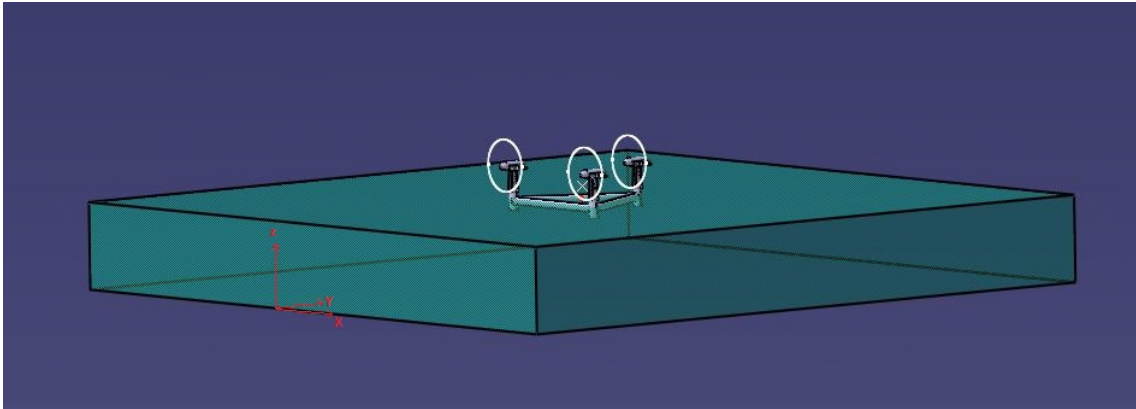


Figure 3-11 Origin for the GZy Calculation

Knowing the Centre of Flotation, Catia is used to calculate the CoB for multiple inclinations, determine the corresponding GZ for each and plot the stability curve. Figure 3-10 displays the structure floating in calm water with the CoF represented. During the process, the structure is rotating around the longitudinal axis passing by the CoF. Therefore, the CoG is also moving considering the origin used (Figure 3-11). In this picture, the plan *xy* is a plan of symmetry for Deltastream. The initial coordinates of the CoG of the whole structure, with the base described earlier, are given in the following table.

CoG.x (mm)	CoG.y (mm)	CoG.z (mm)
0	100,000.00	28,427.00

Table 3-11 Coordinates of the initial Centre of Gravity

With Catia, it is possible to use the function “pocket” and “remove” the tip of the structure in order to calculate the CoG of the part of structure left which corresponds to the CoB of the entire structure. Considering the symmetry of the structure, the *x* coordinate of the CoB is not taking into account as it is included in the *xy* plan. The equation to calculate the GZ_y is a simple subtraction between the *y* coordinates of the CoB and the CoG.

$$GZ_y = CoB.y - CoG.y \quad (3-15)$$

The following table summarises the results obtained with the previous equation.

Θ_y (deg)	GZy (mm)		
0	-390	60	3,811
0.1	-332	70	1,696
0.5	-137.5	80	-500
0.7	-53	90	-2,709
0.85	12.5	100	-4,862
0.86	17	110	-6,895

1	80	120	-8,749
5	2,191	130	-9,595
10	6,032	135	-8,968
15	7,310	140	-8,081
20	8,057	145	-6,963
25	8,888	150	-6,530
30	8,861	155	-6,777
35	8,228	160	-6,991
40	7,485	165	-7,179
45	6,660	170	-7,326
50	5,766	175	-5,728
55	4,812	180	290

Table 3-12 GZ_y according to the angle of inclination

Using the Table 3-12, the following stability curve is plotted.

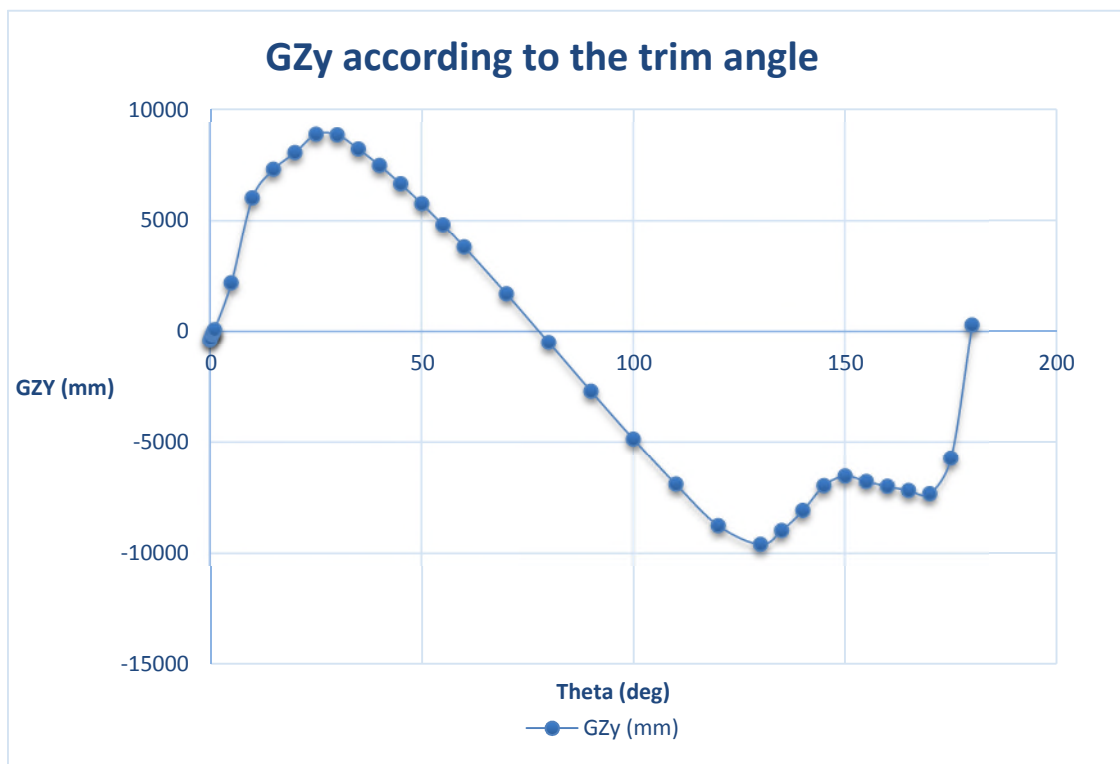


Figure 3-12 Transversal Stability Curve – GZ_y

When the curve is above the abscissa axis, the positive stability is reached. The righting arm helps the structure to come back in its initial equilibrium. Here the Range of Stability is between an angle of approximately 1 degree and the angle of vanishing stability, 77.7 degrees. The maximum \overline{GZ} value is reached in the range of stability, it corresponds to a trim angle of 25 degrees and its value is

8,888.00 mm. Above this trim angle, the \overline{GZ} start to decrease until the angle of vanishing stability is reached. On the contrary, when the curve is below the abscissa axis, the stability is negative. The structure is unstable until it reaches an equilibrium position. The table below summarises the different value of the angles:

θ_0 (deg)	θ_s (deg)
25	77.7

Table 3-13 Value of the particular angles of the stability

In order to find θ_s , the curve between the points of 70 degrees and 90 degrees is approximated by a linear curve; its equation is calculated and the abscissa coordinate of the cross point between this straight line and the abscissa axe corresponds to θ_s .

The small raise of the GZ_y in the negative stability (between 130° and 150°) can be explained by the submersion of the turbine (Figure 3-13). Indeed, this phenomenon brings the CoB close to the CoG, and the temporary raise of the GZ_y is observed.

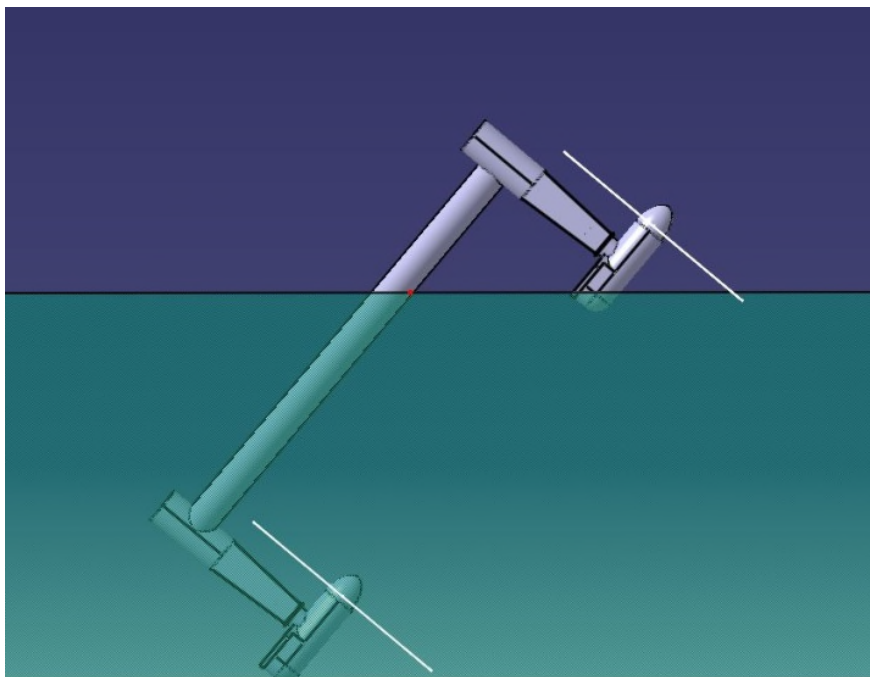


Figure 3-13 Floating Structure - Inclination 130°

With this curve, the angle of equilibrium of the structure can be determined. Indeed, for an angle of zero degree, the \overline{GZ} is negative, which means the stability is negative; the structure will automatically try to reach its equilibrium

position. This position is reached when GZ_y equals to zero. For Deltastream, the angle of equilibrium is 0.82° . This result is found by the same linear method that the one used for θ_0 and θ_s .

Multiplying the Righting Arm by the Weight of the structure, another stability curve is found. The shape of the curve is the same as the previously found curve as the data are just being multiplied by a constant. This curve gives the Righting Stability Moment (M_s) needed by the structure to reach a certain angle.

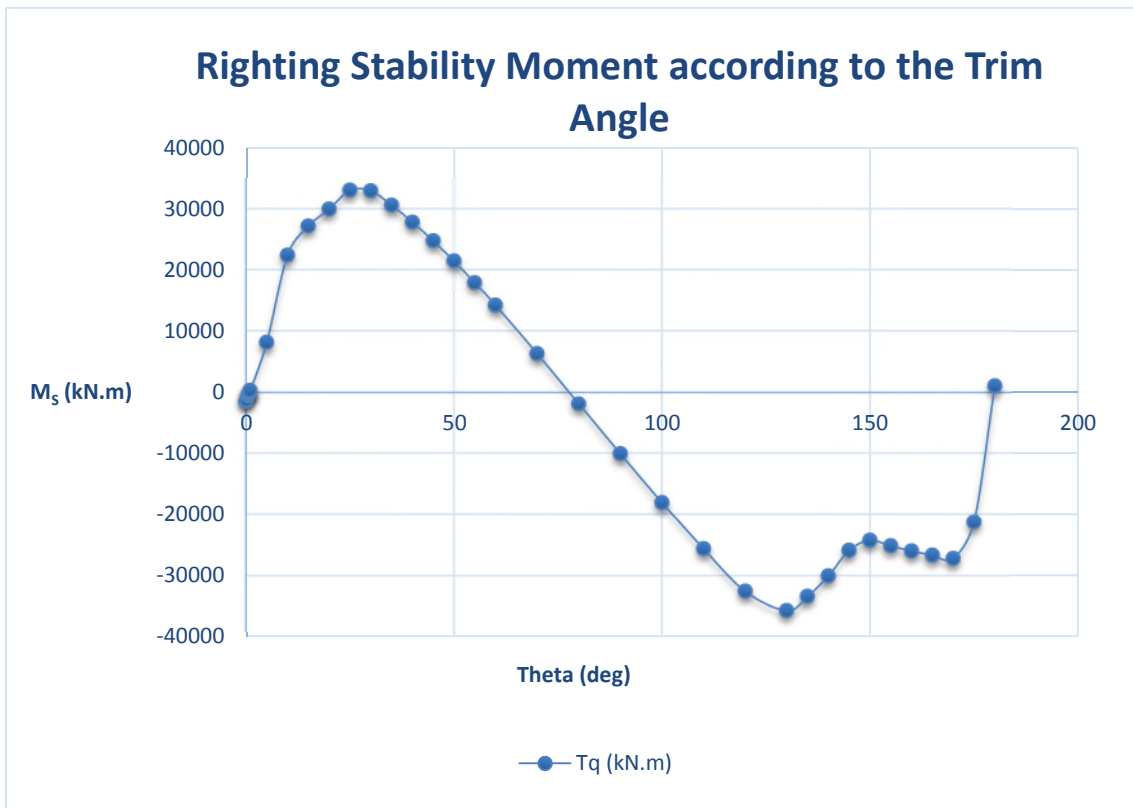


Figure 3-14 Transversal Stability Curves – Righting Stability Moment

With this curve, the amount of energy Deltastream can absorb can be determined using the equation (2-5). The interesting part is the area under the curve in the range of stability. Using Excel, the above curve has been approximate using a polynomial trend line of the 6th order as displayed in Figure 3-15. The small raise of the curve 125 and 152 degree is not approximate by the trend line but it is not a part taken into account for the determination of the energy.

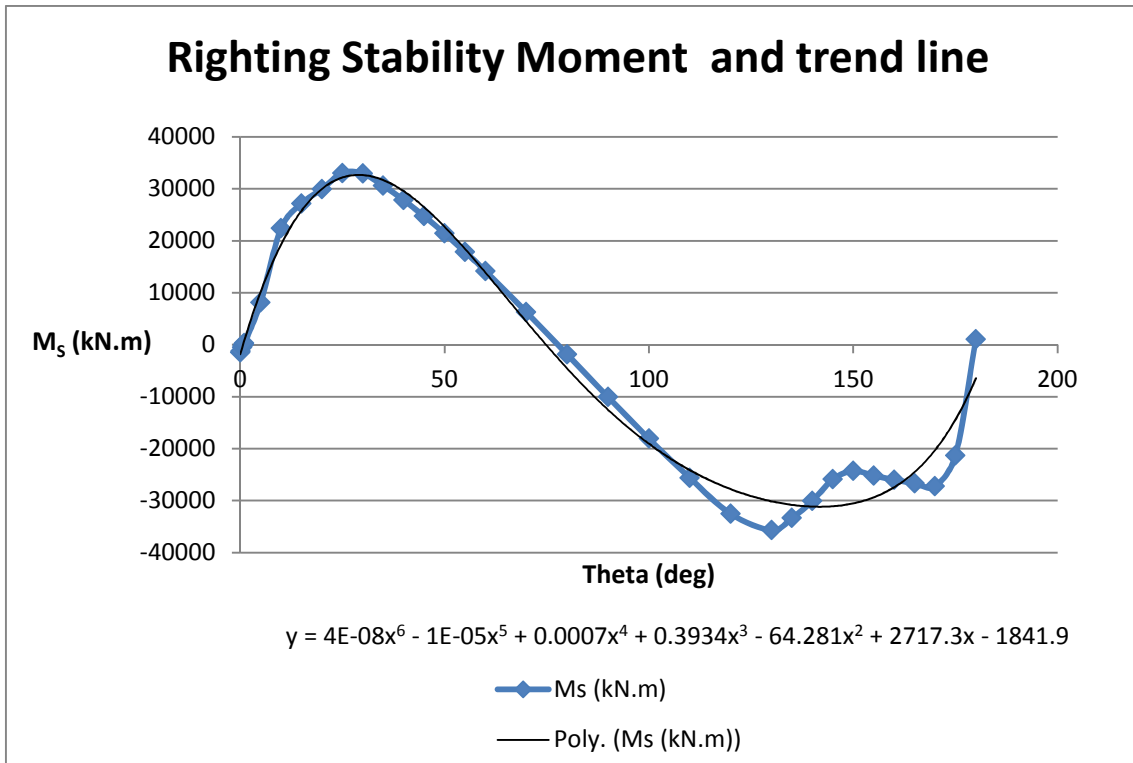


Figure 3-15 Righting Stability Moment curve and its Trend Line

The formula under the graph is the one which is going to be integrated following the equation (2-5). As a polynomial equation, the integration is easy. The integration is made in the range of stability, so between 0.82 and 77.7. The result is displayed in the following table:

P_{θ^*}	$1.72 \times 10^6 J$
----------------	----------------------

Table 3-14 Energy absorbed by Deltastream

For symmetrical reason, the Longitudinal Righting Arm is not possible to find analytically. In this case, the CoB does not stay in the transversal plan, so the inclination is a combined inclination between the transversal and the longitudinal plan.

3.2 Submerged Stability

In this part, Deltastream is considered fully submerged. Therefore, the displacement of the device is constant as well as the CoB. To assess the flooding stability, the quantity of water needed to submerge completely the structure is needed. Once this quantity has been found, a new CoG is calculated, thus the new coordinates of the CoB. Finally the stability is studied given the CoB found with the CAD Software Catia. The physical hypotheses used are equivalent and the geometry used is the one used in the stability curve determination carried out previously.

3.2.1 Determination of the new Centre of Gravity

According to the floating stability study, the z coordinate of the CoG is 6,838mm above the bottom of the structure. The ballasts are located in the tubes linking the three summits of the device. Considering their diameter and the thickness of the steel, the volume available in those three tubes is approximately 311.8m³ if the tubes are considered completely drain. In the following calculation, the volume of water displayed in the ballasts is 309m³, so 103m³ in each tube. By symmetry and knowing the origin of the system, the x coordinate is 0. The z coordinate of each ballast corresponds to the z coordinate of the centre of the tubes containing the ballasts. Which means it is 2.5m above the bottom of the device. As for the y coordinate, it corresponds to the one of the centre of gravity of an equilateral triangle. Thus, it is at a distance of two-third of the height from the summit. The height of Deltastream is 31.177m; the two-third of this value is 20.785m. The Table 3-15 summarises those coordinates.

CoG.x (mm)	CoG.y (mm)	CoG.z (mm)
0	20,785	2,500

Table 3-15 CoG of the ballasts system

In order to calculate the CoG equivalent for the device fully ballasted, a barycentre method similar to the one used in the floating assessment is used. The information needed is displayed in the Table 3-16.

Structure	Weight (kg)	Total Weight (kg)	Weighting (%)
Device without ballasts	379,000.00	695725	54.50
Ballast System	316,725.00		45.50
		Total Weighting	1

Table 3-16 System Information

Using the CoG coordinates displayed in Table 3-1 and the Table 3-15 (ballast CoG coordinates), the final CoG system of coordinate is determined and summarises in the table below.

CoG.x (mm)	CoG.y (mm)	CoG.z (mm)
0	20,573.00	4,863.00

Table 3-17 Final CoG Coordinates – Ballasted Deltastream

3.2.2 Determination of the Centre of Buoyancy

Now that the CoG of the ballasted device has been determined, the CoB must be found in order to see which one is above the other. The structure used for this determination is the structure displayed in Figure 3-10. The CAD software is calculating directly the CoG with this drawing.

CoB.x (mm)	CoB.y (mm)	CoB.z (mm)
0	20,758.00	4,506.00

Table 3-18 CoB coordinates – Fully Submerged Structure

According to Table 3-17 and Table 3-18, the CoG is above the CoB. Moreover, the Y coordinate of the two points are not the same, which means that from the beginning, the device is going to have an inclination. So the structure will start naturally to be inclined and as the CoG is above the CoB, it will roll over completely before finding a static position. Therefore the device is unstable when it is completely submerged. The device will develop a trim angle and the forces applied on it will not be able to stop this trimming movement, they will increase it. A way to avoid this situation is to set up the lift point for the deployment backward to the centre of gravity. Indeed the lifting force develop by the lifting point will offset the loss of stability. The localisation of this point is determined in the following part.

3.2.3 Lifting Point Position

The deployment scenario studied here is a deployment with only one point of lifting. It is the one TEL is using for the deployment of Deltastream during the year 2014. As explained previously, the point must be positioned in such a way that it counterbalances the negative stability of the structure. The resulting force of the Displacement (F_{∇}) and the Lifting Force (F) must offset the Weight (P) in direction and intensity. Moreover, the point of application of those two resulting forces has to be the same. The table below is presenting the three forces applied and there point of application (CoB for the displacement and CoG for the weight). The value of the lifting force is calculated by subtracting the value of the displacement to the value of the weight.

Weight		
CoG.x (mm)	CoG.y (mm)	CoG.z (mm)
0	20,573.00	4,863.00
Intensity (N)		
6,825,062.25		
Displacement		
CoB.x (mm)	CoB.y (mm)	CoB.z (mm)
0	20,758.00	4,506.00
Intensity (N)		
5,068,974.15		
Lifting Force		
F.x (mm)	F.y (mm)	F.z (mm)
0	<i>Unknown</i>	<i>Unknown</i>
Intensity (N)		
1,756,088.10		

Table 3-19 Application points of the forces

As the structure is having a pitch movement, the lift point has to be ahead of the CoG. Furthermore, the point of application of the counterbalancing force of the weight needs to have a y coordinate equivalent to the one of the CoG. It is the only important data of the Lifting Force point of application date which is to be found. The method used to find this data is a barycentre method but it is slightly changed.

$$\frac{F_{\nabla}}{F_{\nabla} + F} \text{CoB}.y + \frac{F}{F_{\nabla} + F} F.y = P.y \quad (3-16)$$

Where

F_{∇} : intensity of the displacement (N)

F : intensity of the lifting force (N)

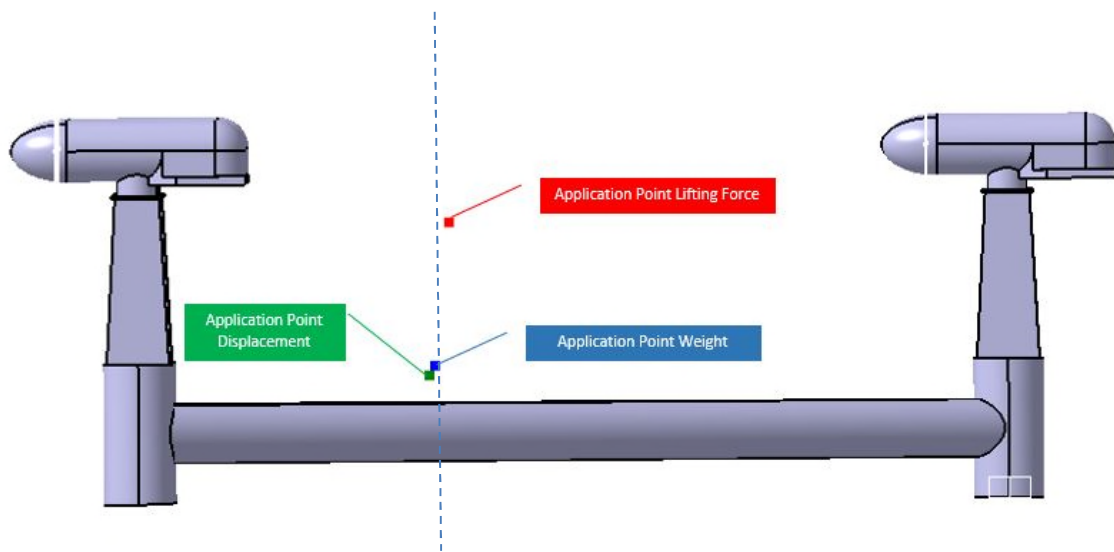


Figure 3-16 Points of Application of the different forces

In this equation, the needed value is $F.y$. By modifying the equation above, the y coordinate found is 20,039.00 mm ahead of the origin. The z coordinate is not important for the balance of the device. The following figure displays the three points of application of the three forces. The z coordinate of the lifting force has been arbitrary put at 10,000.00mm above the bottom of the structure.

3.3 Application to the demonstrator

Considering the lack of information on the geometry of the demonstrator when the preliminary assessment has been done, this part has not been completed right after the end of the previous study. Indeed, the structure designed and presented in this extension is the one which will be fully presented in the fifth part of the thesis. The weight of the structure is 131,000.00 kg. The figures below show the structure, its origin and the principal geometrical data.

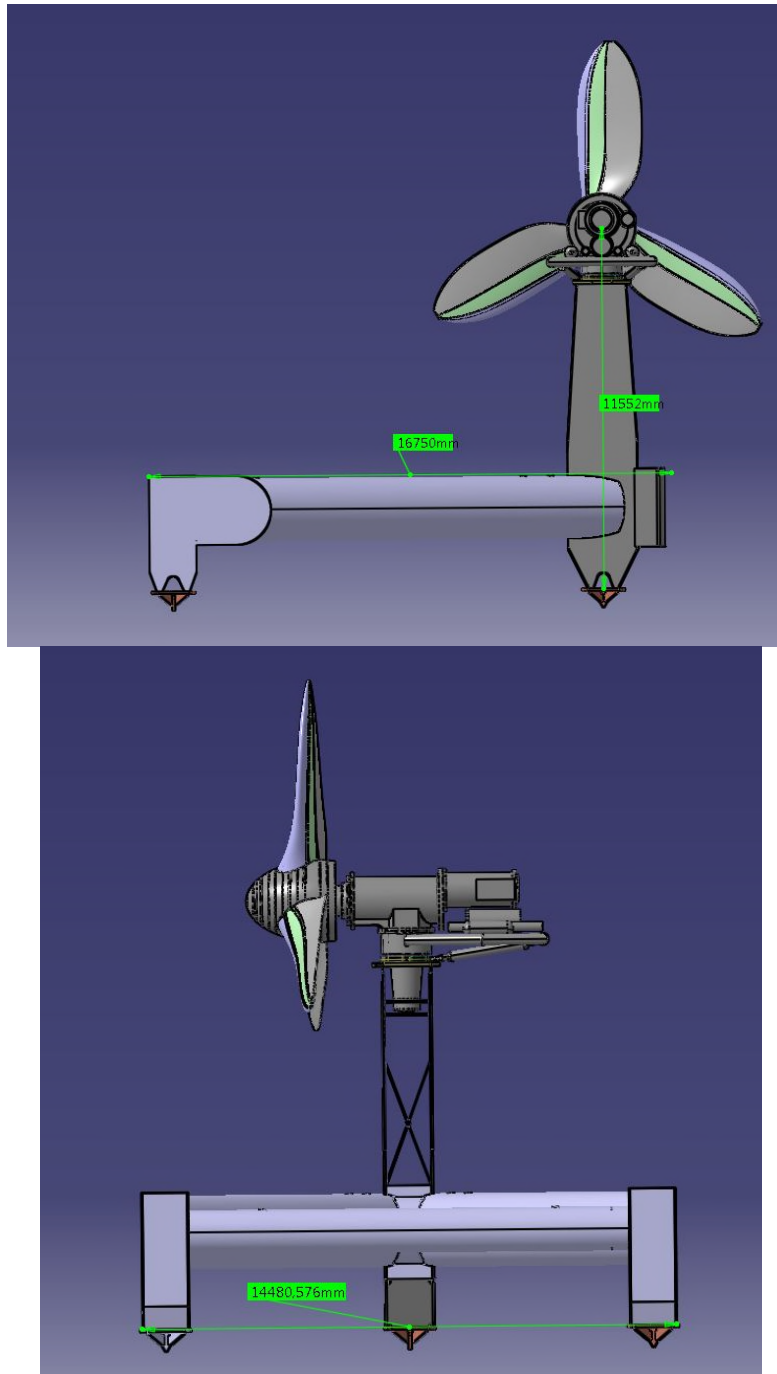


Figure 3-17 Principal Dimensions of the demonstrator

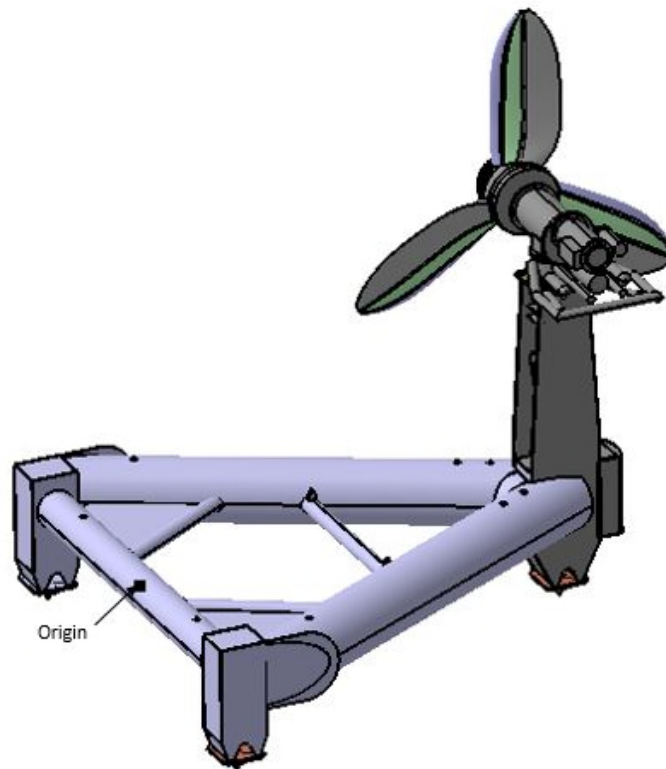


Figure 3-18 Origin of the demonstrator

The main difference remains in the use of only one turbine and the reducing of the size as a result. A loss of stability can be deduced from the use of only one turbine. Indeed this turbine is bringing the CoG close to the principal tower. It induces an important loss of the balance of the device. The turbine is forcing the device to a capsizing movement with a trim angle because the rear part of the device has an important floatability due to its geometry and the two plates installed in the corner when around 30% of the mass is represented only by the turbine. This behaviour has an impact on the way the ballasts will be filled. Indeed, the trim angle experienced by the structure will prevent the multiple ballasts to be filled at the same time, increasing the trim angle and then creating a loss of balance during the splash zone phase.

Concerning the submerged stability, as the geometry has not been significantly modified following the z direction; it can be assumed that the CoB is once more above the CoG, which is inducing a negative stability of the system. In the same way as for Deltastream 1, the lift point has to be located in such a way that it will balance the structure during the descent toward the seabed.

4 Ballast Flooding Assessment on the Demonstrator

4.1 Principle of the Ballast

The principle of using ballasts to submerge a structure is to add water inside the structure without changing the geometry. By adding water, mass is added to the structure and as the geometry is not modified, the displacement is not changed and the structure starts to be submerged. The added mass is depending on the mass of water. Ballasts are considered as constraining structures which constrains the flows inside it. Thus, the Bernoulli equation and the Continuity equation can be used. The flow is considered incompressible so the Bernoulli equation (shown in the part 2.3.1 of the thesis) for incompressible flow along a streamline can be used. Figure 4-1 displays the streamline used:

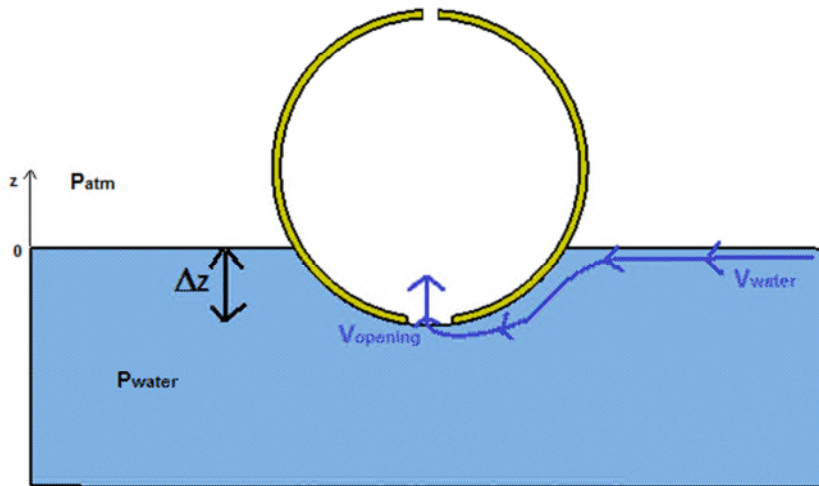


Figure 4-1 Streamline

The scenario with no current is considered, so $v_{water} = 0$. Hence the following equation for $v_{opening}$:

$$\frac{v_{opening}^2}{2g} = 2\Delta z \quad (4-1)$$

Where:

Δz : difference of depth (m)

With the velocity of the water going in the tube, the mass flow rate is determined giving the continuity equation:

$$\dot{m} = \rho_{water} * v_{opening} * A \quad (4-2)$$

Where:

A: area of the opening hole of the ballast (m²)

The added mass is calculated by multiplying the mass flow rate by a time interval. The problem here is that the velocity of the water depends on the depth of the structure and the depth of the structure is evolving because of the actual motion of the structure toward the seabed due to the added mass. A simple way to tackle this issue is to make an iterative calculation with a time interval as small as possible. This method was implemented with Matlab.

4.2 Simulation of the time of descent

4.2.1 Code Architecture

In order to create the architecture of the code, calculations are done first with simple geometry as a hollow cube or hollow cylinders. The structure is considered to descent horizontally to the seabed. The frame of the code is then determined in order to be used for Deltastream. This paragraph resumes the main parts included in the general frame of the code.

- Common architecture

The parameters common to every calculation undertaken with Matlab are the Counter Numbers, the Physical Constants of the problem (density, gravitational acceleration...) and the Physical Parameters needed for the calculation (Pressure, mass flow rate, weight...).

The counter numbers are here to define the number of iteration (n in the code), the maximum draft of the operation (m in the code) and the step of the calculation in the simulation (p in the code). The latter allows the definition of a larger step than 1 for the calculation. It is useful if less data are needed.

The Physical Parameters initialised for the calculation are the following:

- **M**: Mass of the structure in kg.
- **W**: Weight of the structure in N.
- **B**: Buoyancy of the structure in m³.
- **D**: Draft of the structure in m.
- **Delta_P**: Pressure difference between the waterline and the depth of the opening holes in Pa.
- **U_Tube**: Rate of the flows in the opening hole in m/s.
- **MFR**: Mass flow rate in the opening hole in kg/s.
- **AM**: Added mass in the ballast in kg.

Those eight values are calculated successively once; an added mass is found at last. Once this added mass is found, it is added to the mass of the structure and the calculation is done once again. A loop “for” is used with Matlab in order to process this calculation.

- Calculation architecture

For all the code, the step of calculation for the time is 0.1 second.

```

% Creation of the vector column T

T(1) = 0.1;
for j=2:1:n
    T(j) = T(j-1) + 0.1;
end

```

Figure 4-2 Numerical Predictions

A vector column indexing the time is created in order to have all the different values of the time accessible quickly and browse all data easily.

To begin with the iterative calculation, a vector column for each parameter is created and initialised. Then the loop “for” is created to calculate each value of the vectors successively. The following figure is displaying the loop created with Matlab. This loop is creating eight vectors column (one for each parameter). The size of those vectors is the number of iteration *n*.

```

for k=2:1:n
    Ma(k) = Ma(k-1) + AM(k-1);
    We(k) = Ma(k)*g;
    Bu(k) = We(k) / (Rho_W*g);
    Dr(k) = Bu(k) / (a^2);
    Delta_Pr(k) = -Rho_W*g*Dr(k);
    U_Tu(k) = sqrt(U_W^2 + 2*g*Dr(k) - 2*Delta_Pr(k)/Rho_W);
    MFR(k) = Rho_W*A*U_Tu(k);
    AM(k) = MFR(k)*(T(k) - T(k-1));
end

```

Figure 4-3 Loop For – Cube calculation

A vector is listing every values of one parameter according to the time. The function processing the iterative calculation is defined as a matrix made up of nine columns organised as below:

$$(T \quad Ma \quad We \quad Bu \quad Dr \quad Delta_Pr \quad U_Tu \quad MFR \quad AM)$$

Figure 4-4 Matrix Result

With this matrix, the results are accessible easily and some curves can be plot. The following figure displayed four curves plotted with Matlab such as: Draft over Time, Mass over Time, Opening Velocity over Draft and Buoyancy over Time.

4.2.2 Deltastream 1 Calculation

The structure geometry used for the simplified geometry final calculation is an equilateral triangle made of cylinders:

- Three identical horizontal cylinders to represent the edges of the triangle.
- Three identical vertical cylinders to represent the summits of the triangle.
- One smaller vertical cylinder to represent the tower holding the turbine.

It is a structure slightly different compare to Deltastream 1, the cones are replaced by a cylinder of the size of the top cylinders. There are three opening holes on this structure, one on each side of the structure. Those entrances are circular with a radius of 0.05m.

The code explained in the previous part is applied with this geometry. Once the structure is fully submerged and no more mass is added, the calculation is stopped. Therefore, to calculate the depth of the structure over time, the following differential equation has to be solved:

$$M * \frac{dz^2}{d^2t} = P + F_{\nabla} \quad (4-3)$$

Where:

M: total mass of the structure (kg)

With this formula, the z coordinate of the CoG of Deltastream over the time can be assessed when the ballasts are full and Deltastream fully submerged. The first values of the CoG.z are calculated using the code previously presented and adding the known height between the calculated z coordinate of the draft and the CoG.z.

This equation is a second order and linear differential equation in z with P and F_{∇} constant and must be applied for the CoG of the structure.

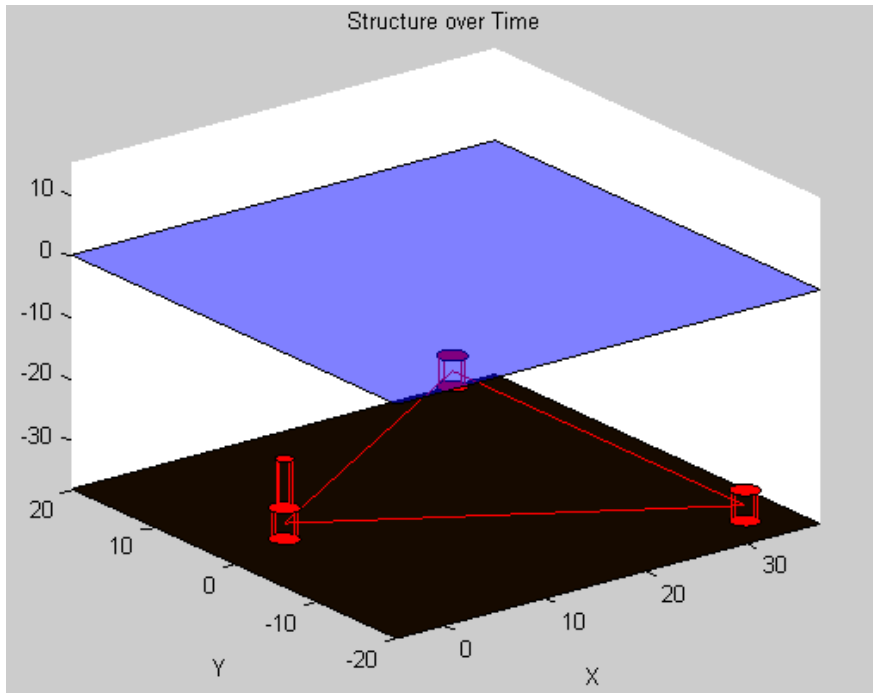


Figure 4-5 Deltastream landed on the Seabed

Finally, the time it takes for the structure to reach the seabed is found. In that case, the seabed is at a depth of 38m. And according to the code, the structure reaches it after 670.2 seconds, so 11 minutes and 10.2 seconds.

With the code, one curve is plotted, the curve giving the z coordinate of the CoG over the time. It gives a shape for the descent of the structure. It is plotted using a vector time and the vector CoG.z calculated the iterative calculation and the equation (4-3).

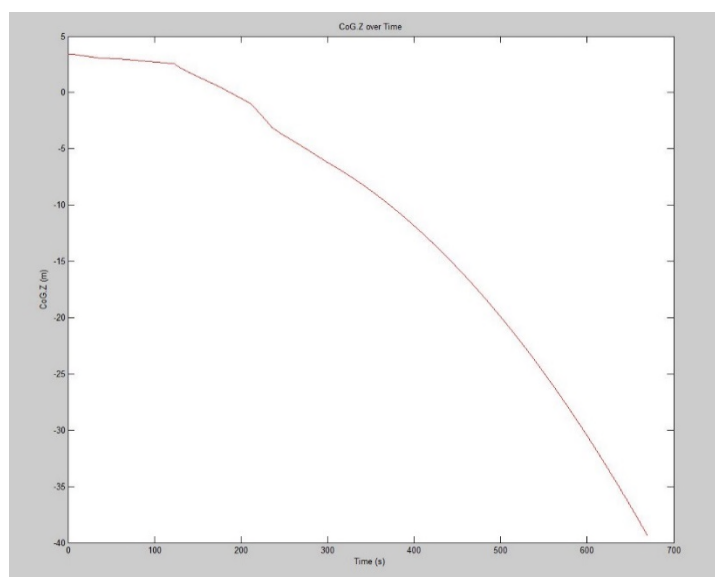


Figure 4-6 CoG.Z over time

Following the same methodology with a structure close to the demonstrator, a Matlab calculation has been undertaken. However, one of the main hypotheses used for this calculation is that the structure remains horizontal during the whole flooding process. In the case of the demonstrator, it has been assessed that the structure will experience an important trim angle due to the important percentage of mass located at the front of the device. The main hypothesis used for the calculation cannot be applied here with this unbalanced device. Nevertheless, the method has been applied and the results are not applicable to the demonstrator.

Considering these issues on the device, it is difficult to assess theoretically the duration of flooding and a mean mass flow rate for the ballasts flooding which needs to be scaled for the reduced scale model.

5 Design of the Model and Test Preparation

5.1 CAD Model

In order to design a scaled model of Deltastream, a full scaled model must be drawn on Catia first. Thus the proper dimension of the structure will be accessible such as the coordinates of the CoG and the Inertia. In this part, the process of the design of the prototype is described. Then the chosen scale for the model is explained. The last part is the design of the prototype.

5.1.1 Full Scaled Design

5.1.1.1 Structure Geometry

The prototype is designed according to the documents given by TEL on the deployment and particularly the document [5] by KML. The turbine tower geometry from the former structure of Deltastream (Deltastream 2) is also used.

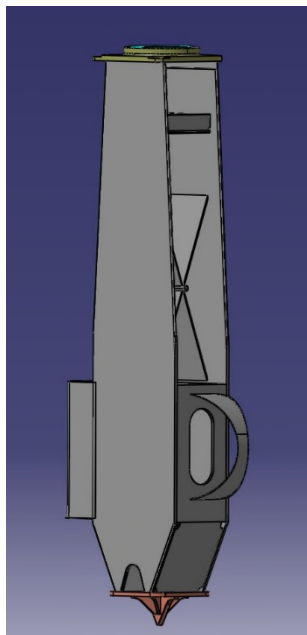


Figure 5-1 Turbine Tower of Deltastream 2

In the KML document [5], some drawings of the deployment with the barge are available. Considering those drawings and the measurements given, a dimension for the prototype is approximated. Those principal dimensions are given in the following table.

Length (mm)	16,750.00
Width (mm)	14,600.00
Height (mm) (centre turbine)	11,627.00
Diameter Side Tube (mm)	2,000.00
Diameter Rear Tube (mm)	1,200.00

Table 5-1 Prototype Data

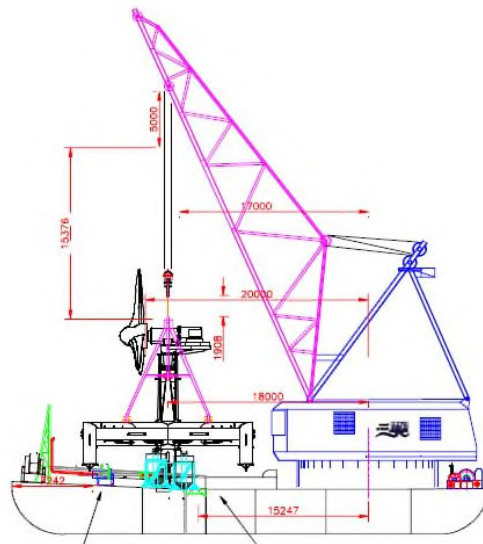


Figure 5-2 KML Document Picture Deployment 1

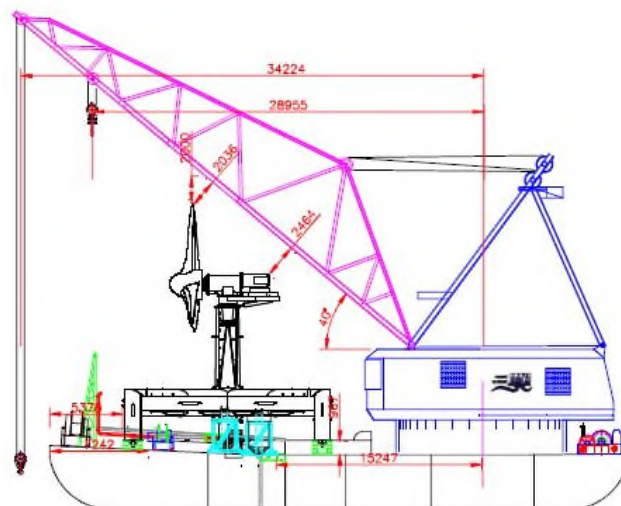


Figure 5-3 KML Document Picture Deployment 2

5.1.1.2 Nacelle Geometry

The turbine used for the design is the one given by TEL. The dimensions of the turbine are the following:

Mass Nacelle (kg)	40,000.00
Mass in the Water Nacelle (kg)	25,000.00
Length Nacelle (mm)	7,977.00
Diameter Nacelle (mm)	2,132.00
Diameter Turbine (mm)	12,000.00

Table 5-2 Nacelle Data

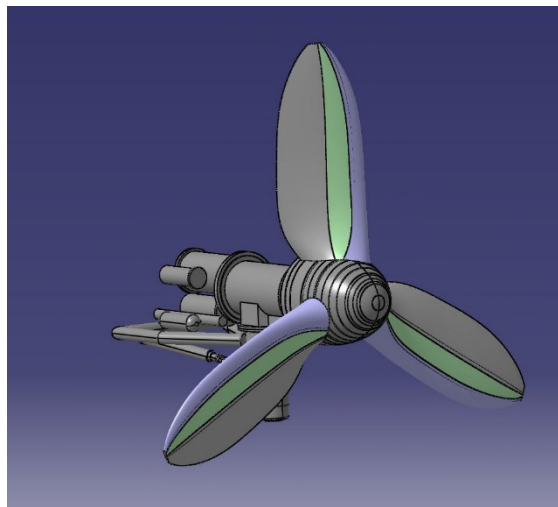


Figure 5-4 CAD of the Nacelle

The turbine is set on the principal tower of the structure and can rotate around its axis of fixation. The parked position is when the turbine has an angle of 90 degrees with the axis of symmetry of the structure. The working position is the one with the turbine in the same axis, with the blades outside the triangle.

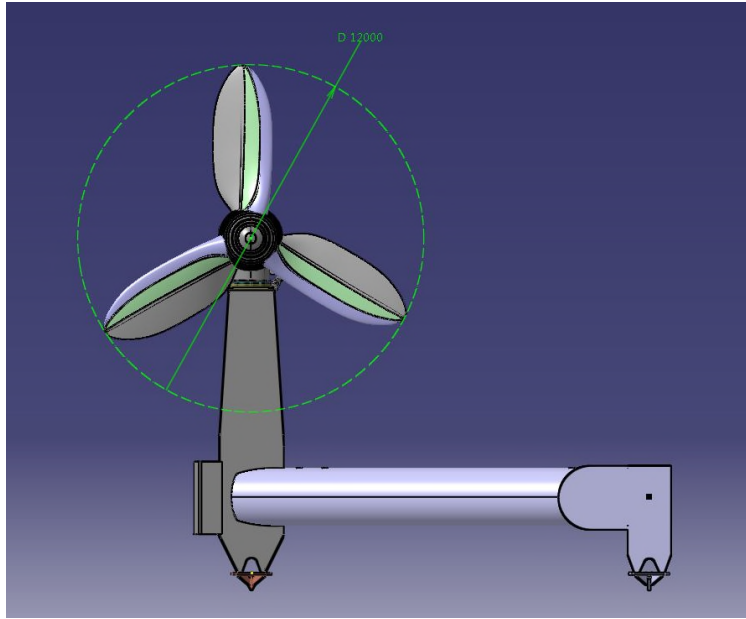


Figure 5-5 Turbine Diameter

5.1.1.3 Ballast Information

The ballasts are located in the tubes forming the triangular shaped frame of Demonstrator. They are using all the volume available in those tubes.

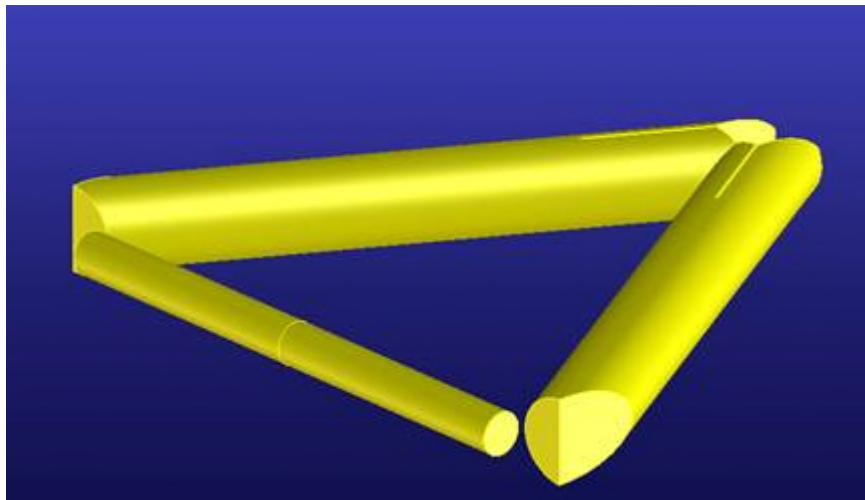


Figure 5-6 Triangular Shaped Frame - Ballast Location

The three tubes are filled by water through multiple openings. Two entrances are located at the bottom of the back summits and the others are near the turbine tower. The two openings at the back are going through the summit with pipes and are divided in two, one in each tube connected to the back summit. As the result, each of the three tubes has two openings for the ballast. The vents of the turbine are at the top of each tube. Three installed on each side tube and two on the back tube.

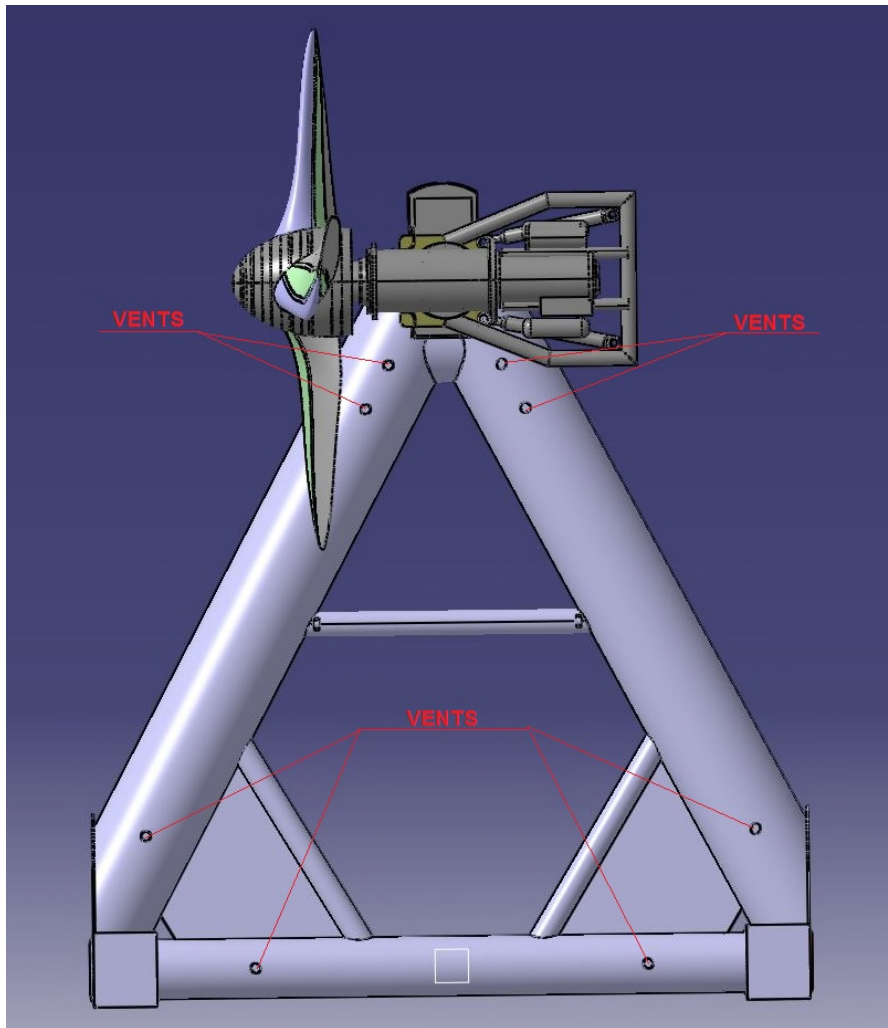


Figure 5-7 Vents Location

The data of the three ballasts for the full scale Model are the following:

Ballast Volume (m³)	95.63
Opening Side Tube Diameter (mm)	600.00
Vents Side and Rear Tube (mm)	200.00

Table 5-3 Ballast information

5.1.1.4 Lift Frame information

The lift frame is made of stainless steel and built with three main pieces. Those three pieces are forming a triangular shape which is linked to the device via the base of the turbine tower and the two side tubes. It is linked to the structure through a pivot link which allows the frame to be raised or lowered depending on the operation. The total weight of the frame is 7.35 tonnes and it has been designed for a lifting capacity of 160.00 tonnes.

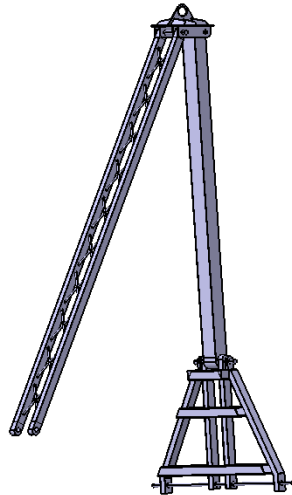


Figure 5-8 Isometric view of the Lift Frame – Full scale

5.1.1.5 Physical Data

The mass of the structure is given by the maximum weight for which the lift frame was designed. According to the KML document [2], the lift frame was design for a weight of 131.00 tonnes.

- Inertia Tensor ($\text{kg}\cdot\text{mm}^2$):

The inertia tensor is given by TEL; the axes used are displayed in the following figure.

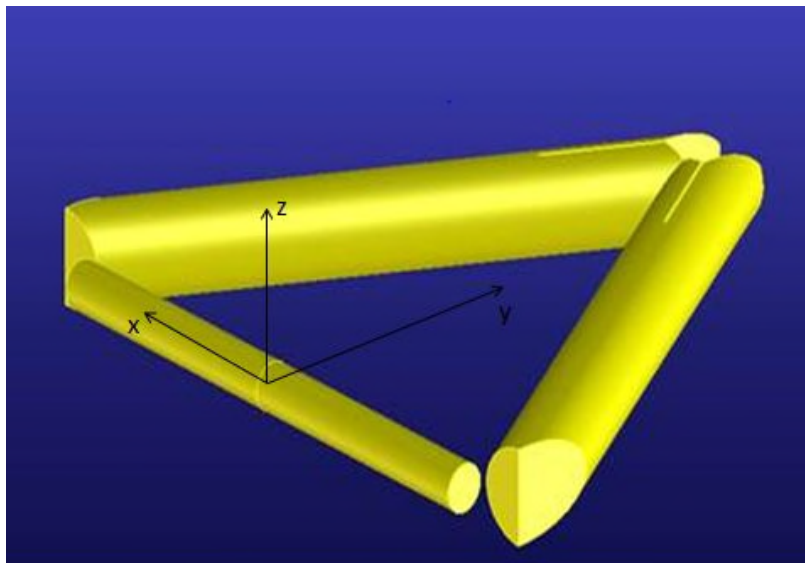


Figure 5-9 Origin and axes for the Inertia Tensor

The following matrix is giving all the results:

$$\begin{pmatrix} 4.48 \times 10^{12} & 0 & 0 \\ 0 & 1.01 \times 10^{13} & 2.19 \times 10^{-4} \\ 0 & 2.19 \times 10^{-4} & 1.24 \times 10^{13} \end{pmatrix} \quad (5-1)$$

- Centre of Gravity:

The coordinates are found using the CAD software.

Centre of Gravity X coordinate (mm)	-2.88
Centre of Gravity Y coordinate without ballast (mm)	9,103.05
Centre of Gravity Y coordinate with ballast (mm)	7,338
Centre of Gravity Z coordinate without ballast (mm)	2,587.37

Table 5-4 CoG Coordinates

The origin taken for these coordinates is the same used for the inertia tensor.

5.1.1.6 General Overview of the Full Scale Model

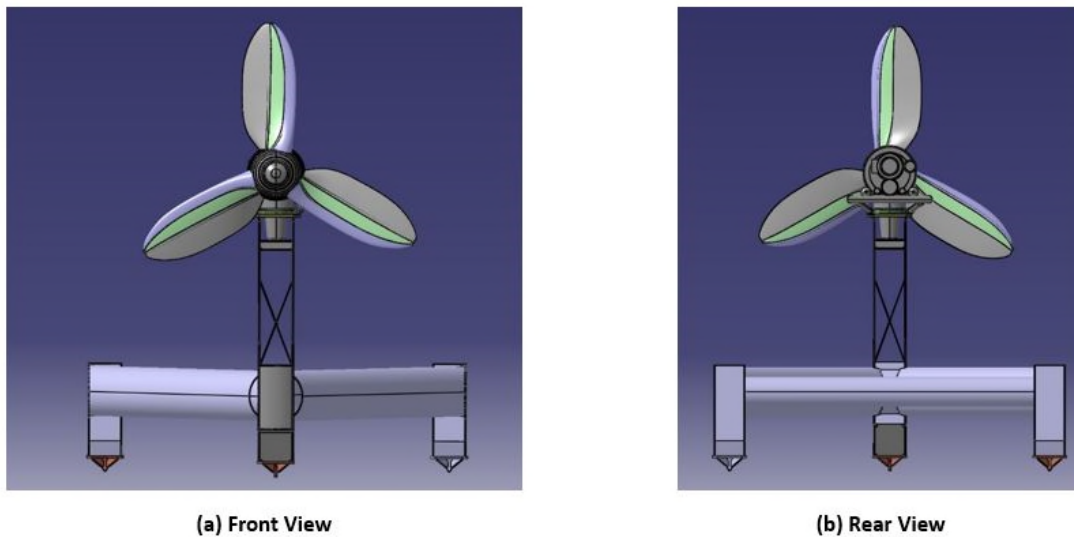


Figure 5-10 Front (a) and rear (b) view

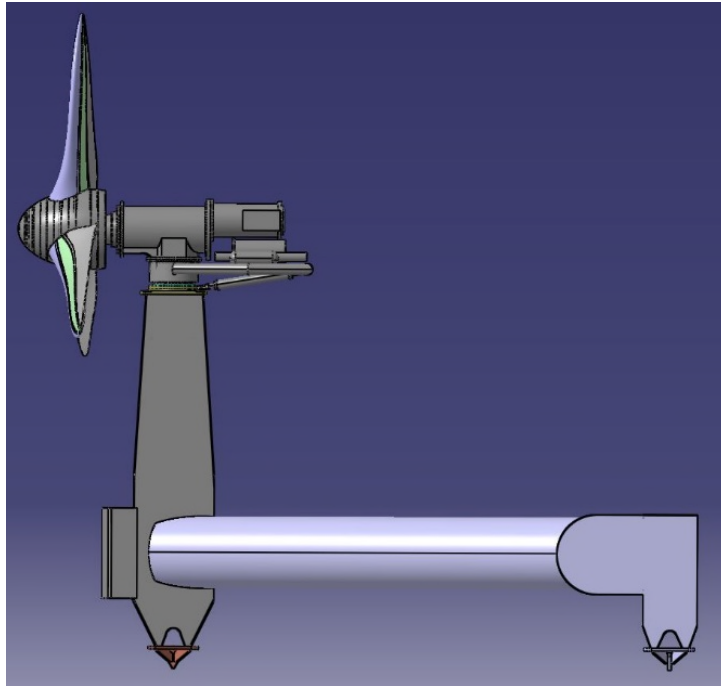


Figure 5-11 Side View

In those pictures, the turbine is set in its working position. The parked position is shown in the next picture.

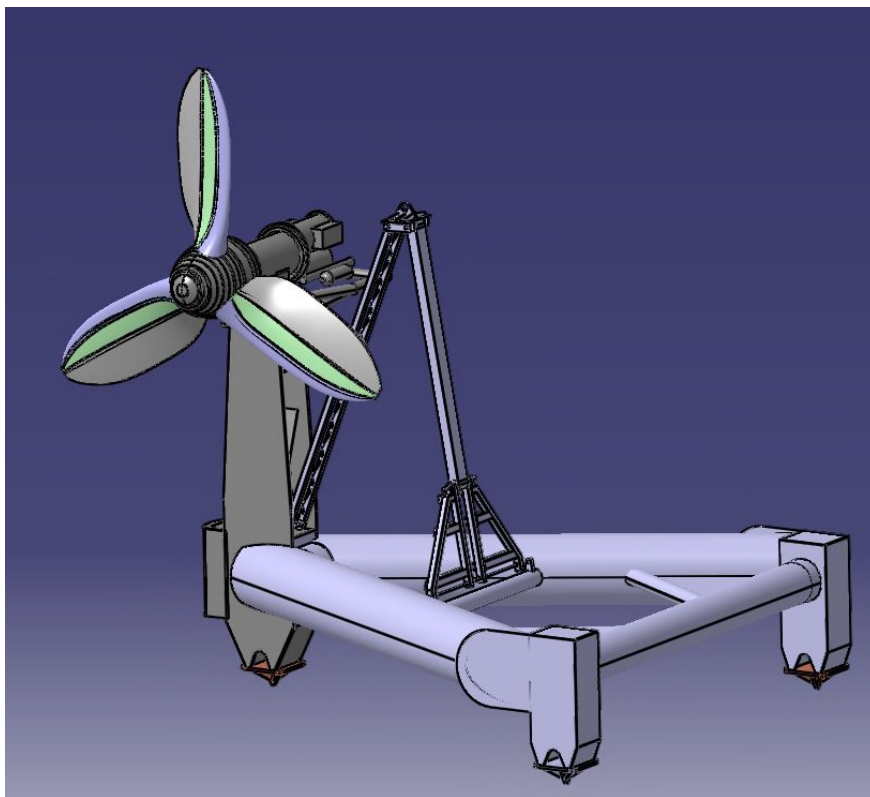


Figure 5-12 Demonstrator with Lift Frame

For the deployment, the position of the turbine is set with an angle of 90 degrees in order to set up the lift frame properly. Indeed, the lift frame cannot fit with a turbine installed in its working position.

5.1.2 Scaled Model Design

5.1.2.1 Scale Factor

The test model is a twentieth scaled model of the previously drawn on the CAD software. To achieve this scale process, the Froude's Similarity is used:

Length	Time	Velocity	Acceleration	Mass	Pressure	Force	Momentum
e	\sqrt{e}	\sqrt{e}	1	μe^3	μe	μe^3	μe^4
e the length scale factor (here 20)							
μ the ratio between the density of the tank water and the real water							

Table 5-5 Scale Factor with the Froude's Similarity

This Froude number is a ratio of inertia to gravitational forces. It is the one used for scaling when the inertial and gravitational forces are predominating and it is important for free surface flows.

For this design, the materials used to create each pieces of the model needs to be chosen considering their effects on the mass and the position of the CoG. Thus the structure is as close as possible to the full scaled model in terms of mass, mass repartition and geometry.

5.1.2.2 Structure Geometry and Materials

To obtain the general size of the model using the Table 5-5, the data of the full scaled model were simply divided by twenty.

Data	Wanted Value	CAD Value
Length (mm)	837.50	837.50
Width (mm)	730.00	730.00
Height (mm)	581.35	557.00

Table 5-6 Scaled Model Geometrical Data

Except for the height of the device, the values obtained with the CAD software are corresponding to the reality. The relative error for the height is 4.19% which is a small error, so with an impact which can be neglected. This difference can be explained by the different turbine used and by the simplification brought to the model for an easier manufacturing.

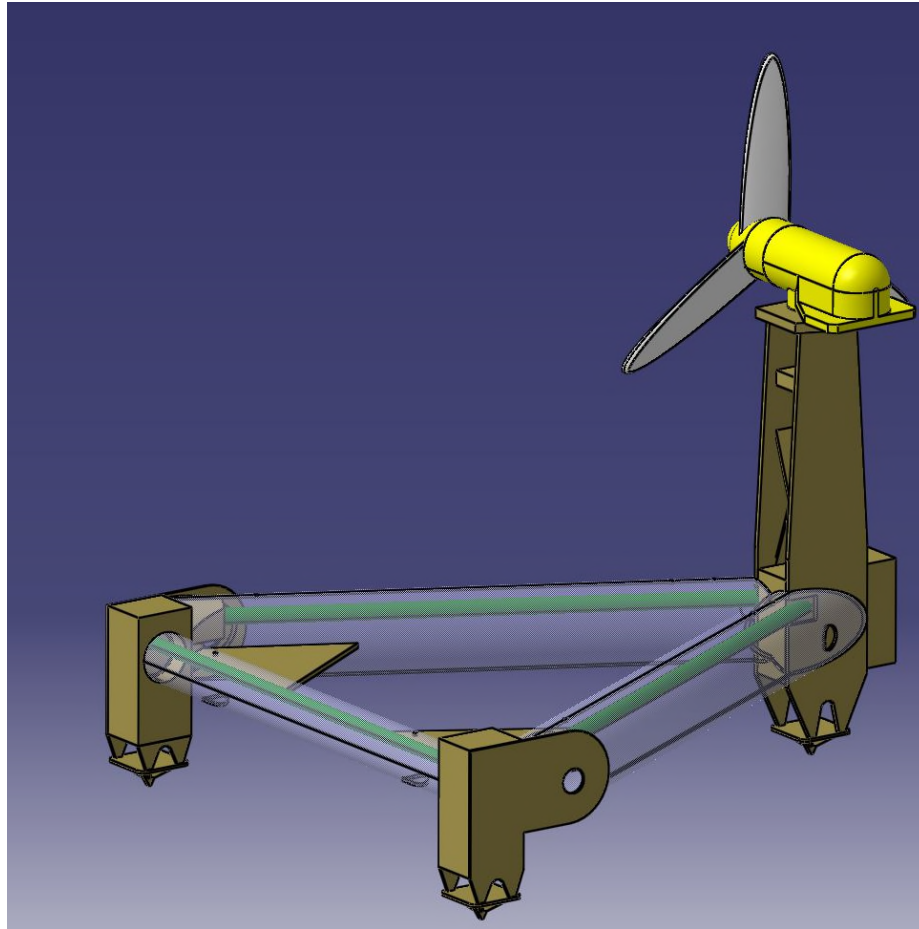


Figure 5-13 Scaled Model View



	Threaded Rod (made of stainless steel)
	Plywood and Planed Pinewood

Table 5-7 Colour Legend of the Scaled Model

The threaded rods used in the design and displayed in green in Figure 5-13 are here to add mass to the structure without changing the geometry. The two rods in the larger tubes are M20 threaded rods; the one in the smaller tube is a M16 threaded rod. The plywood used is 6, 12 and 18 mm thick. Some parts of the summits are carved directly from wooden beams.

5.1.2.3 Ballast Information

In the model, the ballasts are located in the three transparent tubes made of perspex. For the two largest tubes, the dimensions are 100.00 mm diameter and the thickness 3.00 mm; for the smallest one, the diameter is 60.00 mm and the thickness 3.00 mm as well. The vents of the ballasts are scaled and located in the same area as they are on the demonstrator. Concerning the openings

location, it has been modified on the scaled model. The main reason is because the location has been given by TEL shortly after the model was finished and it was impossible to modify the model in order to fit the demonstrator. The following pictures are displaying the openings location:

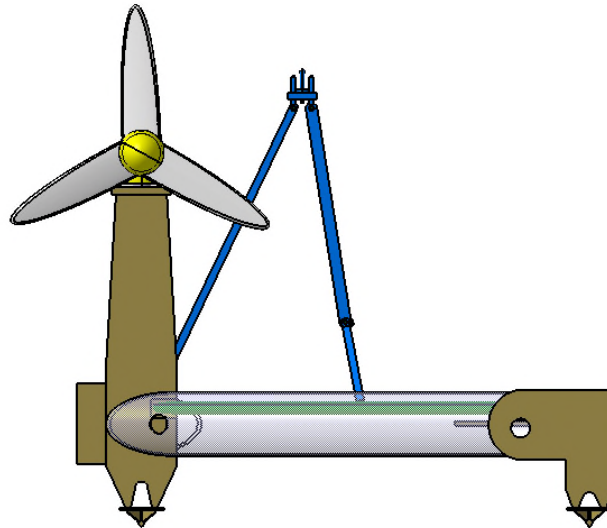


Figure 5-14 Side view - Openings Location

Those two inlets are also present on the other side of the model. Concerning the openings in the rear tube, they are displayed in the figure below:

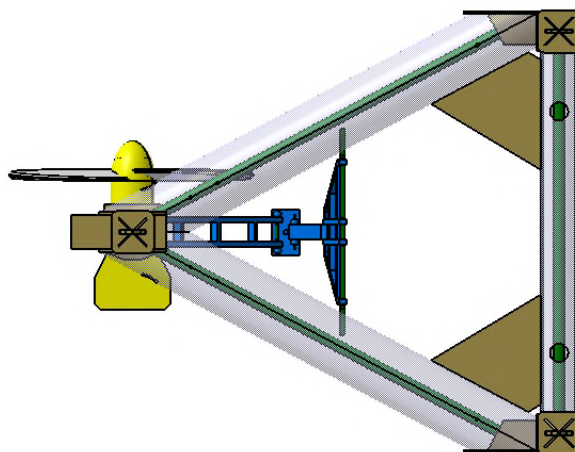


Figure 5-15 Bottom View - Openings location

Respecting the Froude Similarity and the size of the inlets given by TEL, the reduced scaled size of the inlets is 30.00mm diameter. However, it has been assessed in the literature review that this scaling does not allow a fine scaling of

the rate of flooding considering the impact of the atmospheric pressure. A method was found to tackle this issue: scale the volume flow rate of the water entering the ballast. However, it has been assessed that the method permitting the theoretical study of the flooding of Deltastream 1 could not be transposed on the demonstrator, thus the volume flow rate of the flooding cannot be calculated accurately. In that case, it has been chosen to scale the model with respect to the data given by TEL. It is during the transposition to the full scale model that the volume flow rate scaling will be used. Thus, the inlets have a diameter of 25mm and the outlets 10mm. The aim of 30mm for the inlets cannot be reached with the tools available in the laboratory and a drill bit of 30mm is very expensive.

The ballasts volume calculated by the CAD software is described in the following table:

	Desired Volume (m ³)	CAD Volume (m ³)	Relative Error (%)
Ballasts Volume	11.95x10 ⁻³	10.89x10 ⁻³	9.02

Table 5-8 Ballasts volume of the scale model

This difference is explained by the use of threaded rod and wooden part which are placed inside the ballasts to ensure the strength and manufacturing of the structure. Those pieces of material are taking space normally used by water. The space available is also smaller due to the thickness of the tube more important than in reality.

5.1.2.4 Lift Frame design

The lift frame is composed of four different parts made of plywood. The objective is to keep the same degree of freedom of the full scale product while simplifying it for an easier manufacturing. To create the pivot links, eye bolts and threaded rod have been used. The lift head is built with a plate of plywood, four eye bolts and a lift ring strong enough to support the tension during the operations.

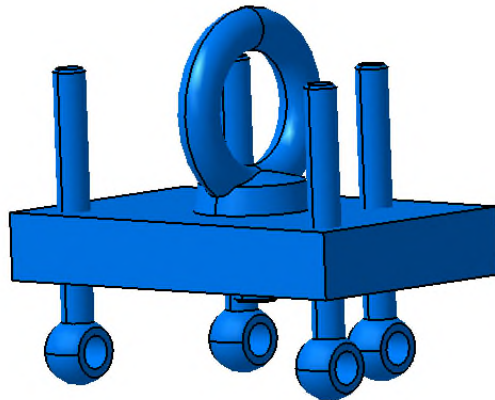


Figure 5-16 Isometric view of the Lift Head - Model Size

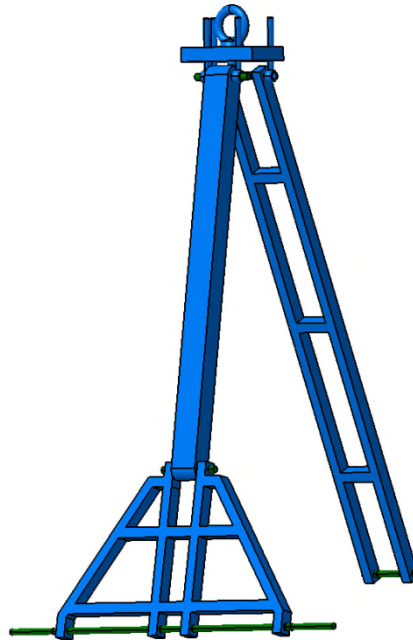


Figure 5-17 Isometric view of the Lift Frame – Model size

5.1.2.5 Physical Data

The first physical data scaled was the mass of the device. Considering the real mass of the device 131,000 kg, the objective is a mass of 15.98 kg for the model scale using the Froude Similarity. According to the CAD software, the mass of the model drawn is 15.50 kg, namely an error of 2.98%. However, the drawing is made with a hub and a turbine different from the one finally used during the tests. The mass will have to be assessed again with the manufactured demonstrator.

- Centre of Gravity:

Using the scale factor and the data summarized in Table 5-4, the coordinates of the centre of gravity wanted are found. The CAD software is giving the coordinates of the designed model.

	Aimed value (mm)	CAD value (mm)	Relative Error (%)
CoG x coordinate	-0.14	-0.03	76.39
CoG y coordinate without ballast	455.15	459.30	0.91
CoG y coordinate with ballast	366.90	401.99	9.56
CoG z coordinate without ballast	129.37	165.73	28.11

Table 5-9 Desired and CAD coordinates of the CoG for the scaled model

Concerning the important error for the x coordinate, it can be neglected considering the small difference between the two values (0.11mm). The difference between the y coordinate with and without ballasts can be explained by the smaller volume of ballasts available in the CAD model than expected from the scaled factor.

- Inertia Tensor (kg.mm²):

The objective given by the scaling factor for the inertia tensor is the following:

$$\begin{pmatrix} 1.37 \times 10^6 & 0 & 0 \\ 0 & 3.06 \times 10^6 & 6.67 \times 10^{-11} \\ 0 & 6.67 \times 10^{-11} & 3.77 \times 10^6 \end{pmatrix} \quad (5-2)$$

I_{yz} and I_{zy} are neglected because they are very close to zero.

According to the CAD software, the inertia tensor of the device is

$$\begin{pmatrix} 1.58 \times 10^6 & 0 & 0 \\ 0 & 2.55 \times 10^6 & 0 \\ 0 & 0 & 2.63 \times 10^6 \end{pmatrix} \quad (5-3)$$

Those values have the same order of magnitude (10^6 kg.mm²). However, the difference between them is still important. It can be explained by the use of a different turbine in the CAD design, so the impact of the mass of the turbine is less important than it should be (smaller I_{zz} and I_{yy}).

5.1.2.6 General Overview

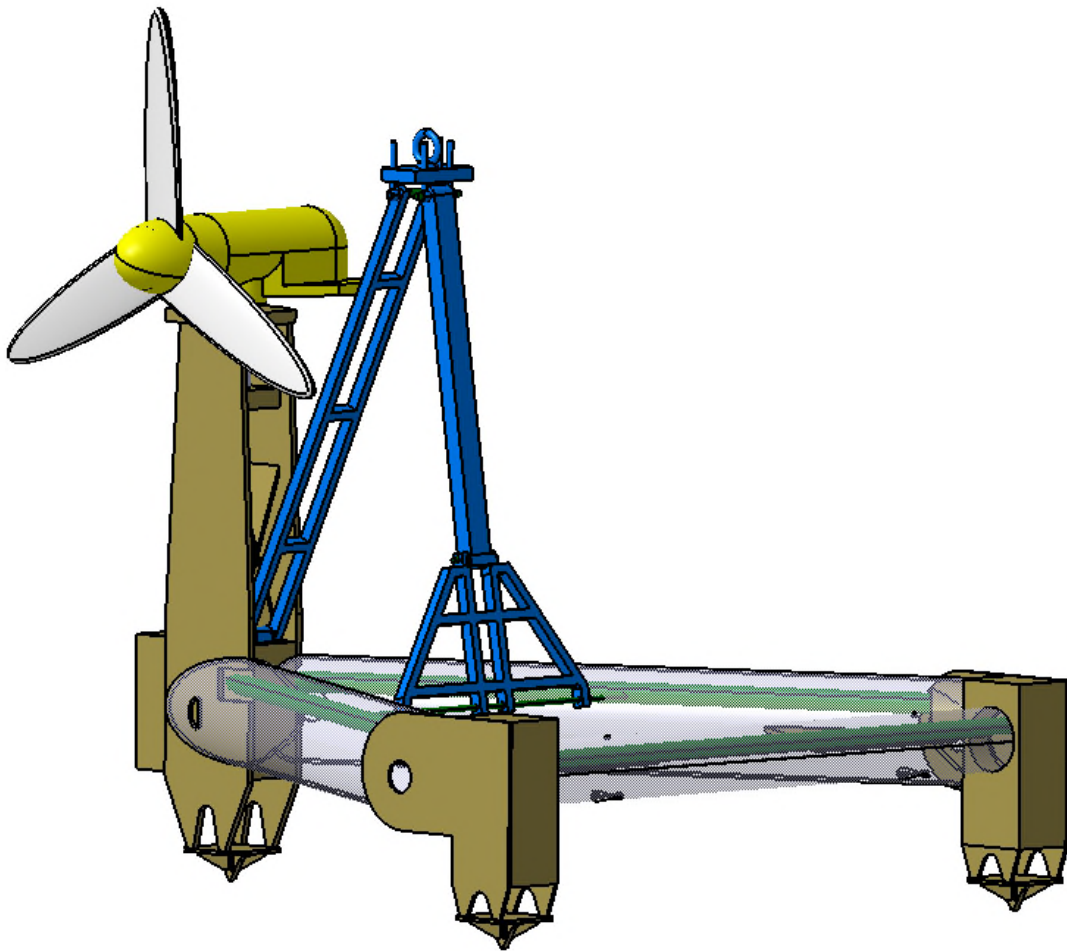


Figure 5-18 Isometric view of the scaled model

This figure is an isometric view of the complete design of the model. Plans have been made out of this design in order to build it in the workshop of the laboratory.

5.2 Model Manufacturing

5.2.1 Manufacturing

The manufacturing was undertaken in the workshop of the Ocean Laboratory in Cranfield.



Figure 5-19 Deltastream Model before assembly and painting

Each tower was built separately, and paint before being assembled. The rear of the demonstrator was first assembled with the threaded rod and the perspex tube linking the two towers.

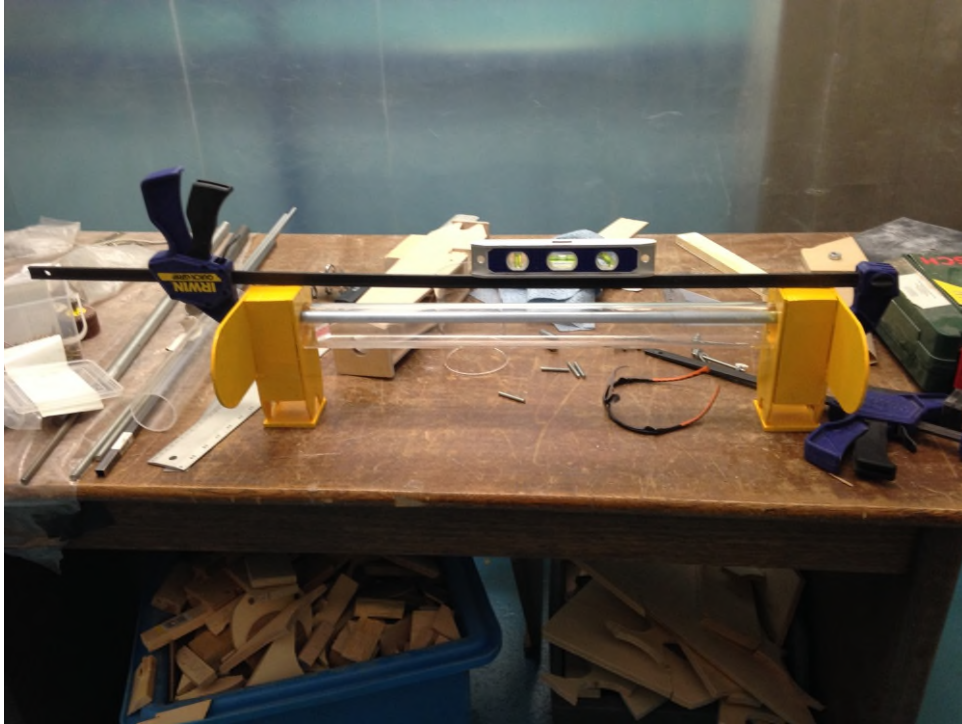


Figure 5-20 Rear of the demonstrator assembly

Once this part was painted and glued, the principal tower can be assembled with the threaded rod, the two tubes and the tower supporting the turbine.



Figure 5-21 Tower Turbine & Tubes

Two plates were built and glued to the tubes (Figure 5-22) to support the two threaded rods in the two side tubes. These two pieces allowed the structure to be divided in two independent parts, which are assembled to create the entire structure of the model.

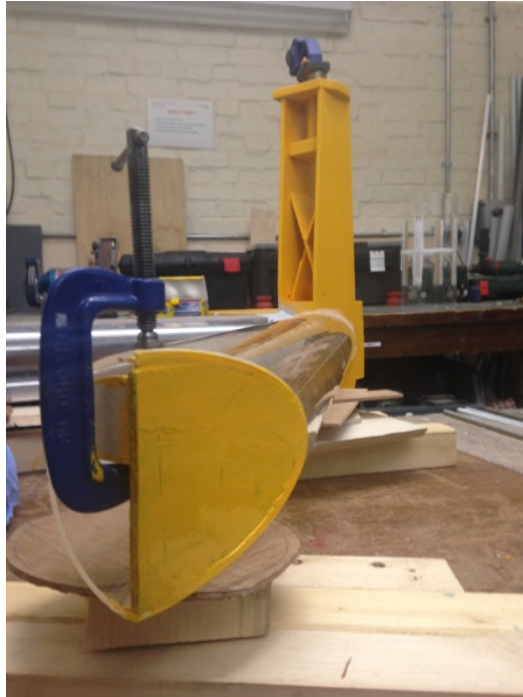


Figure 5-22 Assembly of the principal tower

The next step was to link the two parts in order to have the complete structure assembled (Figure 5-24). Once this was done, the lift frame was installed on the two side tubes using foam to protect those tubes against the pressure of the hose clamps which are linked to the threaded rod used to link the lift frame to the device (Figure 5-23). The pieces used for the lift frame were strengthened using a stratification process with composite (epoxy).



Figure 5-23 Lift Frame linked to the demonstrator

The turbine used is slightly bigger and has been weighted to correspond in mass in water to the data given by TEL.



Figure 5-24 Final Assembled Model

Mass has been added to the device in order to reach the objective of mass fixed by the scale factor. Those added masses are placed on a plate located in the corner on the rear of the demonstrator and at the bottom of the turbine tower. The total mass of added masses is 2,366g.

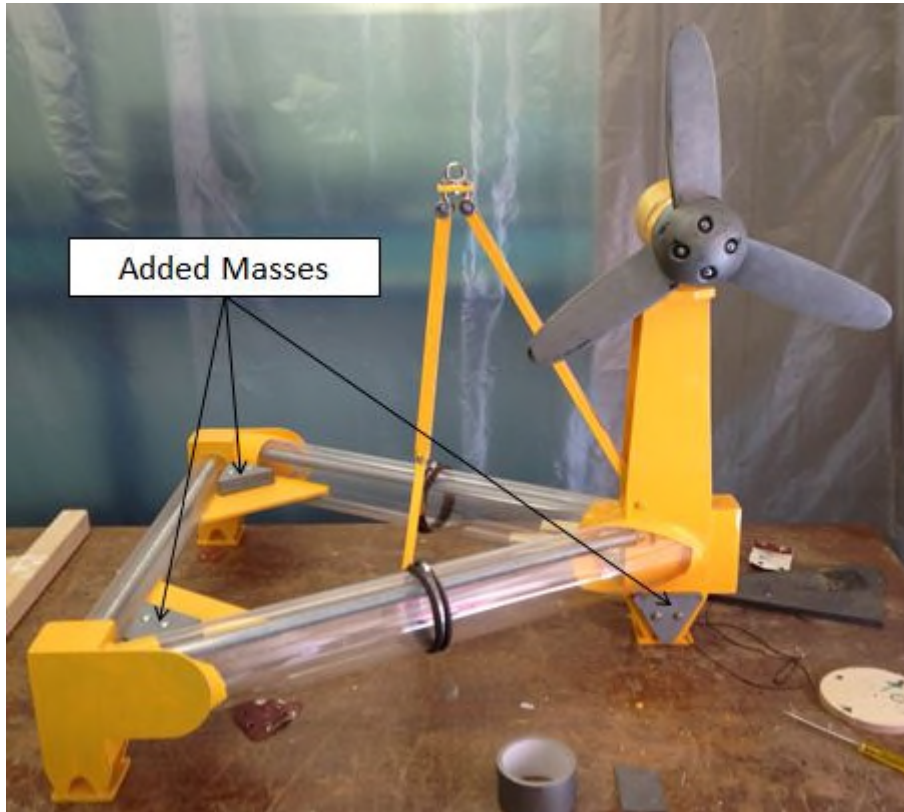


Figure 5-25 Added Masses location

Another mass has been added but it is not visible on this schema. It is located at the same place that the one visible on the turbine tower but on the other side to preserve the symmetry of the device.

5.2.2 Physical Data

The general dimensions of the model are given in the following table.

Data	Wanted Value	Manufactured Value
Length (mm)	837.50	841.00
Width (mm)	730.00	737.00
Height (mm)	581.35	585.00

Table 5-10 General Dimensions of the manufactured model

The values are close in the three principal dimensions. The differences are explained by defaults which occurred during the manufacturing and modifications due to an impossibility to realise the exact CAD model with the tools and materials available in the workshop.

To determinate the CoG coordinates of the demonstrator, a balance is used. The balance is placed below the turbine tower and supports are placed below the two other towers with the same height of the balance to let the xy plan horizontal during the measurement. Noting this value and using the following formula, the y coordinate of the CoG is found.

$$y_G = L - l * (1 - \frac{m_1}{M}) \quad (5-4)$$

In which:

L: length between the centre of the tower turbine and the chosen origin (mm)

l: length of the complete device (mm)

m₁: mass displayed on the balance (g)

M: total mass of the device (g)

Considering the z coordinates, it has been measured qualitatively by suspending the device by one point of lifting with a xz plan as horizontal as possible. Once an equilibrium position is found, the distance along the z axis between the point of lifting and the origin is taken, thus giving the z coordinate of the CoG.

As for the x coordinate, the approximate symmetry of the device allows to put it at zero. The following table is summarising the results with the relative error between them and the coordinates wanted.

	Measured value (mm)	Relative Error (%)
CoG x coordinate	0	
CoG y coordinate	-376.09	17.37
CoG z coordinate	139.1	7.52

Table 5-11 CoG coordinates of the manufactured model with relative error

The use of the new turbine allows a z coordinate closer to the one delivered by the CAD software. Moreover, the y coordinate has a relative error larger which can be explained by the new turbine as well.

To determinate the inertia tensor in the three principal directions, an experience has been made. This methodology is explained in [9]. With this method I_{xx} , I_{yy} and I_{zz} are calculated. The main part of this method is to determinate for each axes the natural period of oscillations of the device around these axes. In order to have a look to those oscillations, an ultrasonic sensor is used with the data acquisition software Labview. Plotting the curve of the oscillations, the period is assessed and the following formulas are used.

$$I_{xx} = \left(\frac{T_N}{2\pi}\right)^2 * M * g * z_G - M * z_G^2 \quad (5-5)$$

$$I_{yy} = \left(\frac{T_N}{2\pi}\right)^2 * M * g * z_G - M * z_G^2 \quad (5-6)$$

$$I_{zz} = \left(\frac{T_N}{2\pi}\right)^2 * M * g * x_G - M * x_G^2 \quad (5-7)$$

In which

T_N : period of the oscillations (sec)

M : mass of the device (kg)

g : gravitational acceleration (m/sec²)

The inertia tensor of the manufactured model is:

$$\begin{pmatrix} 2.64 \times 10^6 & 0 & 0 \\ 0 & 2.20 \times 10^6 & 0 \\ 0 & 0 & 3.79 \times 10^6 \end{pmatrix} \quad (5-8)$$

The repartition of mass of the manufactured model is good along the z-axis with a very small difference between the objective value and the one obtained. However, the values along the x and y axes y are still far from the objective values. This issue can be explained by a mass repartition different due to the use of different material and weight to reach the correct mass.

5.3 Test Rig Design

5.3.1 Functional Analysis

In order to test the model, a test rig has been designed. This test rig will allow the complete deployment and recovery operation of the demonstrator by modelling the action of the crane on the barge. To analyse the needs and identify the targets of the test rig, a functional diagram is drawn

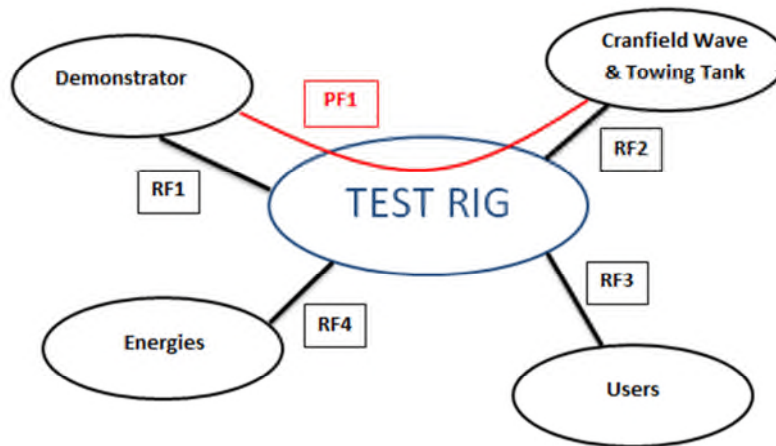


Figure 5-26 Functional diagram interaction test rig

Here, the test rig is interacting with the demonstrator, the Cranfield Wave & Towing tank, users and energies. The Principal Function (PF) and the Requirement Functions (RF) are listed in the functional specification table below which is characterising the functions by criteria themselves defined by flexibility and levels.

Functions	Functions characteristic		
	Criteria	Levels	Flexibilities
PF1: to test the demonstrator in the Cranfield wave and towing tank	Stroke	≥ 2,200.00mm	F0
	Pull Force	≥300.00N	F0
	Rate	Adaptable	F1
RF1: to hold the demonstrator	Assemblage ability	Easy	F1
RF2: to be adaptable to the wave & towing tank of Cranfield	Dimension	as small as possible	F0
	Weight	< 20.00 kg	F0

RF3: to collect data	Data acquisition	Easy interface	F1
RF4: to use energies	Electric	24V - 5A	F0

Table 5-12 Functional Specifications of the test rig

5.3.2 Design



Figure 5-27 Actuator ROBO Cylinder RCP2-SA7C

In order to achieve the requirements of the principal function of the test rig, the actuators available in the Ocean System Laboratory in Cranfield are used (Figure 5-27).

The complete technical data are given in the 7Appendix B. According to these data, the actuator has a stroke of 800.00 mm and can pull a weight of 35.00 kg at a minimal speed and in a horizontal position. To match the first criteria of the PF of the test rig, the stroke has to be multiply by three. It is reach using a pulleys system displayed in Figure 5-28.

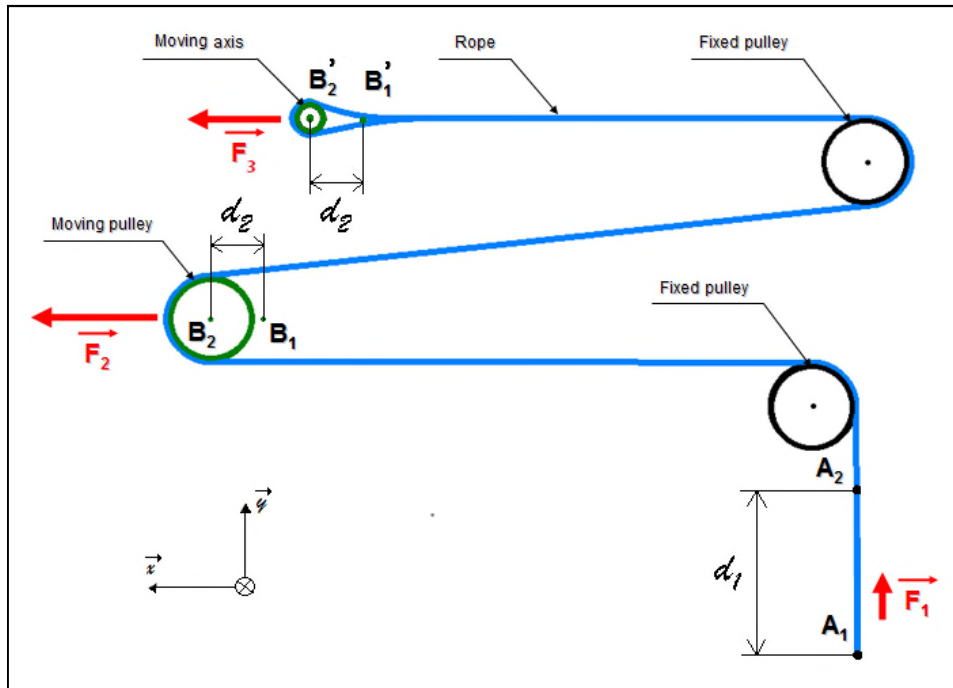


Figure 5-28 Configuration of the motion transmission system

The legend of the configuration is explained below:

- Moving axis: it is the axis links to the actuator, it is moving along the x axis.
- Moving Pulley: it is the pulley installed on the moving axis, therefore it is also moving along the x axis.
- B_1 is the point representing the initial position of the centre of the pulley.
- B_2 is the point representing the moving position of the centre of the pulley during the operation.
- B'_1 is the point representing the initial position of the centre of the moving axis.
- B'_2 is the point representing the moving position of the centre of the axis during the operation.
- d_2 is the distance B_1B_2 which is also equal to the distance $B'_1B'_2$.
- A_1 is representing the point where the demonstrator is attached to the test rig
- A_2 is representing the moving point of the demonstrator during the operation.
- d_1 is the distance A_1A_2 .
- F_1 is the tension produced by the system to lift the demonstrator.
- F_2 is the tension developed by the actuator in point B.
- F_3 is the tension developed by the actuator in point B'

Considering the geometry of the system, the point B_1 and B'_1 are the same in the plan xy . They have been defined separately because they have a different z coordinate. It is the same for the point B_2 and B'_2 .

Thanks to this configuration, when the actuator is moving of a certain distance, the demonstrator has a movement of three times this distance. This means that $d_1 = 3 * d_2$. The stroke of the actuator has been tripled, thus reaching a maximal stroke of 2,400.00 mm.

However, this configuration is dividing the force developed by the actuator to lift the device by three. Indeed, if the system wants to produce a force F_1 to lift the demonstrator, it has to develop a tension three times more because the winch lifting the demonstrator is attached once to the actuator and it is passing through a pulley also attached to the actuator. The maximal tension which is needed for the operation is 300.00 N. Therefore, an actuator must develop an tension three times more, so 900.00 N. The limit of the actuator is 35.00 kg of weight for a low velocity, which correspond to a force of 343.35 N. It is clearly not enough for the deployment and recovery operations. A way to fix this issue is to divide by three the force needed by attaching the demonstrator with three winches, each one of them connected to a different actuator installed with the same configuration. The three winches will be connected to the demonstrator at the top of the lift system. With this configuration, each actuator will need to produce a tension F_1 of 100.00 N which corresponds to a tension of 300.00 N as the origin of the transmission system. It is in the range of action of the actuator for a maximal speed of 100.00 mm/sec.

The final system is displayed in Figure 5-29; it is showing the three actuators fixed one next to the other on a wooden beam with the system of pulleys installed. The load cell is installed vertically between the two fixed pulleys in order to detect directly the tension F_1 . Prior to the test, a calibration of the captor has been undertaken to know exactly the meaning of the values it will give. This study has given a coefficient to apply to the results to have workable data. This coefficient is 2.

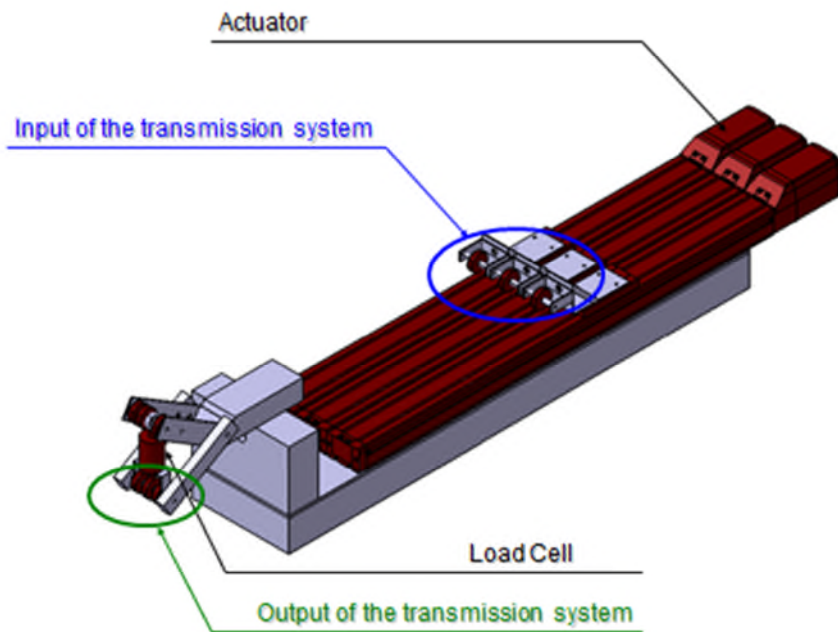


Figure 5-29 Final Test Rig

The power supply needed for the test rig must generate 24V of tension with an intensity of at least 1A, even more during the operation. The software necessary to monitor the actuators is installed on the computer used for the data acquisition.

6 Test Program

6.1 Set-up in the Cranfield wave-towing tank

The test rig was installed on the carriage of the wave-towing tank. By its weight, the test rig does not need to be attached to the platform. The power supply for the actuators is installed on the carriage with the controller of the actuators connecting them to the laptop with the recommended software previously installed.

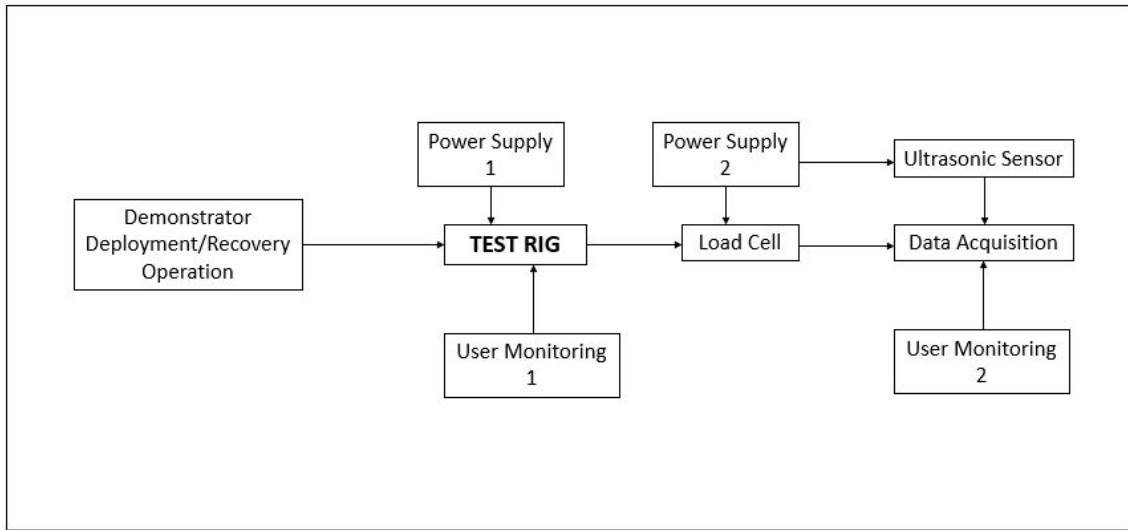


Figure 6-1 Drawing of the complete set-up

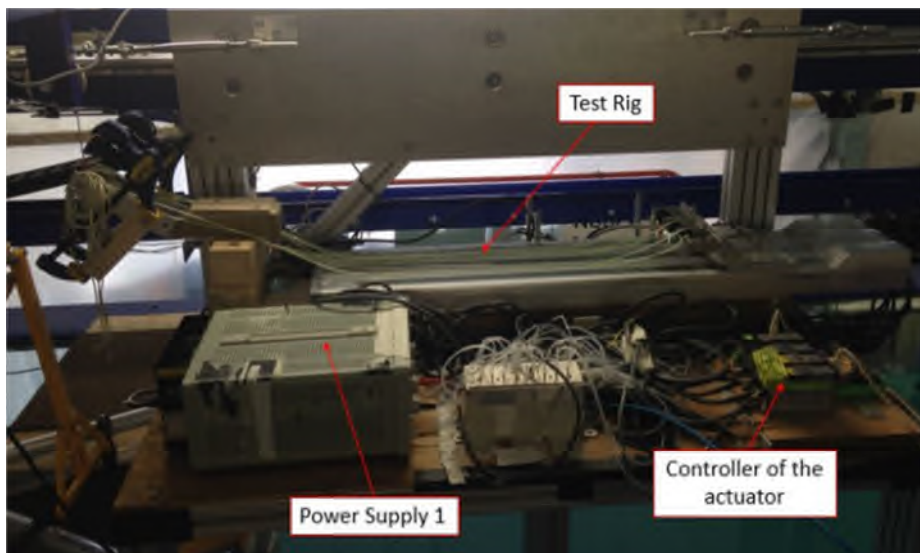


Figure 6-2 Set-up on the carriage

A second part of the set-up was installed on the desk of the platform, with another power supply and the acquisition system for the data acquisition.

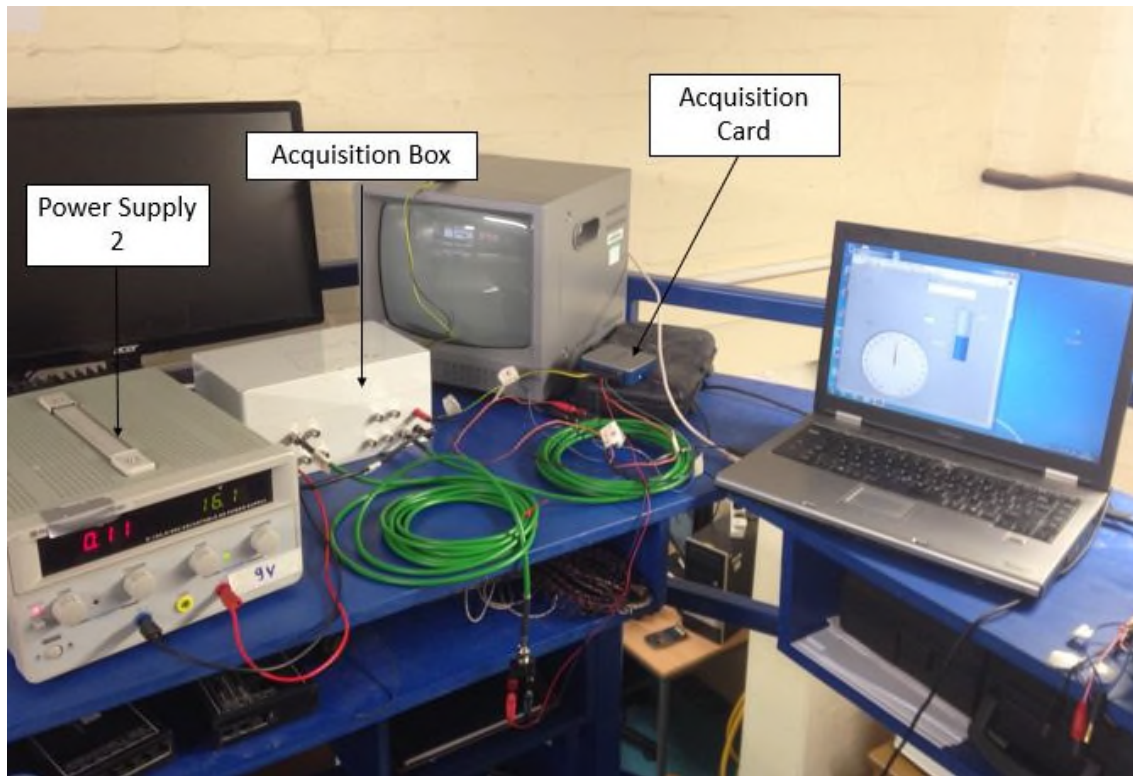


Figure 6-3 Set up on the desk

6.2 Instrumentation and data acquisition

In this part, the Labview interface is presented. It has permitted the recording of the data during the tests. The two captors used for the data acquisition are:

- The load cell installed on the test rig to measure the lifting tension experienced by the crane. This load cell has a 1,000.00 N limit in tension/compression and needs to work with a tension of 16V.
- The ultrasonic sensor which is measuring the wave height during the data acquisition. This ultrasonic sensor is installed 40.00 cm above the waterline because it is calibrate to measure data from 20.00 cm to 60.00cm. An equation is used to calibrate the sensor to return value from -20.00 cm to 20.00 cm. Thus, the 40.00 cm distance of the sensor without calibration corresponds to the 0 cm distance with calibration. The sensor also needs to work with a tension of 16V.

The signals of these sensors were acquired by an acquisition card: the NI USB 6000. The following Graphical User Interface (GUI) was created using the software Labview 2010.

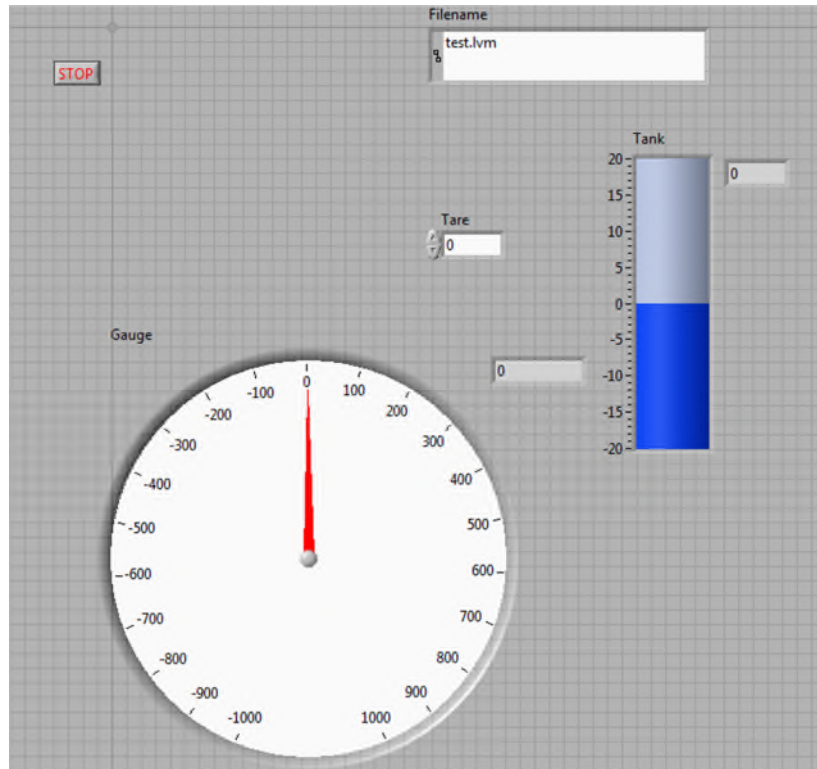


Figure 6-4 Labview Interface of the data acquisition

The GUI is made of:

- One gauge from -1,000.00 N to 1,000.00 N for the load cell. A tare has been created to offset the load cell to 0 in the beginning of the data acquisition.
- A second gauge displayed as a level for the water height from -20.00 cm to 20.00 cm. Here no tare has been use; the offset is adjusted with the installation of the ultrasonic sensor on the tank.
- A filename window to name the file which is created during the data acquisition.
- A stop button to stop the acquisition.

The acquisition is designed to last until the stop button is used, allowing long acquisition for the recovery for example. The time laps is 0.01s and the returning file is a text file which needs to be import in Excel. This acquisition is returning three columns: one for the time, one for the load cell and one the ultrasonic sensor.

6.3 Test runs

The tests have been run in the wave and towing tank in Cranfield with the set-up described in the previous part. During the test operation, 60 tests have been carried out, 30 tests of deployment and 30 tests of recovery. The first aim was to define the influence of the sea state on the operation by detecting the maximal tension and the oscillations of this tension along the time. The second aim was to determinate the time of the deployment and the time of the recovery and the influence of the inlets/outlets of the ballast on it.

Concerning the first objective, multiple inputs are modified during the tests:

- Wave amplitude: the range of amplitudes is from 0.01 to 0.035 m. It corresponds at full scale to a range in-between 0.2 and 0.7 m from the waterline to the crest. So 0.4 to 1.4 m crest to crest.
- Wave frequency: the range of frequencies used is from 0.5 Hz to 1.4 Hz. It corresponds to wave periods in-between 0.7 and 2 seconds. At full scale, it means wave periods from 3.13 to 8.94 seconds.
- Positioning of the model: the orientation of the demonstrator through the wave is changed from 0 to 180 deg. Five positions are tested to see their impact (Figure 6-5).

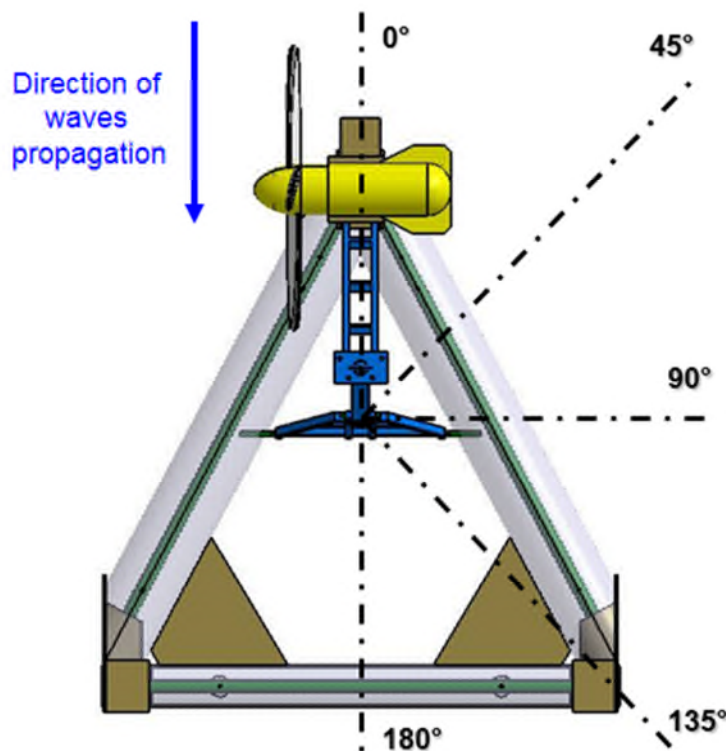


Figure 6-5 Deltastream orientations

As for the second aim, two different configurations have been test. They are explained with Figure 6-6 and Table 6-1.

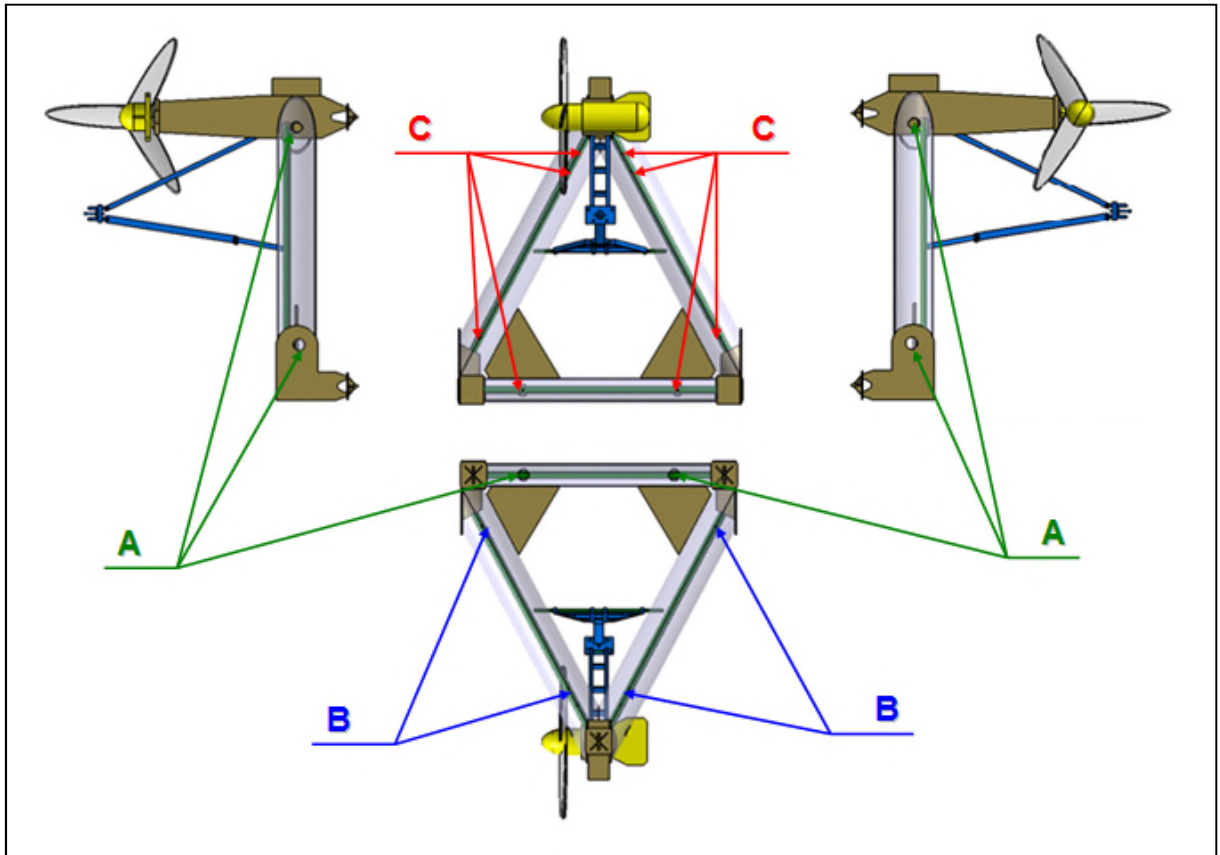


Figure 6-6 Inlets/Outlets Position

On the figure, the inlets A are the principal inlets for the filling when the inlets B are the secondary inlets, smaller. C represents the vents of the ballasts.

Data	Configuration 1	Configuration 2
Number of inlet	A (6x) + B (4x)	A (6x) + B (4x)
Diameter of inlet	10.00 mm + 5.00 mm	25.00 mm + 5.00 mm
Number of Vents	C (8x)	C (8x)
Diameter of Vents	5.00 mm	5.00 mm
Speed of Descent	8.00 mm/sec	8.00 mm/sec

Table 6-1 Two configurations data

- The first configuration is made to have a first idea of the behaviour of the demonstrator with a longer time of submersion.
- The second configuration is the scaled one.

6.4 Data processing

6.4.1 Tests with the first configuration

6.4.1.1 Presentation

Twenty-four tests have been carried out in this configuration, twelve for the deployment and twelve for the recovery. Only the sea state has been modified in those tests. The first test was made without waves. It has for objective to calibrate the other tests by observing the behaviour of the demonstrator and setting a time slicing which allows a clear understanding of all the phases the demonstrator is going through during both deployment and recovery.

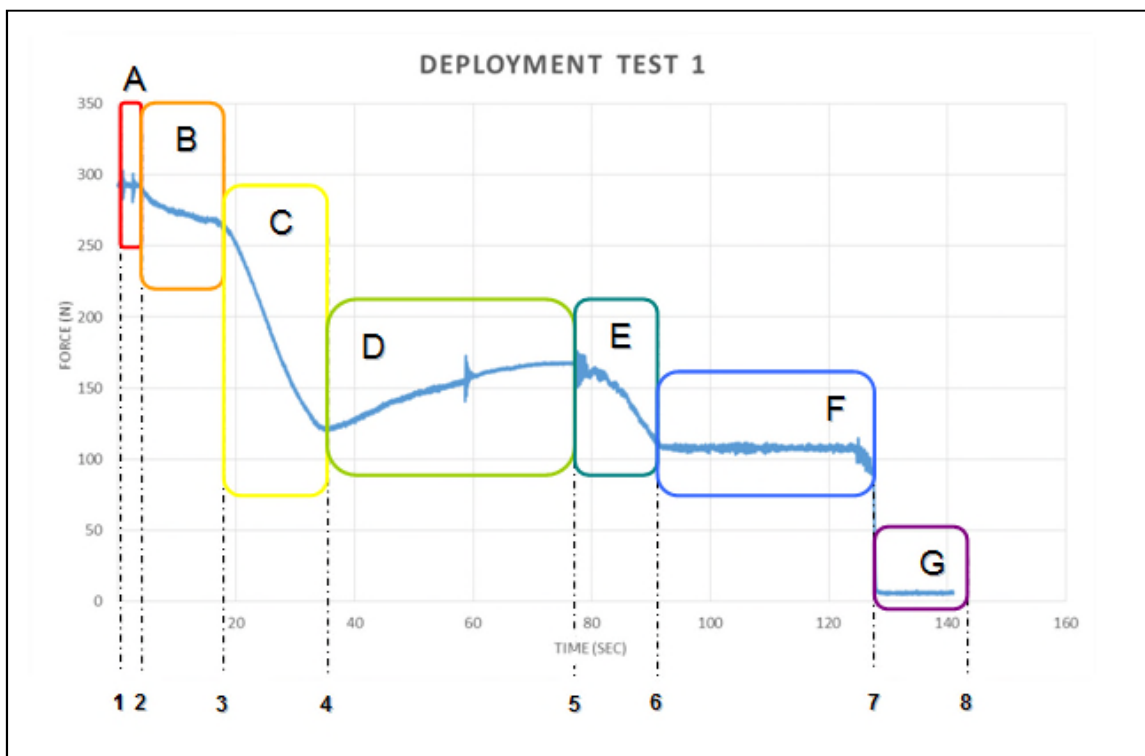


Figure 6-7 Deployment curve with time-slicing

The curve is divided in seven phases described below:

- Phase A: waiting phase between the beginning of the acquisition and the launch of the actuator. The vibrations can be explained by the jerks experienced by the actuators while they are stopped.
- Phase B: the demonstrator is starting its descent toward the waterline; the diminution can be explained by the beginning of the motion of the actuators in the same direction that the force developed by the demonstrator on them.

- Phase C: the demonstrator starts to be submerged. The drop is due to the Displacement developed by the raising submerged volume of the demonstrator. The ballasts are also starting to be filled but the filling is slower than the submersion of the device, so the drop is experienced.
- Phase D: during this phase, the actuators are stopped until the ballasts filling are complete. The slight raise is explained by the fact that the mass raises without a change of the displacement.
- Phase E: the device is starting its descent toward the seabed. The drop is explained by the displacement being raised by the submersion of the turbine.
- Phase F: the demonstrator is completely submerged and descending toward the seabed, the tension is constant. The value of the tension here corresponds to the weight in water of the device.
- Phase G: the device is landed on the seabed, the actuators are not experiencing tension anymore so the load cell is returning 0 N.

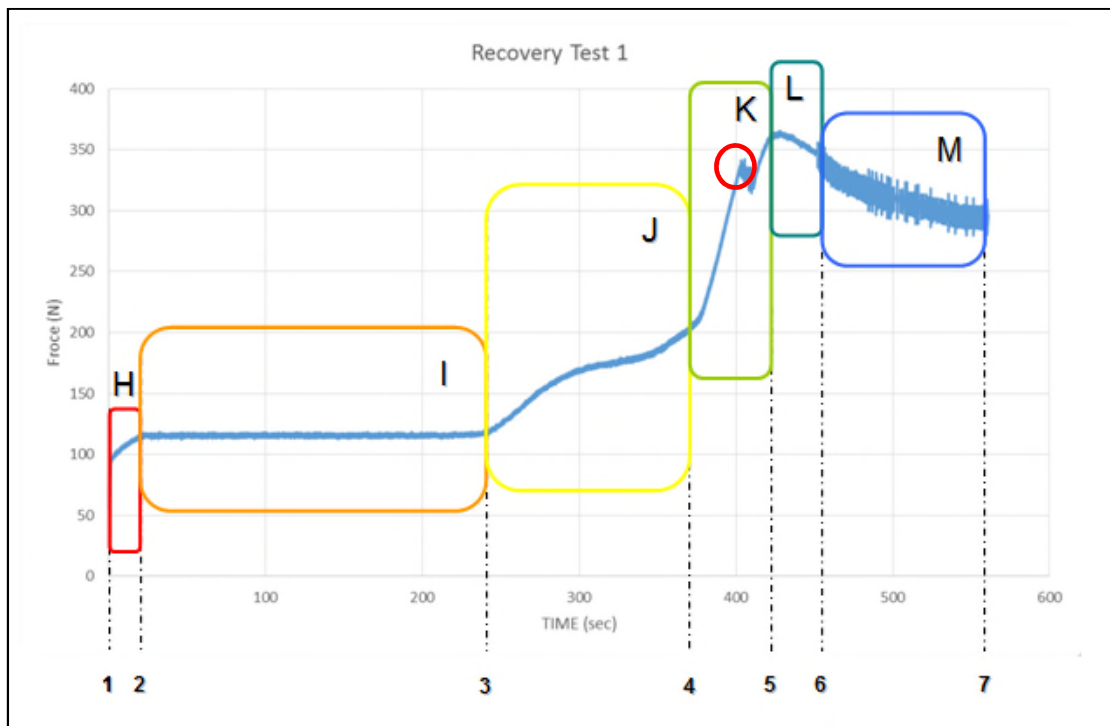


Figure 6-8 Recovery curve with time-slicing

The curve is divided in six phases described below:

- Phase H: the device is starting its recovery; it is progressively being detached from the seabed, so the augmentation of the tension is progressive.
- Phase I: this phase is the equivalent of the phase F during the recovery.

- Phase J: the structure is getting progressively out of the water, inducing a reduction of the displacement. So the tension is rising.
- Phase K: the ballasts start to be drained. But the process is slower than the diminution of submerged volume, so a raise is experienced. During this raise, a small drop is experienced (red circle in the figure). It can be explained by the interruption of the actuator. The demonstrator is still partly submerged but the ballasts are being drained, so the tension is slightly dropping.
- Phase L: during this phase, 90% of the demonstrator is outside the water, the displacement is constant while the draining of the ballasts is still on-going. Thus the tension is dropping.
- Phase M: the actuators are stopped in their initial position but the ballasts are not drain yet. The demonstrator is fully out of the water, a drop is once again experienced. The oscillations are due to the immobility of the actuators and the jerks they are experienced because of it.

In addition to those phases, eight actuator phases have been used for the first tests: three phases for the deployment, one when the demonstrator is landing on the seabed and four for the recovery (Table 6-2).

Actuator Phase		Deltastream Estate
0	Holding the structure above the waterline	Completely unsubmerged structure and holding in position
1	Descending to the waterline	Partly submerged structure, flooding of the ballasts
2	Descending to the seabed	Equilibrated structure, simply descending
3	Landing on the seabed	Equilibrated structure, landing on the seabed
4	Ascending to the water line	Slow recovery operation until the structure starts to go of the water - Start Draining of the ballasts
5	Holding the ballasts inlets above the waterline	The demonstrator is hold in position to allow the water to come out of the ballasts
6	Second ascending	Slow ascending until the structure is fully out of the water
7	Holding the structure above the waterline	Completely unsubmerged structure and holding in position

Table 6-2 Actuator phases and Deltastream estate during tests

The shape of the graphs plotted with the data and the actuator phases is the following:

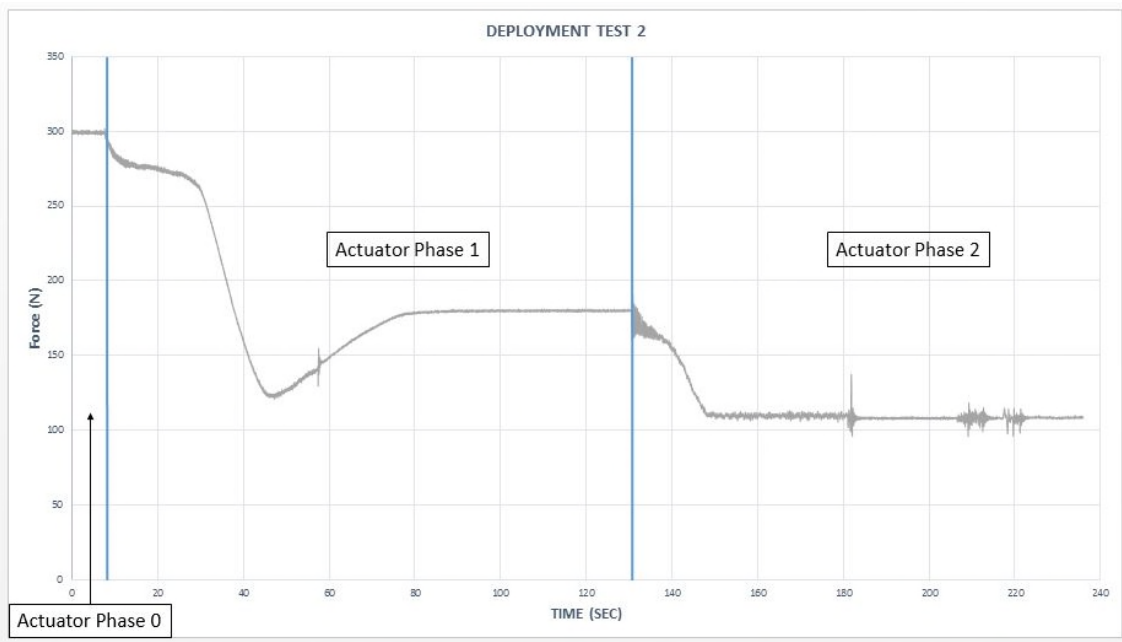


Figure 6-9 Deployment Test 2 - Graph Shape

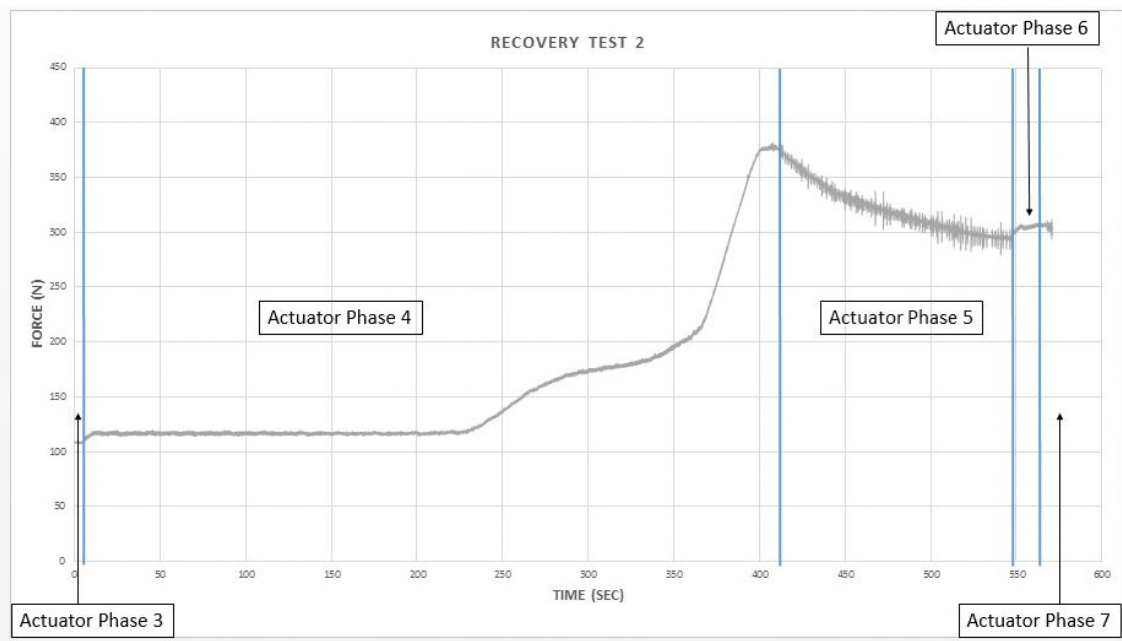


Figure 6-10 Recovery Test 2 - Graph Shape

The horizontal axis is representing the time of the acquisition. The grey curve is the curve of the tension developed during the deployment and the recovery.

The following table is giving the different sea states used during the tests:

Amplitude (m) \ Frequency (Hz)	0	0.02	0.025	0.03	0.035
0	Test 1				
0.5				Test 11	Test 12
1		Test 3	Test 4	Test 5	Test 6
1.2		Test 7	Test 8	Test 9	Test 10

Table 6-3 Wave Data for the first configuration

6.4.1.2 The influence of the wave height

In this part, the influence of the amplitude is assessed through two key points:

- Influence of the wave height on the shape of the curve.
- Influence of the wave height on the maximal tension measured.

To determinate the impact of the wave height, the frequency is fixed and the wave height is modified. For the impact on the shape, the deployment tests 3 to 10 are used. The oscillations during deployment and recovery are similar, the data are equivalent. The oscillations are the strongest while the ballasts are flooded. The actuators are stopped and the demonstrator is progressively flooded (beginning of phase D).

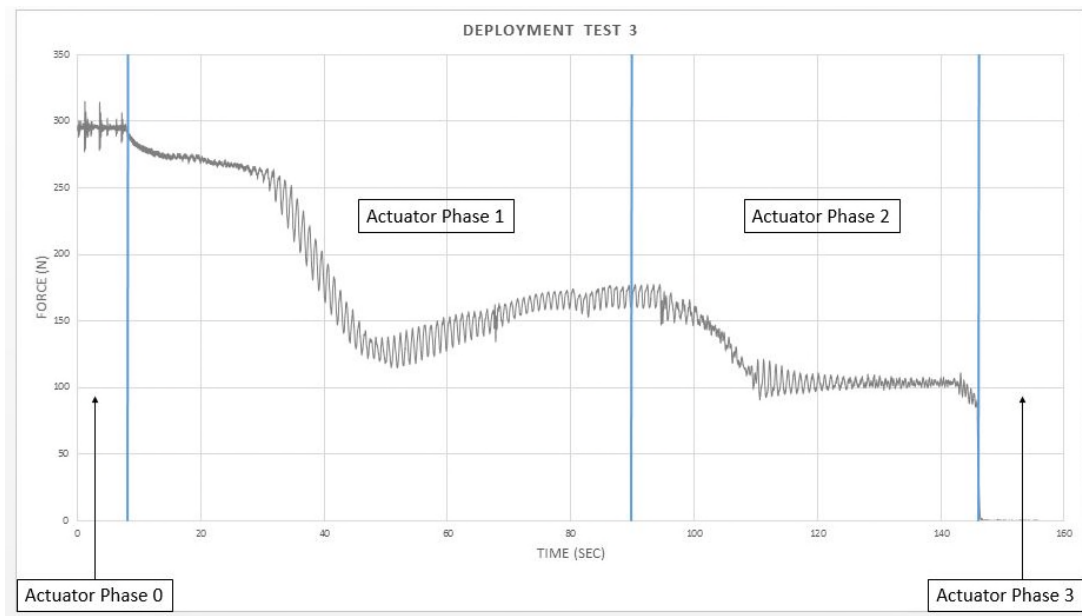


Figure 6-11 Deployment Test 3 - Configuration 1

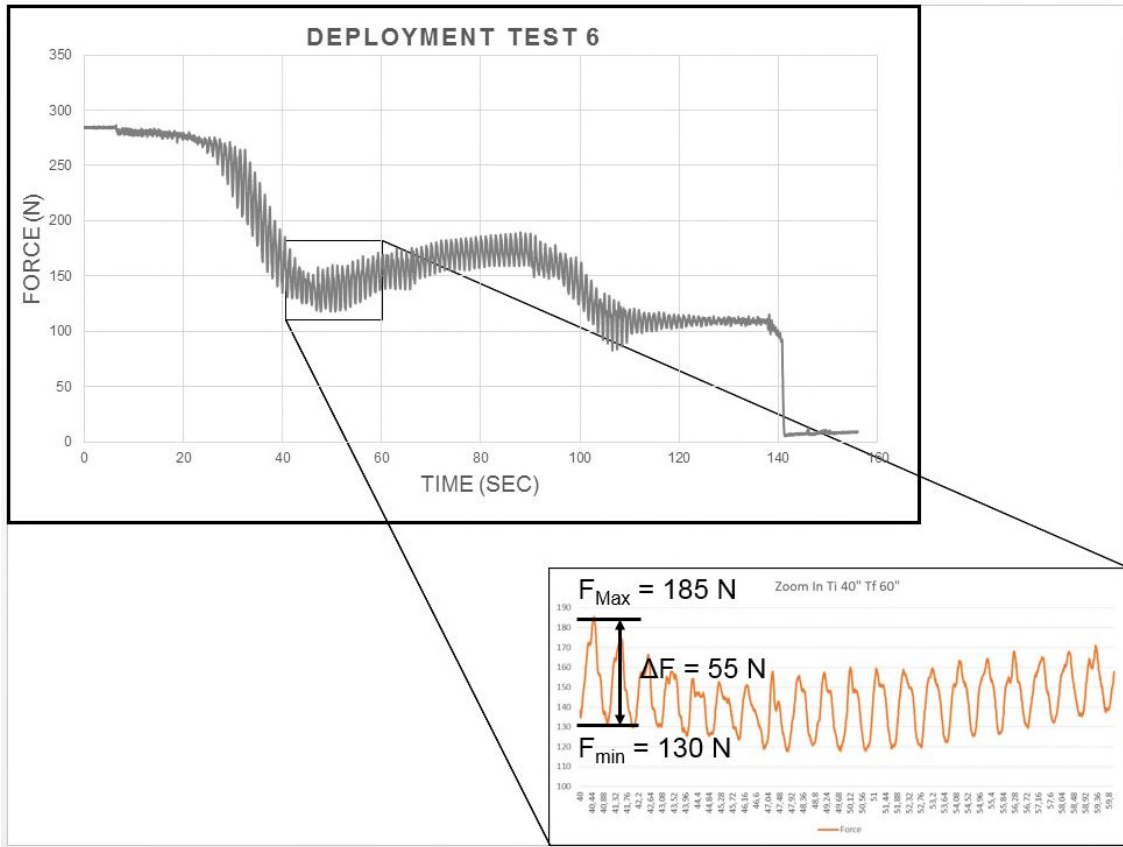


Figure 6-12 Deployment Test 6 with zoom-in– Configuration 1

For a direct understanding, the following histograms drawn are done with the values divide by two, the coefficient needed to obtain the tension on the cable.

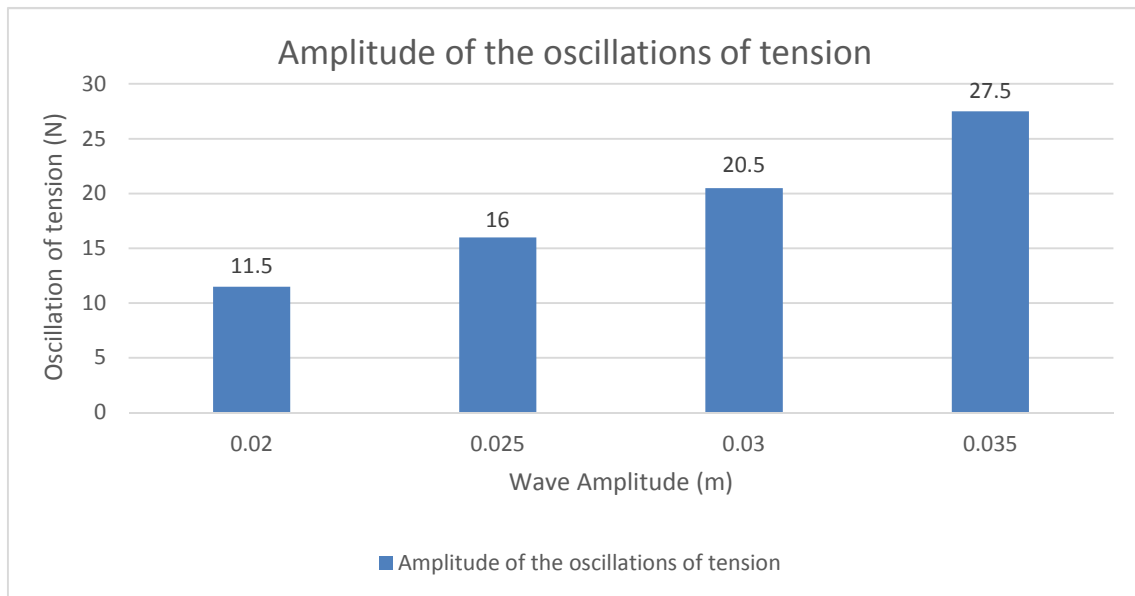


Figure 6-13 Influence of the wave amplitude on the amplitude of the oscillations of tension – deployment tests 3/4/5/6

This histogram is representing the different amplitude of oscillation detected by the load cell during the test 3, 4, 5 and 6. The tendency shown on this histogram is that the amplitude of the oscillations is rising in proportion to the raise of the wave height.

Wave Height (m)	Amplitude of the oscillation of tension (N)	Mass equivalent (kg)	% of the total mass
0.02	11.5	1.17	7.31
0.025	16	1.63	10.19
0.03	20.5	2.09	13.06
0.035	27.5	2.8	17.5

Table 6-4 Summarised Results and percentage – deployment test 3/4/5/6

For 0.02 m amplitude, the oscillations are of 7.31% of the total weight (unballasted) of the device in the worst condition. But for 0.035 of amplitude, the percentage is 17.5%, almost one fifth of the total weight. At full scale, this percentage represents 22.93 tonnes (trough to crest) so a variation of the tension of ± 11.47 tonnes. The snatch load in that case is very important and cannot be neglected.

To confirm this tendency, another histogram was plotted with the tests 7, 8, 9 and 10. The results are in the following table:

Wave Height (m)	Amplitude of the oscillation of tension (N)	Mass equivalent (kg)	% of the total mass
0.02	17	1.73	10.81
0.025	21.5	2.19	13.69
0.03	28	2.85	17.81
0.035	35	3.57	22.31

Table 6-5 Summarised Results and percentage – deployment test 7/8/9/10

The tendency is identical; the oscillations are more significant here because the frequency is smaller, so the waves longer. A percentage of 22.31% is obtained, corresponding to a variation of the mass at full scale of ± 14.61 tonnes. The snatch load experienced by the crane is again very important and cannot be neglected.

Those snatch loads are experienced from the first contact with the waterline to the descent toward the seabed. During the descent, the demonstrator is pulled away from the waterline so the impact of the waves drops.

Concerning the maximal tension detected by the load cell, a histogram has been plotted to evaluate the evolution of this tension with a variation of amplitudes.

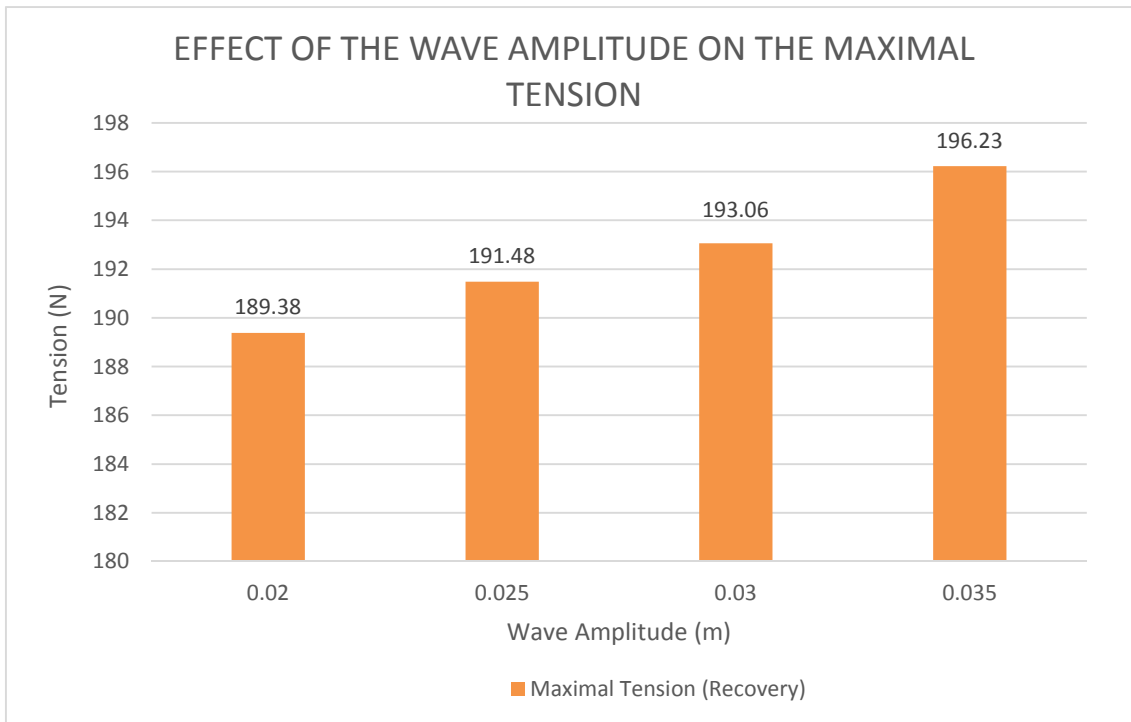


Figure 6-14 Influence of the wave amplitude on the maximal tension – Recovery test 7/8/9/10

The tests used here are the number 7, 8, 9 and 10 (frequency 1.2 Hz). The maximal tension has been detected each time during the recovery operation, at the end of phase K in Figure 6-8. The tendency observed is an augmentation of the maximal tension with the raise of the wave amplitude. For those four tests, the difference between 0.02 and 0.035 of amplitude is 6.85 N. At full scale, this raise corresponds to an augmentation of the tension of 56,170 N.

In order to confirm this tendency, the tests 3, 4, 5 and 6 have also been compared with a histogram (frequency 1Hz). The same tendency is observed, with a slight diminution of the difference with 3.8 N. At full scale, this is corresponding to a raise of 31,160 N of the tension.

6.4.1.3 The influence of the frequency

In this part, the same key aspects are investigated, with the same methodology. But this time the amplitude is fixed and the frequency modified.

The following graphs are displaying the curves for the deployment test 10 and 12 with identical amplitude (0.035m) but a different frequency (respectively 1.2 and 0.5Hz).

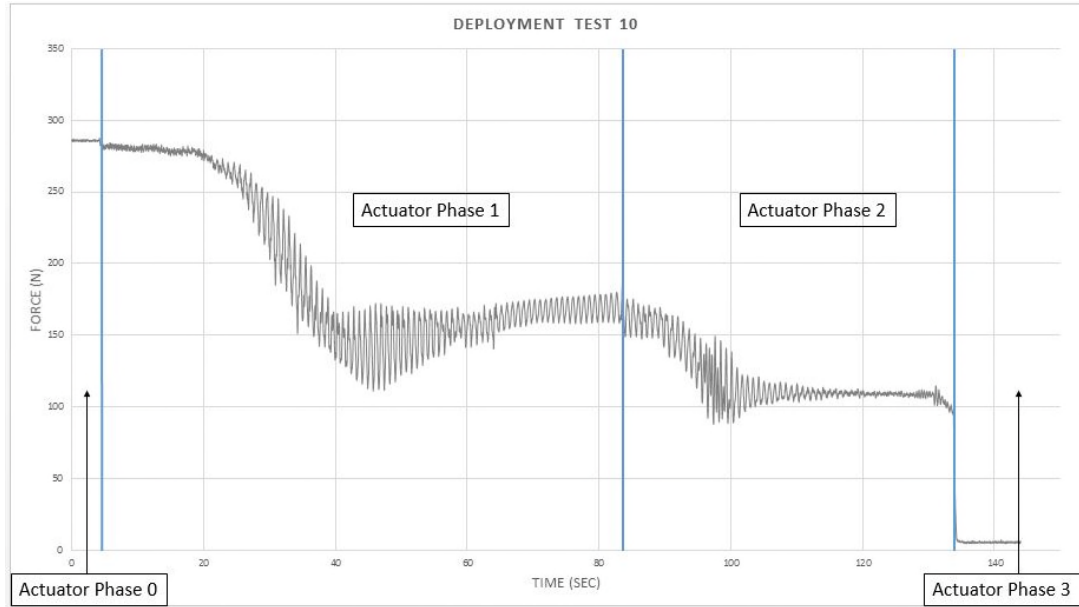


Figure 6-15 Deployment test 10 - Configuration 1

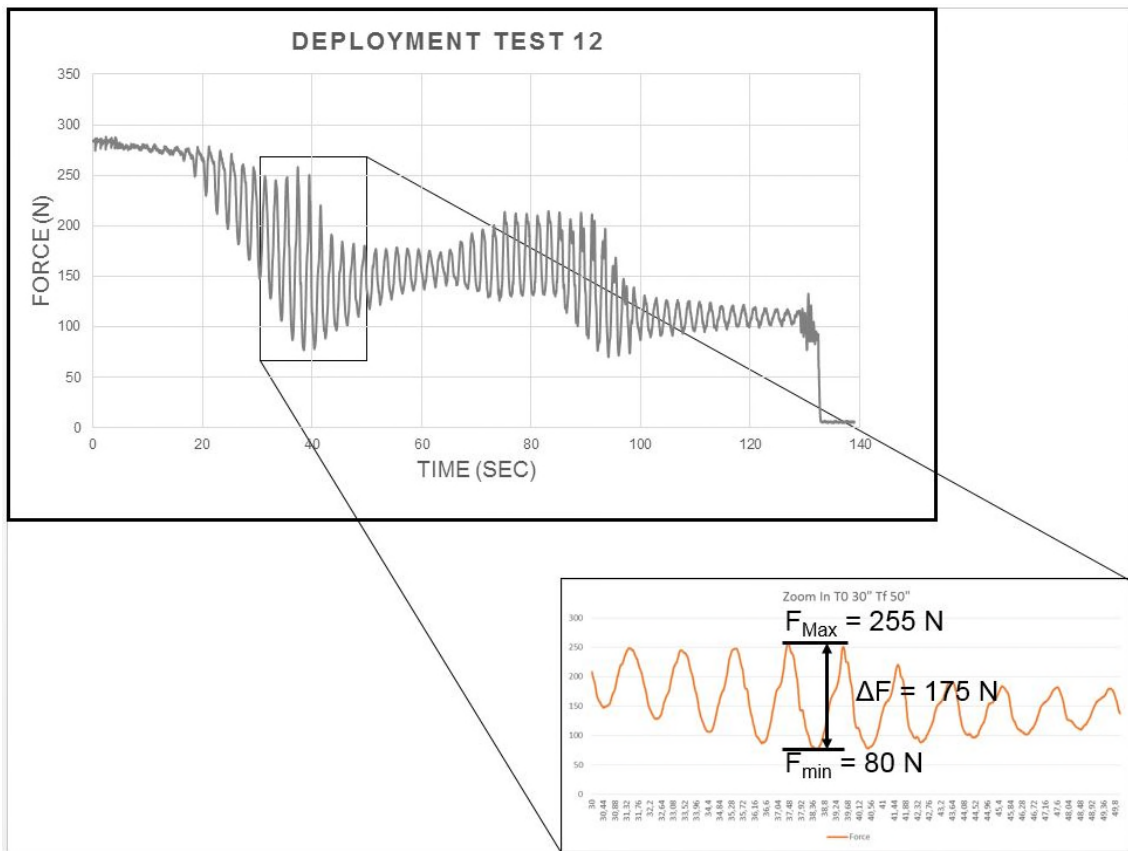


Figure 6-16 Deployment test 12 with zoom-in - Configuration 1

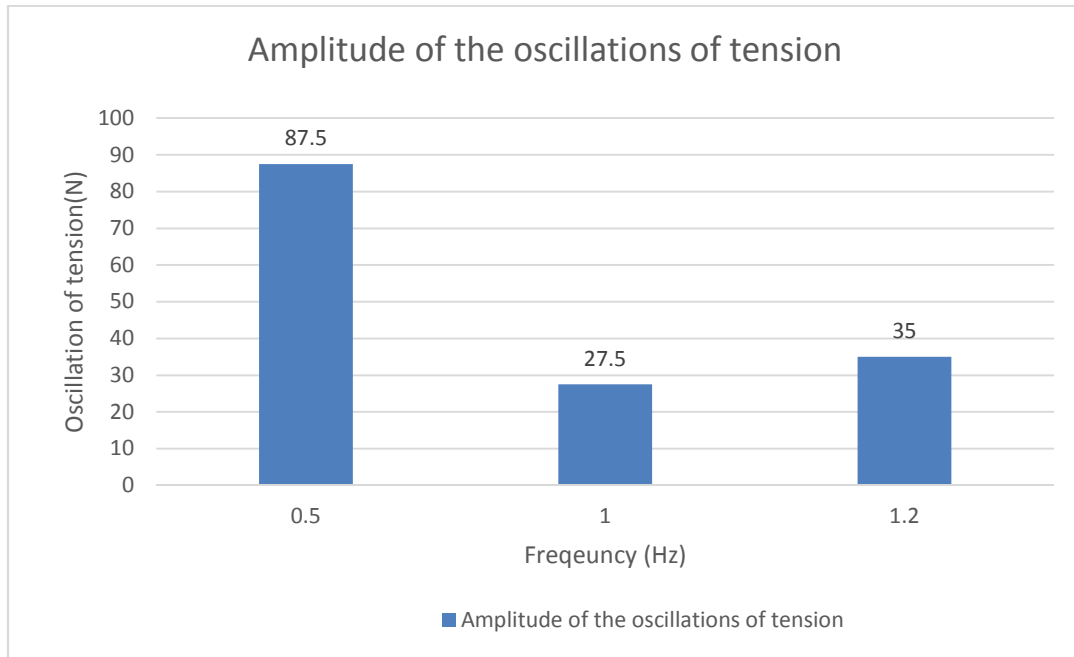


Figure 6-17 Influence of the frequency on the amplitude of the oscillations of tension – deployment test 12/6/10

In opposition to the wave height impact, the amplitude of the oscillations is not evolving in proportion to the frequency. As shown on Figure 6-17, a frequency of 1Hz is the most favourable for the deployment.

Frequency (Hz)	Oscillation (N)	Mass equivalent (kg)	% of the total weight
0.5	87.5	8.92	55.75
1	27.5	2.80	17.5
1.2	35	3.57	22.31

Table 6-6 Summarised Results and percentage – deployment test 12/6/10

The impact of the change of frequency is more important than the impact of a change of wave height. The worst case is with a frequency of 0.5 Hz, with a fluctuation of the cable tension of 55.75% of the unballasted mass of the demonstrator. At full scale, it corresponds to a variation of ± 36.52 tonnes of mass on the crane.

To confirm this tendency, a histogram has been plot with the test 11, 5 and 9.

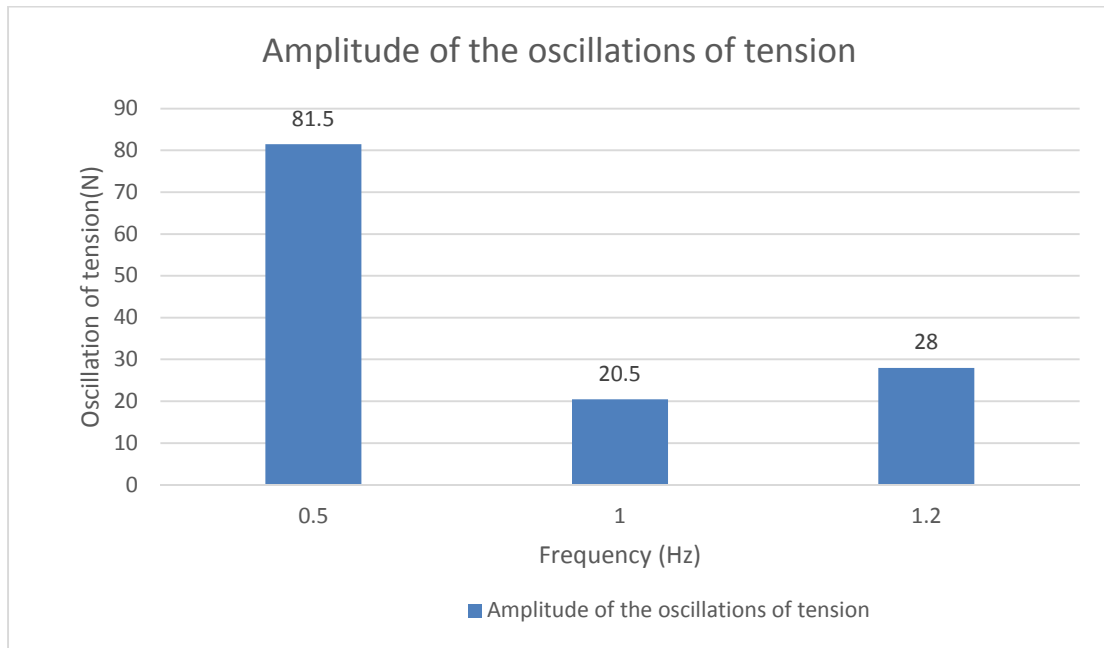


Figure 6-18 Influence of the frequency on the amplitude of the oscillations of tension – deployment test 11/5/9

The results are showing a similar tendency, with a maximal oscillation once more for a frequency of 0.5 Hz. These oscillations correspond to a fluctuation of 51.92% of the unballasted mass of the device. Full scale, it is equivalent to a variation of 34.01 tonnes of the mass applied on the crane.

Concerning the maximal tension detected by the load cell, a histogram has been plotted to evaluate the evolution of this tension with a variation of frequencies.

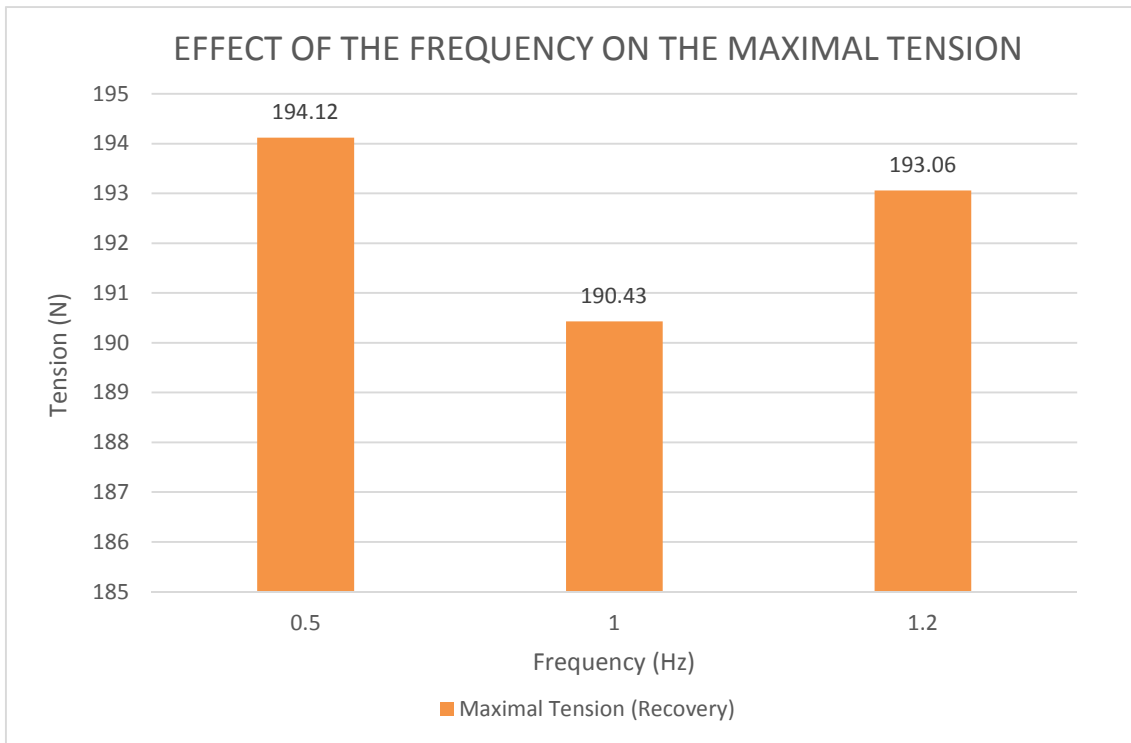


Figure 6-19 Influence of frequency on the maximal tension – recovery test 11/5/9

The tests used here are the number 11, 5 and 9 (wave height 0.03 m). The tendency observed is that the most favourable scenario is with a frequency of 1 Hz because it is the one with a smaller tension on the cable. However, the difference between those values is small.

The same histogram was plotted with the tests 12, 6 and 10 (wave height 0.035 m). The tendency observed is the same; the most favourable scenario seems to be the one with a frequency of 1 Hz. Due to the raise of the wave height, the difference of maximal tension between the scenarios is slightly higher but still small.

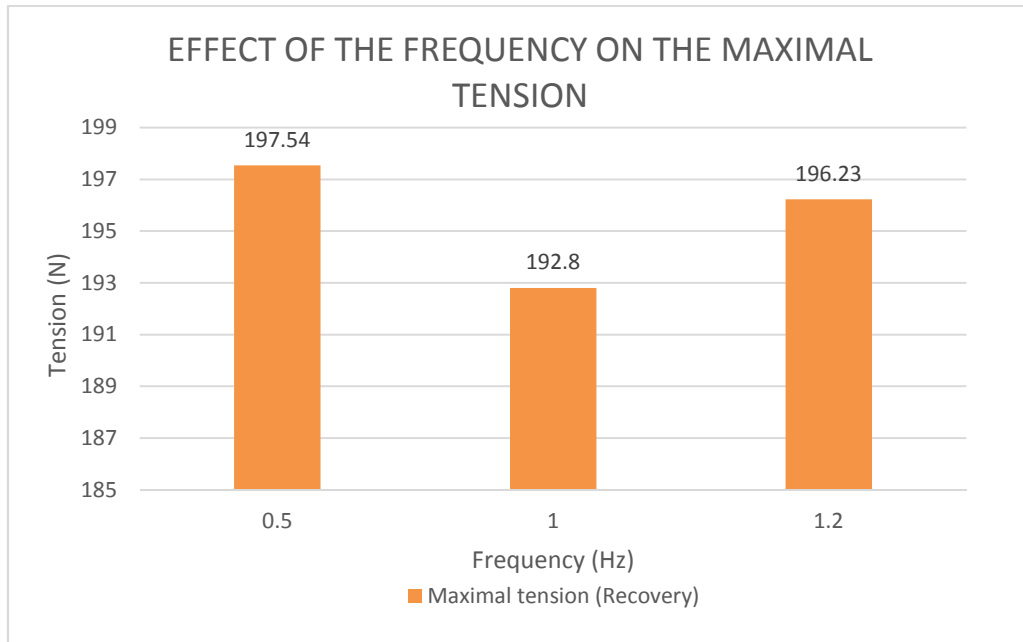


Figure 6-20 Influence of frequency on the maximal tension – recovery tests
12/6/10

A general conclusion of the influence of the frequency on the demonstrator is that a frequency of 1 Hz is preferable. The lowest pick of tension and the smallest oscillations of the tension are observed with a frequency of 1 Hz. However, the impact of the frequency on the maximal tension is not significant considering the small differences of tension between the different frequencies (max 5 N).

6.4.1.4 Phase shift between oscillations of tension and wave

The waves during the tests are inducing oscillations of the tensions collected by the load cell. The aim of this part is to study the phase shift between the period of the oscillations and the period of the waves. The deployment test 12 is used to assess this aspect. The sea state during test 12 is the following:

	Frequency (Hz)	Period (sec)	Wave height (m)
Input wave maker	0.5	2	0.07
Full Scale	0.11	8.94	1.4
Output ultrasonic sensor	0.5	2	0.087
Full Scale	0.11	8.94	1.74

Table 6-7 Sea state of the test 12

A small difference is observed for the wave height in output, but the period is the same. Figure 6-21 is displaying the results obtained during the data acquisition according to the time. Here the actuator phases are not displayed. During this state, the demonstrator will be floating in the beginning and then submerged. The phase shift will be assessed in those two different cases.

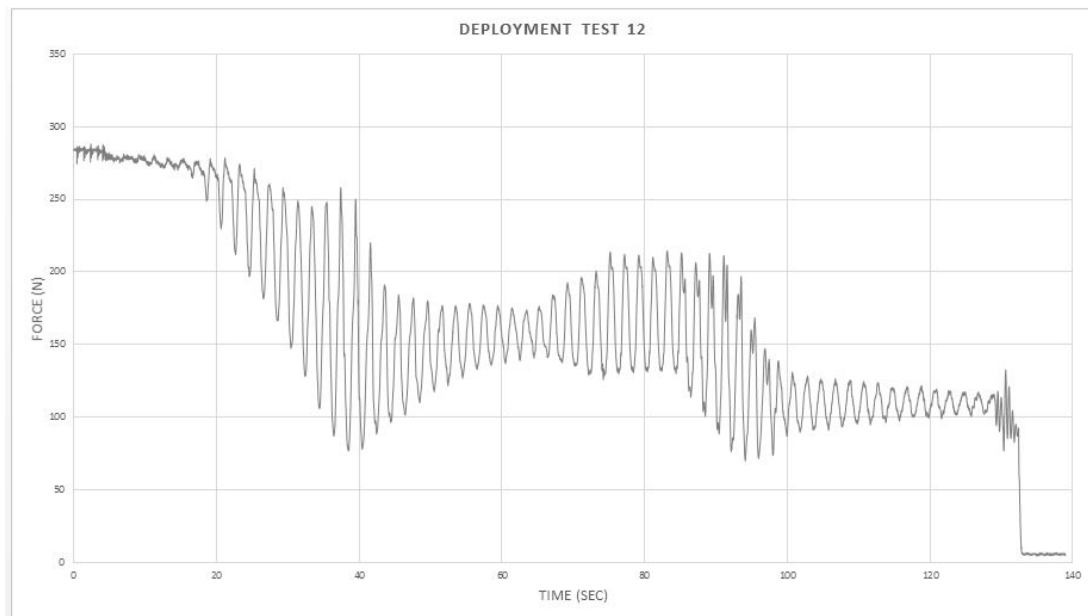


Figure 6-21 Deployment Test 12 – Configuration 1

To begin with, the phase shift during the floating phase of the device is assessed. To comprehend this aspect, a graph has been plot with the tension and the wave height with an identical time scale from 15 to 47 seconds. During this interval, the device is reaching the waterline and then starts its floating phase. The impact of the waves here is a lack of the tension during a crest and a pick during a trough.

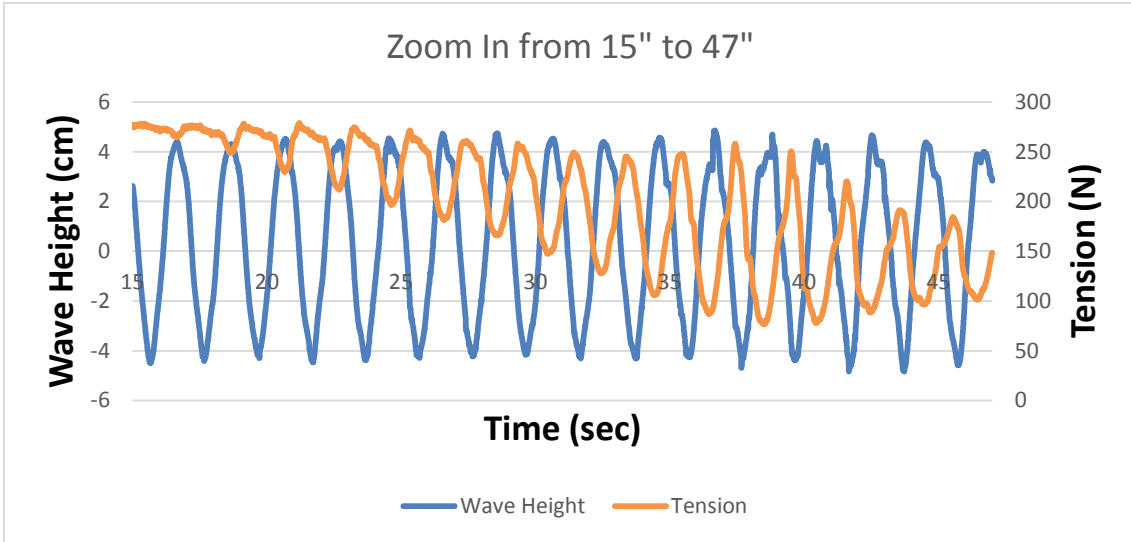


Figure 6-22 Zoom-in from 15 to 47 seconds

According to this graph, the phase shift is π . The oscillations are in opposition of phase. It can be explained by the motion of the demonstrator which is similar to the motion of the waterline. The device is being raised during a crest and lowered during a trough inducing a release of the tension during the crest and an over tension during the trough.

However, a change of the phase shift is observed during the operation. Indeed, a second zoom-in has been plotted while the demonstrator is completely submerged and the phase shift is different.

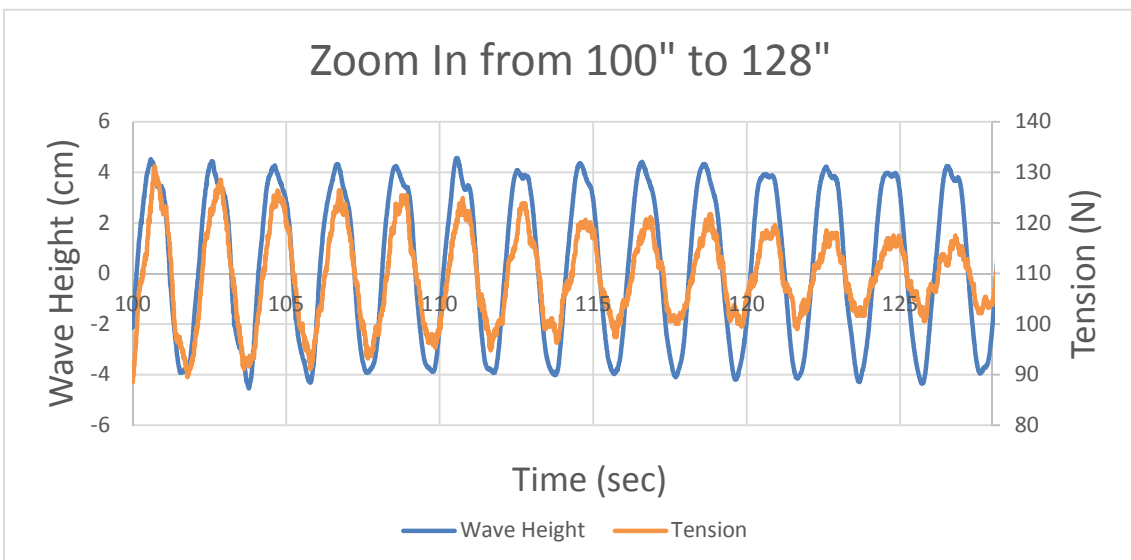


Figure 6-23 Zoom-in from 100 to 128 seconds

Here the phase shift is close to zero. The lacks on the cable are experienced during the troughs and the over-load during the crest. This phenomenon can be explained by a loss of buoyancy during a crest and a gain of buoyancy during a trough.

6.4.2 Tests with the second configuration

6.4.2.1 Presentation

Thirty tests have been carried out in this configuration, fifteen for the deployment and fifteen for the recovery. Here the sea state was changed only in frequency as well as the orientation of the demonstrator and we are on configuration two, with larger inlets/outlets for the ballasts. The aim of those tests is to assess the impact of the orientation of the demonstrator as well as the impact of the inlet/outlet size of the ballasts. A time slicing has been undertaken again to have a clear understanding of the different phases of the tests.

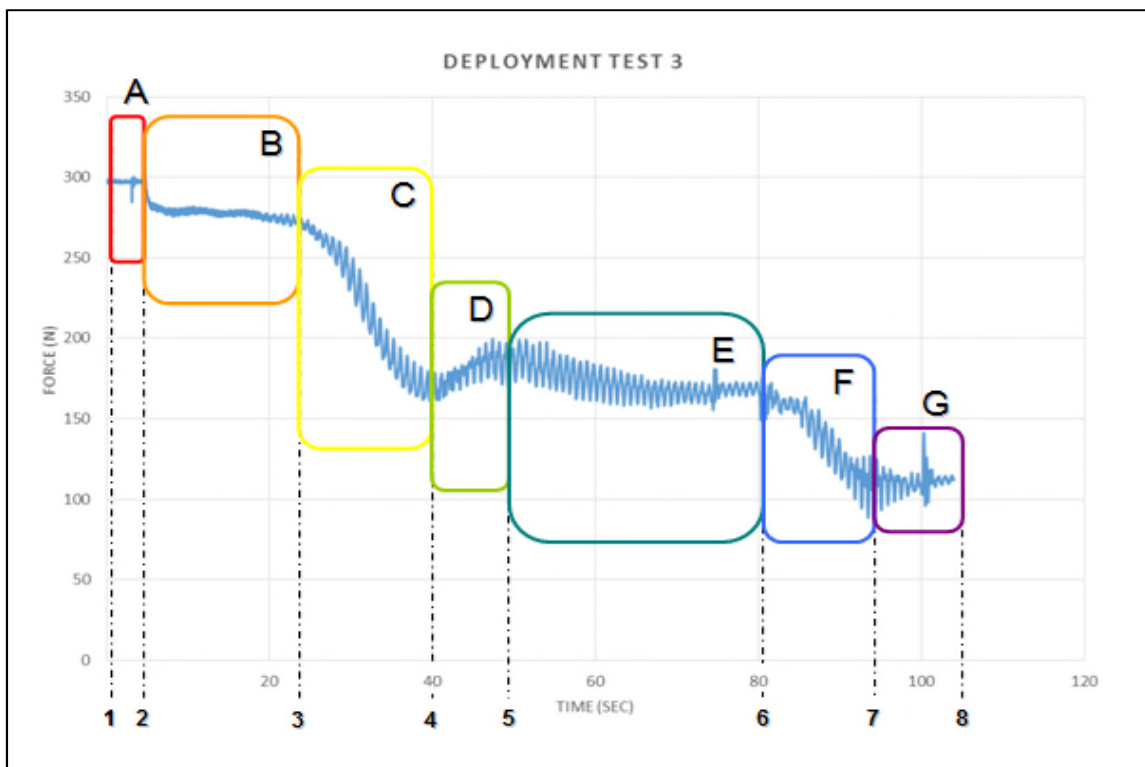


Figure 6-24 Deployment curve with time-slicing

The curve is divided in seven phases described below:

- Phase A: waiting phase between the beginning of the acquisition and the launch of the actuator. The vibrations can be explained by the jerks experienced by the actuators while they are stopped.

- Phase B: the demonstrator is starting its descent toward the waterline; the diminution can be explained by the beginning of the motion of the actuators in the same direction that the force developed by the demonstrator on them.
- Phase C: the phase starts after the first contact of the ballasts with the water line. As the rate of the submersion of the demonstrator is more important than the rate of the raise of the mass due to the ballast flooding, a drop is observed.
- Phase D: during this phase, the ballasts are underwater but not completely filled. The slight raise is explained by the fact that the mass raises without an important change of buoyancy.
- Phase E: the ballasts are flooded, the mass is constant. The slight drop is explained by a small raise of the displacement.
- Phase F: the important drop here is due to the entrance of the turbine in the water.
- Phase G: the demonstrator is fully submerged; the tension is constant and corresponds to the weight in water of the device.

The following figure is illustrating the multiple phases describe hereinabove.

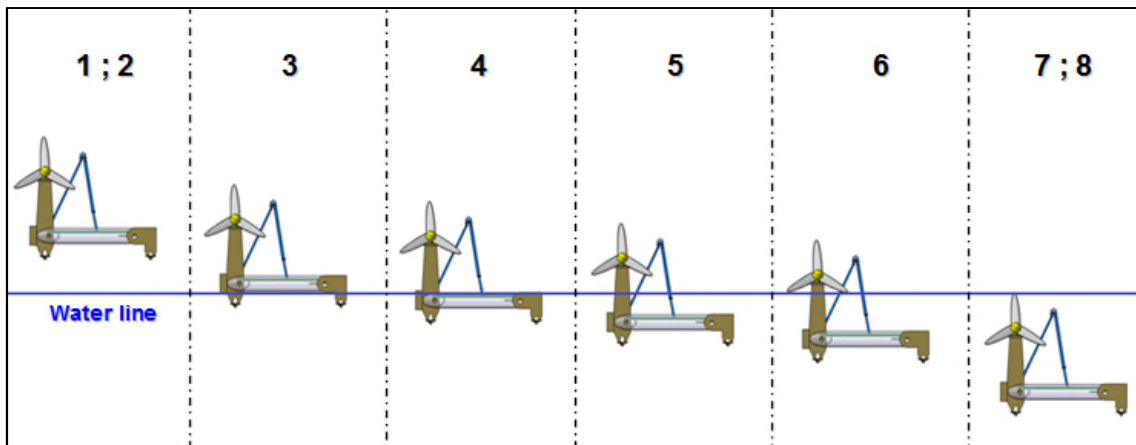


Figure 6-25 Deltastream position during deployment operation

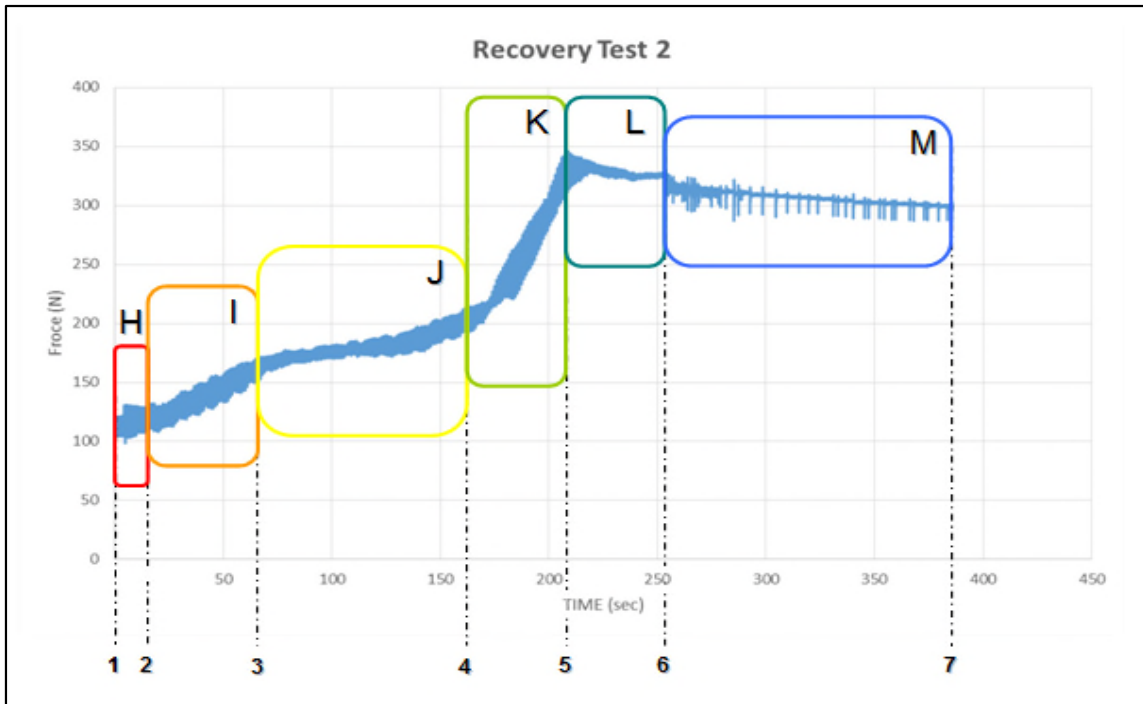


Figure 6-26 Recovery curve with time-slicing

The curve is divided in six phases described below:

- Phase H: the device is starting its recovery; the weight is constant because the demonstrator is not starting yet to be out of the water.
- Phase I: the first part of the turbine is off the water; the displacement is decreasing causing a raise of the tension.
- Phase J: the turbine is completely out of the water, the structure is still going out of the water, inducing a reduction of the displacement. The tension is then rising. The slope is less important because it is the structure of the tower which is going out and it has a less important volume than the turbine.
- Phase K: the ballasts start to be drained. But the process is slower than the diminution of submerged volume, so a raise is experienced.
- Phase L: during this phase, 90% of the demonstrator is outside the water, the displacement is constant while the draining of the ballasts is still on-going. Thus the tension is dropping.
- Phase M: the actuators are stopped in their initial position but the ballasts are not drain yet. The demonstrator is fully out of the water, a drop is once again experienced. The oscillations are due to the immobility of the actuators and the jerks they are experienced because of it. The acquisition is stopped when the ballasts are drain.

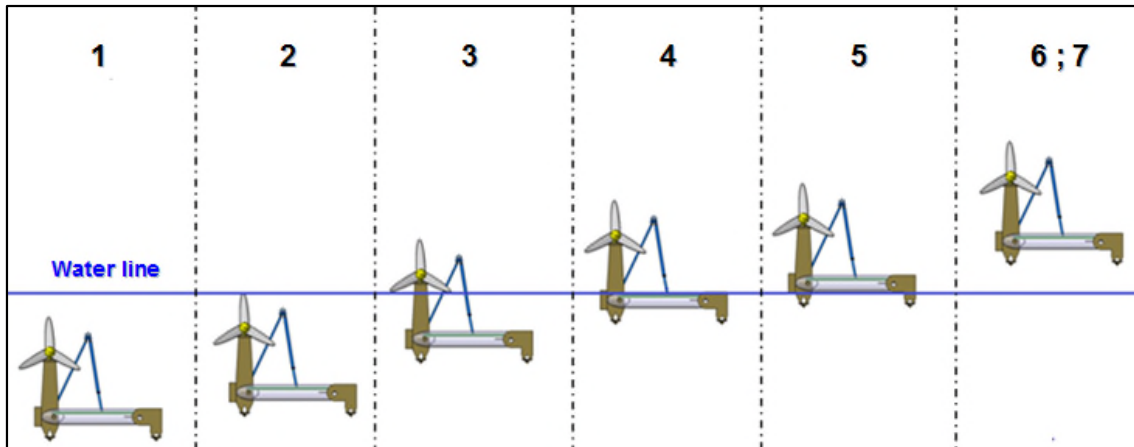


Figure 6-27 Deltastream position during recovery operations

During those tests, the demonstrator is not landed to the seabed. Indeed, the data will be equivalent to the one collected during the tests in configurations one.

For this configuration, the actuator phases are identical except that the actuators are not going to bring the demonstrator to the seabed.

The following table is giving the different sea states used during the tests:

Amplitude (m) \ Frequency (Hz)	Angle 0	Angle 45	Angle 90	Angle 135	Angle 180
	0,02	0,02	0,02	0,02	0,02
0,5	Test 1	Test 4	Test 7	Test 10	Test 13
1	Test 2	Test 5	Test 8	Test 11	Test 14
1,2	Test 3	Test 6	Test 9	Test 12	Test 15

Table 6-8 Wave Data and angle for the second configuration

6.4.2.2 Influence of the angle

Five different angles have been tested. The same aspects as in the configuration one are assessed:

- Influence of the angle on the maximal tension on the cable
- Influence of the angle on the shape of the curve

Considering the maximal tension applied on the cable, three groups of test are used; they are distinguished by a different frequency and once again the maximal tension is detected during recovery operations.

- Group 1: Recovery tests 1/4/7/10/13 with 0.5 Hz frequency

- Group 2: Recovery tests 2/5/8/11/14 with 1 Hz frequency
- Group 3: Recovery tests 3/6/9/12/15 with 1.2Hz frequency

For each group, a histogram is plotted with the maximal tension corresponding to the angle. The aim is to determinate the most favourable angle for the maximal tension.

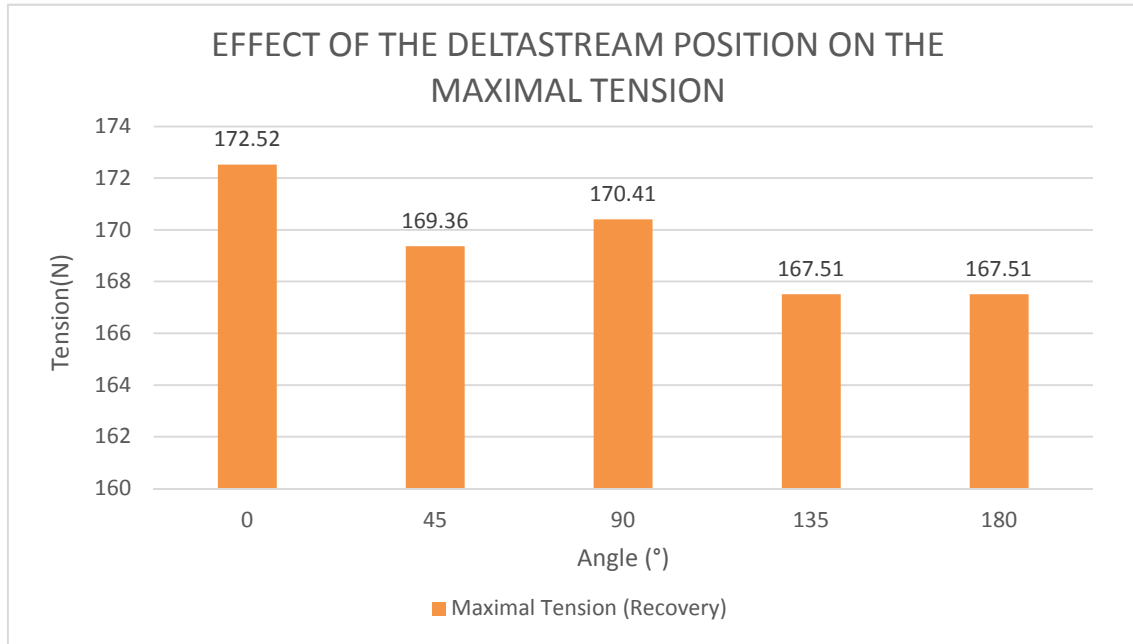


Figure 6-28 Influence of the angle of the demonstrator on the maximal tension – recovery tests 1/4/7/10/13

According to this histogram, the impact of the angle is not significant. The higher difference is 5.01N between the 0 angle and the 135/180 angle. However, the angle of 135 and 180 degrees are the one with a lower maximal tension when the 0 angle is the worst scenario (turbine facing the waves). A second histogram is displayed to confirm this tendency.

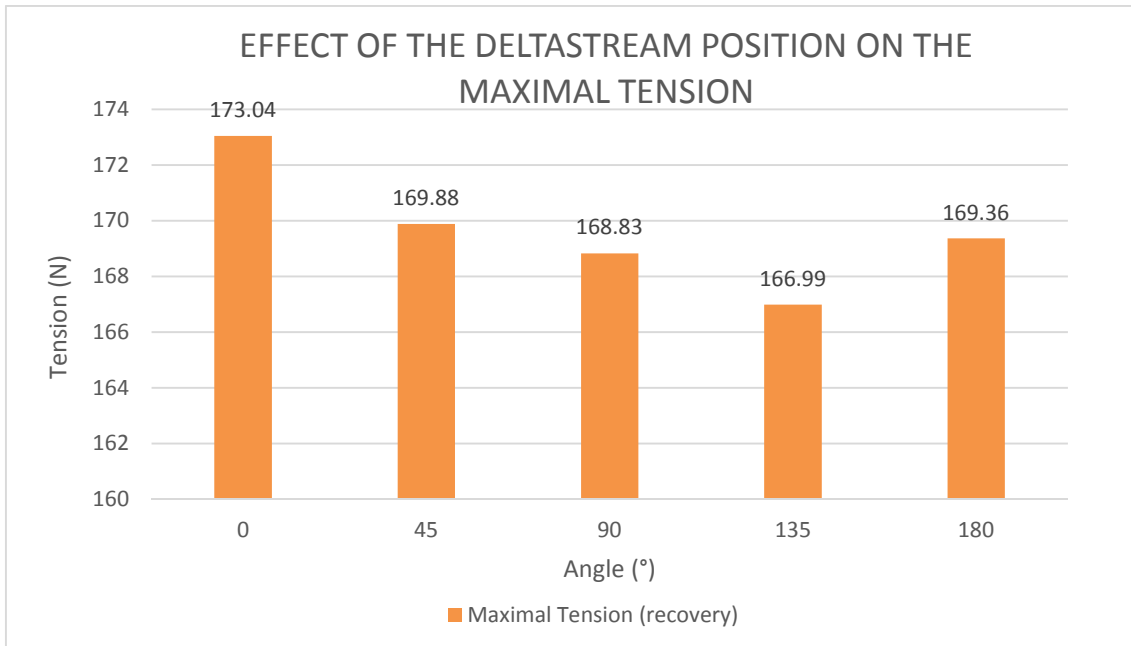


Figure 6-29 Influence of the angle of the demonstrator on the maximal tension – recovery tests 2/5/8/11/14

The second histogram is partly confirming the tendency displayed in the first one. The most favourable angle is 135 degrees and the worst scenario is an angle of 0 degree (turbine facing the waves). Those results can be explained given the fact that the turbine is the part of the demonstrator with the higher inertia; the energy developed by its movement is higher inducing a higher tension on the cable. The movement of the turbine is more important when it is facing the waves. In the opposite, with an angle of 135 or 180 degree, the movement of the turbine are less important, developing less energy so a tension less important.

Concerning the impact of the angle on the oscillations of the tension, the same histograms have been plot with the amplitude of the oscillations corresponding to the angle of the model.

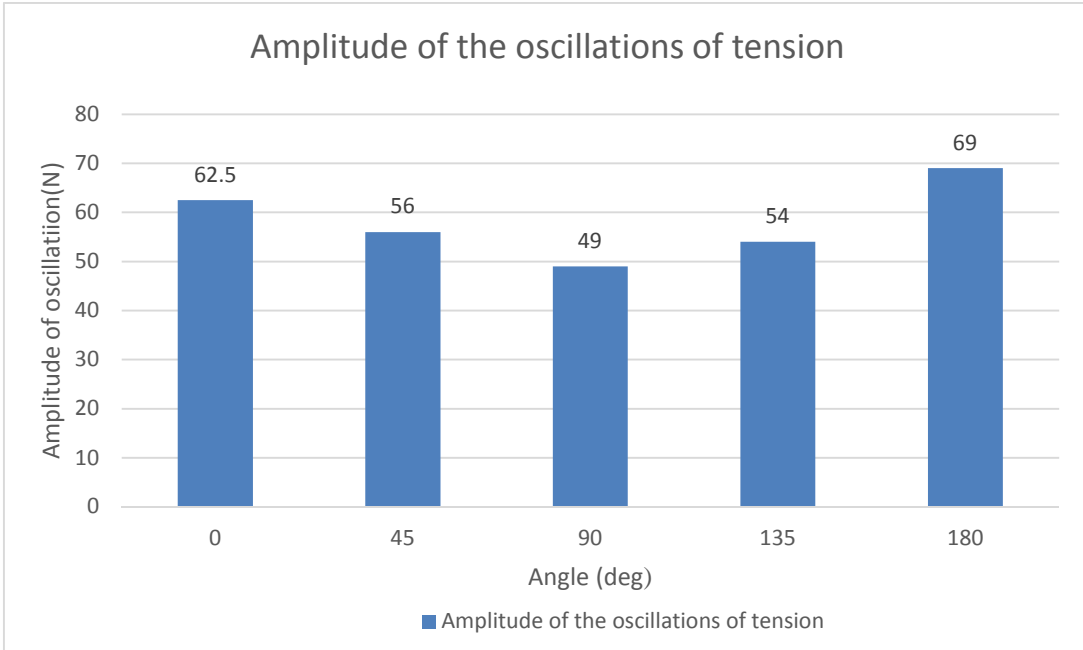


Figure 6-30 Influence of the frequency on the angle of the oscillations of tension – deployment test 1/4/7/10/13

According to this graph, the most favourable angle is 90 degrees. The angle 0 and 180 degrees seem to be the less favourable angle for a deployment, the oscillations are more important on this case. A second histogram is plotted to confirm or not this hypothesis.

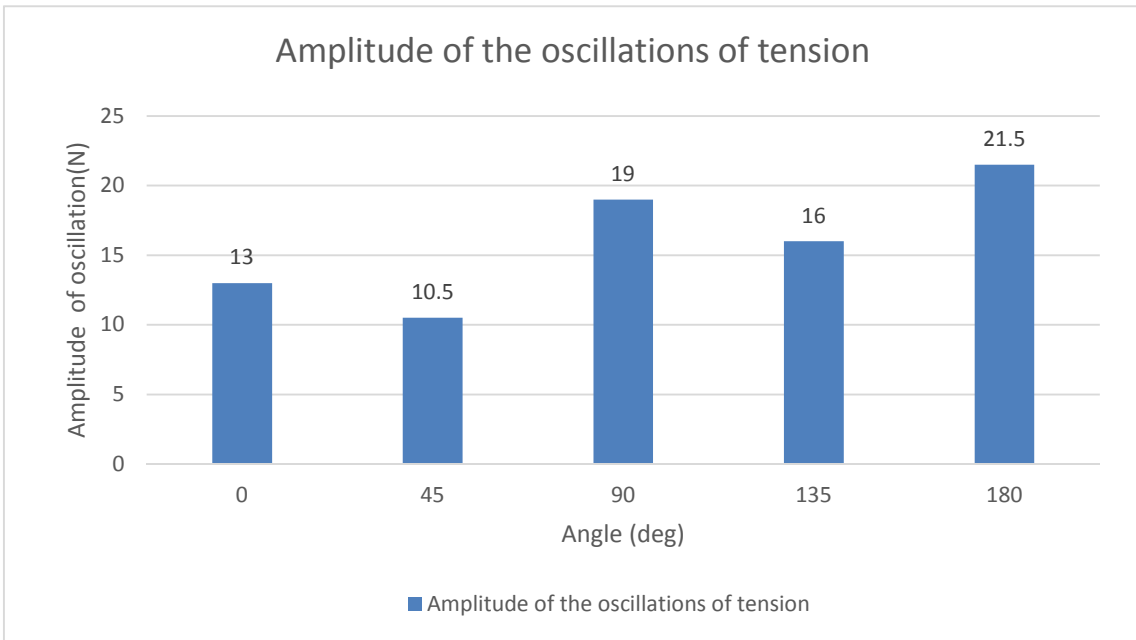


Figure 6-31 Influence of the angle on the amplitude of the oscillations of tension – deployment test 2/5/8/11/14

The tendency is not confirmed by the second series of tests. A hypothesis cannot be accurately deduced from those tests. However, the disparities between the different angles are not very significant, so the impact of the angle is small.

6.4.2.3 Influence of the inlet/outlet size

The first impact assessed is the time of the flooding. The time elapsed between the first water going in the ballast and the end of the flooding has been timed for each test in order to compare between the configurations one and two. The second impact assessed is the impact of the flooding rate on the general shape of the curves and thus the general behaviour of the tension on the crane.

Concerning the flooding rate, a histogram is plotted to have a quick view of the different phases and their respective timing.

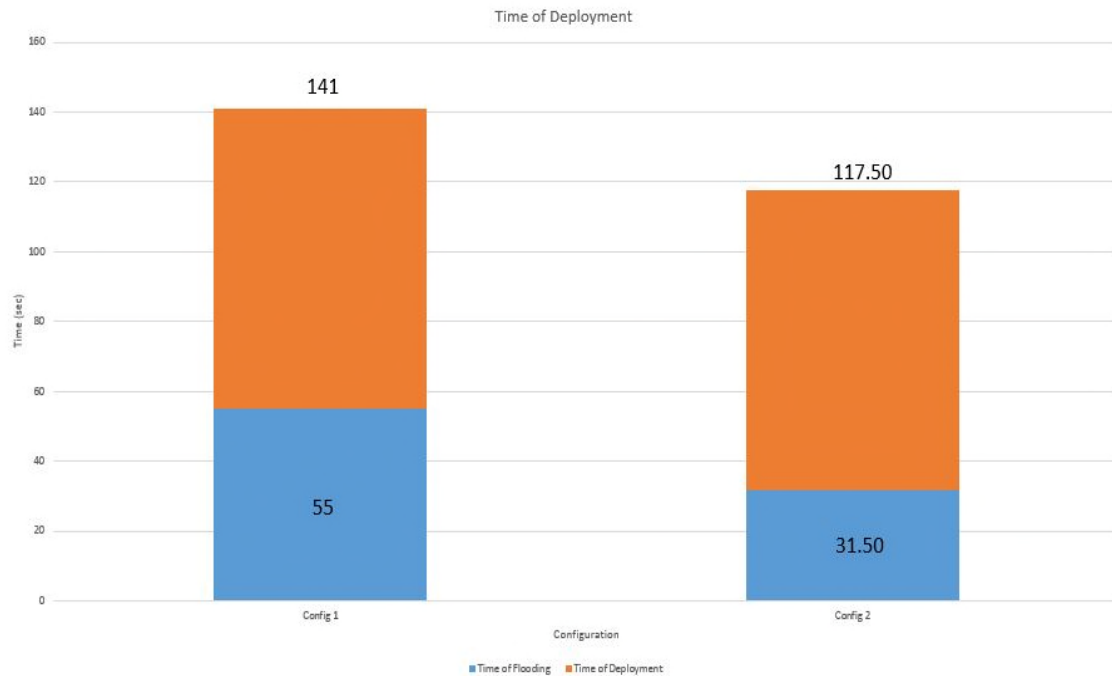


Figure 6-32 Time of Deployment - Configuration one and two

The impact of the size of the inlets and outlets of the demonstrator is the time of the flooding. The flooding is shortly quicker. The main impact is on the recovery operation, with a difference for the rate of draining greater.

The mass flow rate is assessed using this time and the volume of water stored in the ballasts. Using Table 5-8, the mass of water stored in the ballasts is 10.89kg. Divided by the time of flooding, a mass flow rate of 0.189kg/sec for the configuration 1 and 0.346kg/sec for the configuration 2 are found for the deployment. For the recovery, the results are: 0.06kg/sec for the configuration 1 and 0.068kg/sec for the configuration 2.

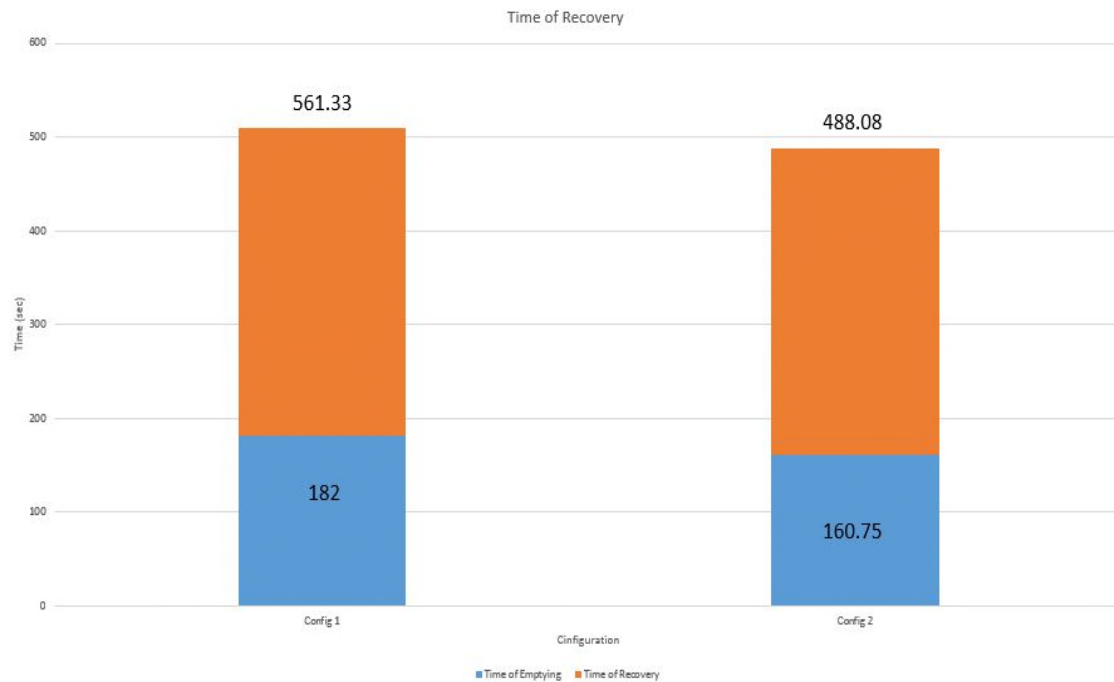


Figure 6-33 Time of Recovery - Configuration one and two

The second assessment undertaken is on the behaviour of the tension. In order to compare, two tests has been made with the same wave configuration. The two set of data collected have been plotted in the same curve to compare the shape:

- Deployment and recovery test 3 of the configuration 1 compared with the test 14 of the configuration 2.
 - Wave height: 0.02 m
 - Frequency: 1 Hz
 - Deltastream orientation: 180 degrees
- Deployment and recovery test 7 of the configuration 1 compared with the test 15 of the configuration 2
 - Wave height: 0.02 m
 - Frequency: 1 Hz
 - Deltastream orientation: 180 degrees

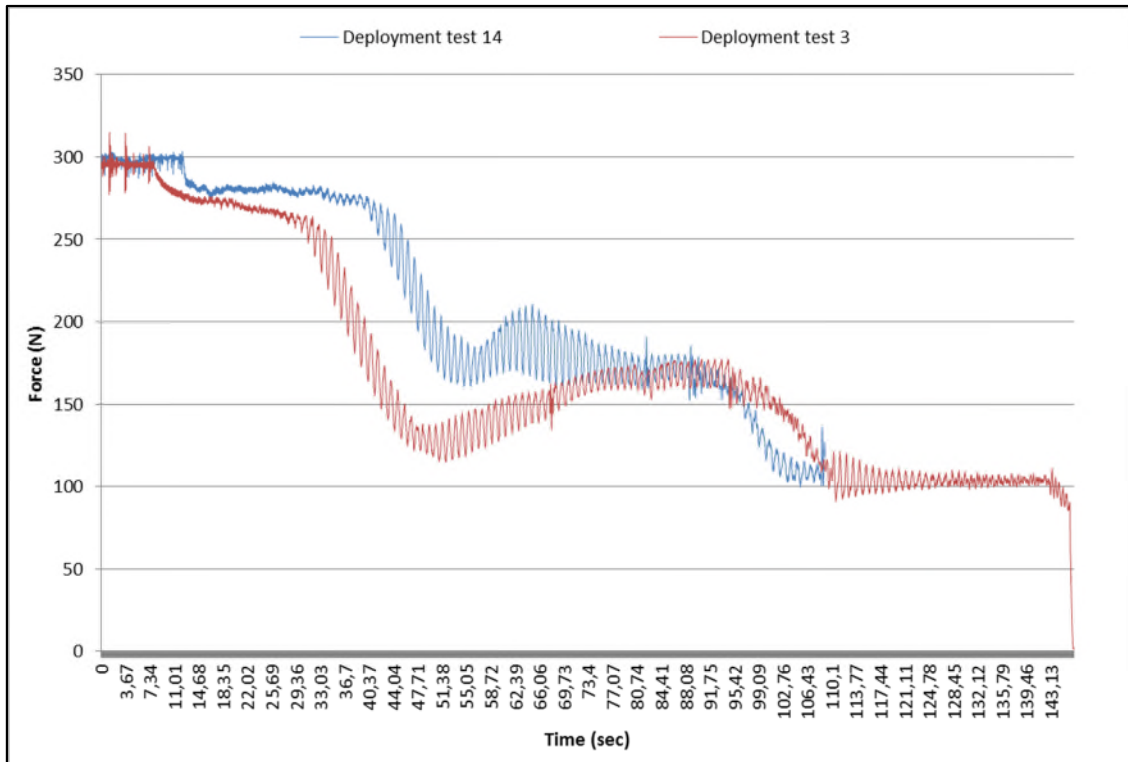


Figure 6-34 Comparison Graph – Deployment tests

The main differences between those two curves are located in the phase C and D of the time slicing. Those phases correspond to the phases of the flooding process of the device. During the first drop (phase C), when the openings are larger (test 14) the drop is not as significant because the ballasts are flooded more quickly. So the ratio between the raise of the displacement and the raise of the weight is smaller. Concerning the small raise after the drop (phase D), it is shorter due to the rate of the flooding. The demonstrator is being flooded more quickly so the second phase of the descent can be started sooner. The impact is mainly on the time of the operation. However, the tension is higher during the flooding operation but during a shorter time.

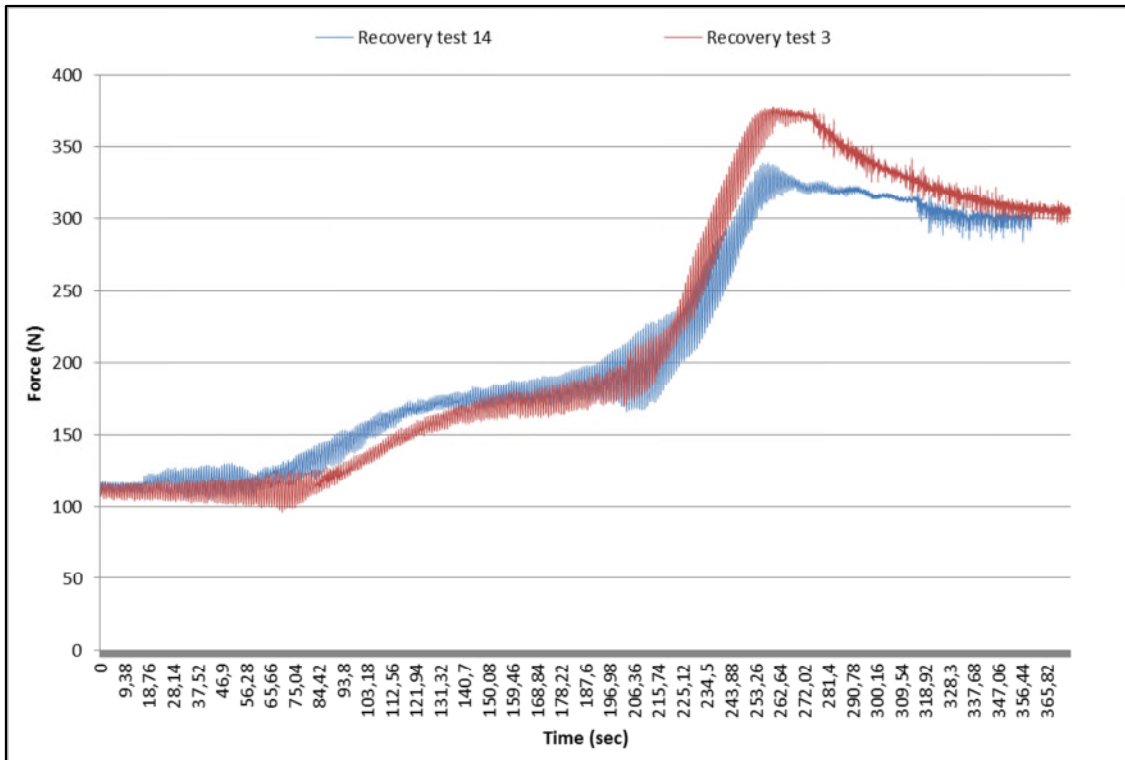


Figure 6-35 Comparison Graph - Recovery

Concerning the recovery operations, the difference of time is not significant. The main difference is in the pick of tension detected at the end of the operation. As the ratio between the rate of the loss of weight and the rate of the loss of displacement is larger, the slope of the raise during the phase K of the operation is less important and the pick of tension as well. The drop of the maximal tension is of 10.4%, which corresponds to a drop of 159,900 N for the full scale. Divided by two, the equivalent in real weight is 8.15 tonnes of difference.

6.5 Analysis and comparison with numerical predictions

6.5.1 Analysis and best scenarios

6.5.1.1 Deployment scenario

According to the KML document [3], the maximal tension supported by the heavy lift crane of the barge is 150 tonnes with an inclination of 20 degrees for the crane. It can already be assessed that the maximal tension on the crane will not be experienced during a deployment scenario in the range of the sea states tested. During most case of deployment tested, the maximal tension is around 150N. This correspond full scale to a tension of 122.32 tonnes.

Considering the sea state, it can be assessed from the results that the quieter the sea is the better. The parameter with the most important influence is the frequency of the waves. With a low frequency (i.e. long waves), the demonstrator will experienced important movements when it will be floating and submerged close to the water surface. Those movements will induce important variations of tension on the lift crane. The cable will be successively tighten and untighten. Thus the snatch loads experienced by the crane can be very important and induce a risk for the safety of the deployment. The maximal oscillations detected during the tests are with the longer waves with a frequency of 0.5Hz which correspond full scale to a wave period of 8.94sec. With this wave period and an important wave height, the variations of tension can reach a value of 87.5N trough to crest. At full scale, this value corresponds to a variation of the tension of ± 36.52 tonnes on the lift crane. However, those snatch load experienced cannot bring the lift crane to an overload situation because they occur when the demonstrator is already partly submerged or completely submerged, so with a buoyancy reducing the tension. The impact of the wave height for an identical frequency is not as important.

6.5.1.2 Recovery scenario

Considering the maximal tension experienced by the lift crane, the recovery scenario is worse than the deployment scenario in the range of sea state tested. Indeed, the maximal tension experienced during a recovery test was 196N. This correspond full scale to a tension of 159.84 tonnes. This value is above the maximal tension supported by the lift crane. This tension is experienced when the demonstrator is fully unsubmerged but the ballasts are still containing water, adding mass to the system. However, this tension was detected in the first configuration, when the inlets and outlets of the ballasts were not scaled yet. The maximal tension experienced during the second configuration was 173.05N. This correspond full scale to a tension of 141.12 tonnes. It is below

the crane limit. Concerning the sea state, the impact on the recovery operation is equivalent to the impact on the deployment.

6.5.2 Comparison with numerical predictions

The behaviour of the device examined during the tests while the structure is floating and the ballasts flooded is in accordance with the hypothesis made in 3.3 in the range of the sea state tested. The stability of the demonstrator is first unbalanced and the device cannot be left loose floating. To counterbalance this effect, the device must be constrained to a certain depth during the flooding process. A quick flooding is also recommended to limit the time of over-tension experienced by the crane during the operation. In the tests carried out and presented previously, a slow flooding process was inducing a waiting time while the descent was stop and the crane was experienced an over-tension. With a flooding quite faster, no stopping was necessary during the deployment process. The cap sizing of the device was limited and the over-tension was shorter even if it was a slightly more important over-tension which was experienced. However, during the descent between the end of the ballasts flooding and the beginning of the submersion of the turbine, the device is still experiencing a trim angle not favourable to the tension on the crane and the strength of the lift frame. However, the buoyancy of the turbine is counterbalancing this issue by rebalancing the device and lowering the trim angle to almost the zero value. The turbine which is an issue to the floating stability and the flooding process is becoming an advantage important for the submerged phase of the deployment and recovery operation. Figure 6-36 displays the aspect described above.

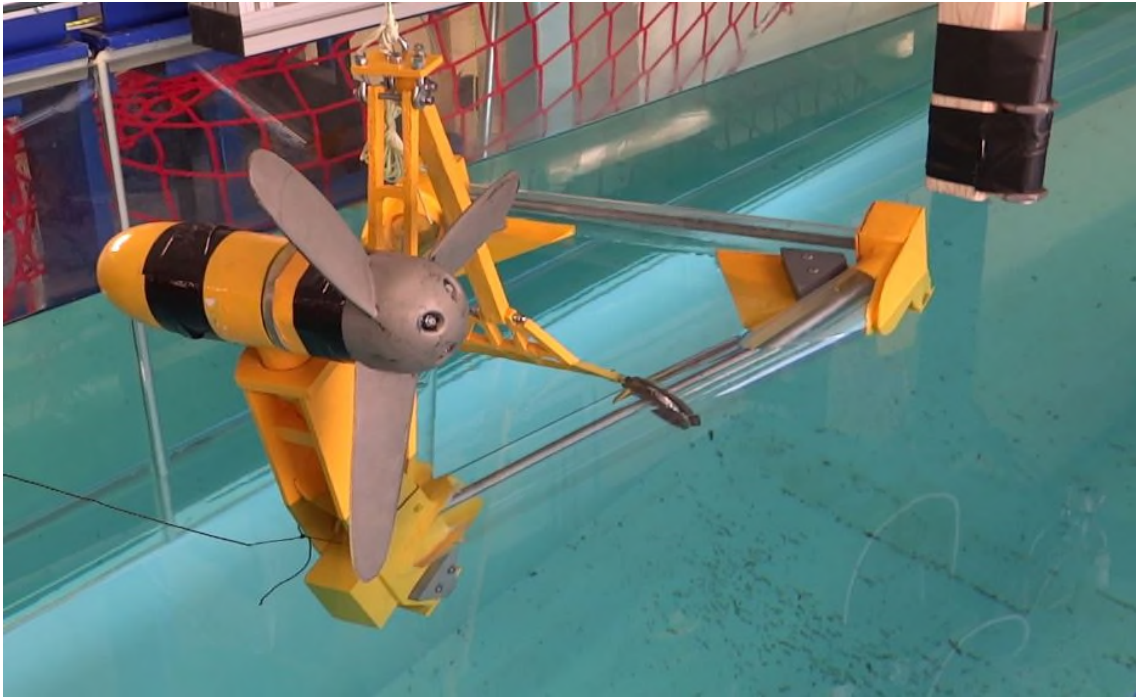


Figure 6-36 Floating Deltastream with a trim angle

The following table is summarising the mean volume flow rate determined during the experiments and the full scale value corresponding:

	Configuration 1		Configuration 2	
	Deployment	Recovery	Deployment	Recovery
Reduced Scale Volume flow rate (m³/sec)	$1.84 * 10^{-4}$	$0.6 * 10^{-4}$	$3.46 * 10^{-4}$	$0.68 * 10^{-4}$
Full Scale Volume flow rate (m³/sec)	$3.37 * 10^{-1}$	$1.1 * 10^{-1}$	$6.34 * 10^{-1}$	$1.25 * 10^{-1}$

Table 6-9 Comparative results of volume flow rate

The average full scale volume flow rate given above are used to calculate analytically the time needed for the ballasts to be flooded. Indeed, the volume of ballasts available is known from TEL. By dividing the total volume by the volume flow rate, a duration for the flooding is obtained. However; it is not possible to determine the inlet and outlet full scale size corresponding to the tests carried out: Indeed, the average flow velocity at the entrance of the ballasts is needed but it cannot be found accurately.

7 Conclusions

Through this thesis, a literature review has been done to present the analytical methodologies used during the research. The stability of a simplified structure has been assessed along with a work on the ballasts flooding process. The test session presented in the thesis has given a great deal of information on the deployment and recovery operations with a single lift point: snatch load effect, maximal tension experienced, and rate of flooding.

The tests carried out in the wave-towing tank of Cranfield are an introduction to further tests, more complicated and more complete in the modelling of the scenarios. For instance, other tests can be carried out with a more complete modelling of the operation including first the barge in a fixed position and then with the complete mooring system. However, in order to achieve these tests, a larger tank is needed.

Further work can be undertaken in the post processing such as a physical explanation of the change in the phase shift between the oscillations of the tension and the wave height. Why Deltastream is experiencing sudden buoyancy effects which are inducing those oscillations while it is fully submerged and the influence of the wave in those buoyancy effects. A full assessment can be carried out on the flooding process with a scaled pressure and inlets and outlets scaled accurately.

REFERENCES

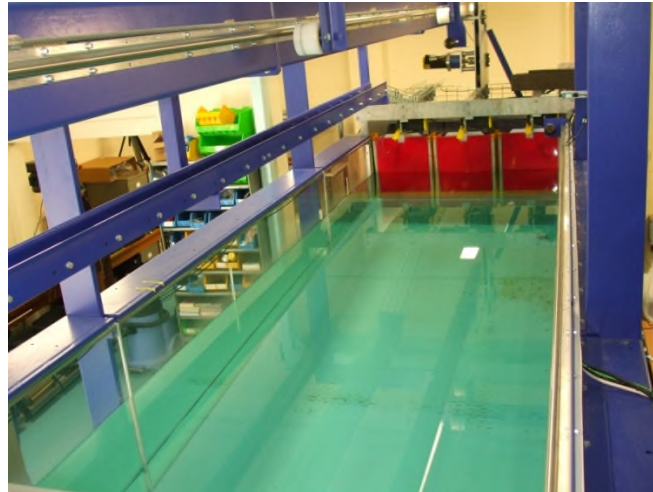
- [1] Minoo H. Patel, "Dynamics of Offshore Structures", *Butterworths*, 1989.
- [2] Keynvor MorLift Ltd, "Lift Frame Concept Design Report", *Deltastream Tidal Device Installation, Wales, UK*, 2013.
- [3] Keynvor MorLift Ltd, "Procedures for Mooring Lay & Recovery Operations", *Deltastream Tidal Device Installation, Wales, UK*, 2013.
- [4] Keynvor MorLift Ltd, "Preliminary Mooring Study Report", *Deltastream Tidal Device Installation, Wales, UK*, 2013.
- [5] Keynvor MorLift Ltd, "Procedures for Outline Deployment & Recovery Operations", *Deltastream Tidal Device Installation, Wales, UK*, 2013.
- [6] Det Norske Veritas, "Modelling and Analysis of Marine Operations", 2009.
- [7] Bunnik T., Buchner B., "Experimental Investigation of Subsea Structures During Installation and the Related Wave Loads, Added Mass and Damping", *International Offshore and Polar Engineering Conference*, Toulon, France, May 23-28, 2004.
- [8] Paulet D., Presles D., "Architecture Navale, Connaissance et Pratique", *Les Editions de la Villette*, 1999.
- [9] Subrata Kumar Chakrabarti, 1994, "Advanced Series on Ocean Engineering – Vol. 9: Offshore Structure Modelling", *World Scientific*, 1994.

APPENDICES

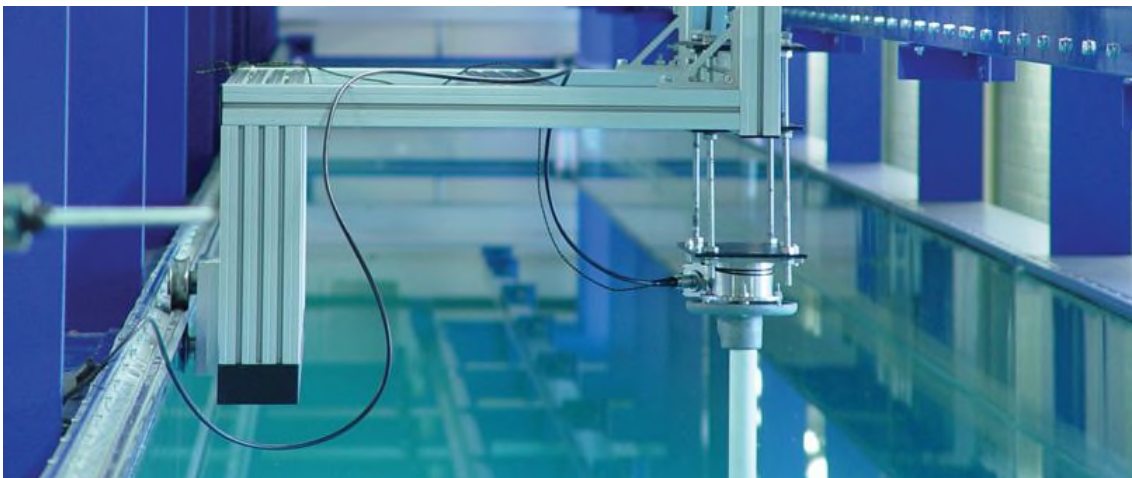
Appendix A Cranfield Wave-Towing tank

The facility has the following characteristics:

- Tank Length: 30.0 m
- Tank Width: 1.5 m
- Tank Height: 1.8 m
- Water depth: 1.5 m
- Wave height: 280mm peak to trough
- Working frequency: 0.10Hz to 1.1Hz
- Towing speed: 0-2.5m/s
- Max drag: 200 N
- Max payload: 30 kg
- Multi-Component Balances



Figure_Apx A-1 Wave maker



Figure_Apx A-2 Towing carriage

Appendix B Actuator Technical Data

RCP2 ROBO Cylinder

RCP2-SA7C

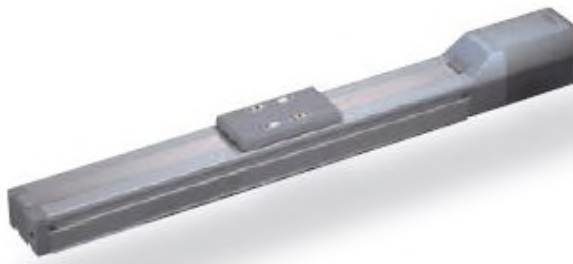
ROBO Cylinder, Slider Type, Actuator Width 73mm, Pulse Motor, Straight

Model Specification Items: **RCP2 - SA7C - I - 56P**

Series: RCP2, Type: SA7C, Encoder type: I, Motor type: 56P Pulse motor, Lead: 16, Stroke: 100-100mm, Applicable controller: P1, Cable length: P, Options: P1

Incremental specification: 56P size, Lead: 16: 16mm, 8: 8mm, 4: 4mm, Stroke: 100-100mm, 800-800mm (Set in 100mm steps), Applicable controller: P1: PCON, PSEL, Cable length: N: No cable, P: 1m, S: 3m, M: 5m, X: Specified length, R: Robot cable, Options: BE: Brake (existing on the end), BL: Brake (existing on the left), BR: Brake (existing on the right), NM: Reversed-home positioner, SR: Slide roller positioner

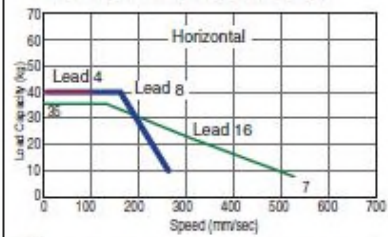
* Refer to p. 31 of the form reader for details on the model specification items.



- When the stroke increases, the maximum speed will drop to prevent the ball screw from reaching a critical speed. Use the actuator specification table below to check the maximum speed at the stroke you desire.
- The RCP2 series uses a pulse motor, so the load capacity will decrease as the speed increases. Use the correlation diagram of speed and load capacity on the right to check the load capacity corresponding to the speed you desire.
- The load capacity is based on operation at an acceleration of 0.3 G (or 0.2 G if the lead is 4 or the actuator is operated vertically). This is the maximum acceleration.

Correlation Diagram of Speed and Load Capacity

With the RCP2 series, the load capacity will decrease as the speed increases due to the characteristics of the pulse motor used in the actuator. Use the table below to check if the desired speed and load capacity are satisfied.



Actuator Specifications

Lead and Load Capacity

(Note 1) Take note that the maximum load capacity will decrease as the speed increases.

Model	Lead (mm)	Maximum load capacity (Note 1)		Stroke (mm)
		Horizontal (kg)	Vertical (kg)	
RCP2-SA7C-I-56P-16-①-P1-②③	16	-35	-5	100 - 800 (Set in 100mm steps)
RCP2-SA7C-I-56P-8-①-P1-②③	8	-40	-10	
RCP2-SA7C-I-56P-4-①-P1-②③	4	40	-15	

Explanation of numbers: ① Stroke, ② Cable length, ③ Options

Stroke and Maximum Speed

Lead	Stroke	100 - 700	800
		(Set in 100-mm steps)	(mm)
16	100	533	480
8	100	266	240
4	100	133	120

(Unit: mm/s)

Options

Name	Model	Page
Brake (Cable existing the end)	BE	P381
Brake (Cable existing the left)	BL	P381
Brake (Cable existing the right)	BR	P381
Reversed-home specification	NM	P385
Slide roller specification	SR	P388

Actuator Specifications

Item	Description
Drive method	Ball screw ø12mm, rolled C10
Positioning repeatability	±0.02mm
Backlash	0.1mm or less
Base	Material: Aluminum with special alumite treatment
Allowable load moment	Ma: 13.9N·m, Mb: 19.9N·m, Mc: 38.3N·m
Overhang load length	Ma direction: 230mm or less, Mb/Mc directions: 230mm or less
Ambient operating temperature, humidity	0-40°C, 85% RH or below (non-condensing)

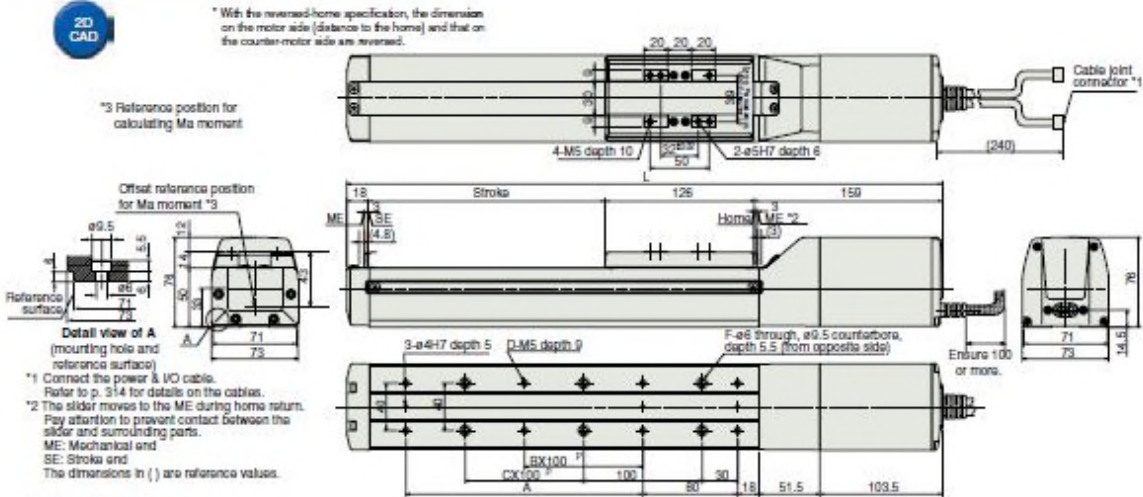
Direction of allowable load moment



25 RCP2-SA7C

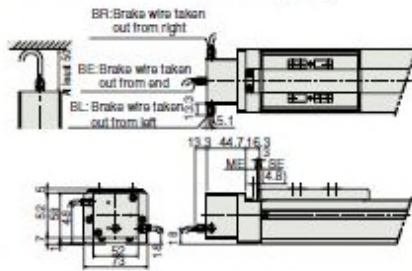
Dimensions

You can download CAD drawings from our website: www.intelligentactuator.com



Brake dimensions

* Models with brake have their overall length extended by 43 mm (or 56.3 mm if the wire is taken out from the end) and weight increased by 0.6 kg.



■ Dimensions and Weight by Stroke

Stroke	100	200	300	400	500	600	700	800
L	403	503	603	703	803	903	1003	1103
A	100	200	300	400	500	600	700	800
B	0	1	2	3	4	5	6	7
C	0	1	2	3	4	5	6	7
D	6	8	10	12	14	16	18	20
F	4	6	8	10	12	14	16	18
Weight (kg)	3.3	3.8	4.2	4.7	5.1	5.6	6.0	6.3

Controller

Applicable Controllers

RCP2 series actuators can be operated using the following controllers. Choose the type that best suits your specific purpose.

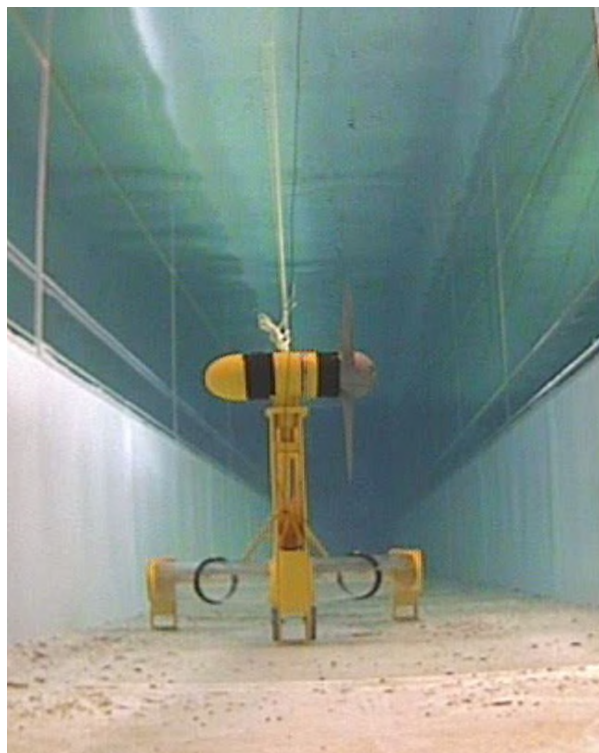
Name	External view	Model	Features	Maximum number of positioning points	Input power supply	Power supply capacity	Reference page
Positioner type		PCON-C-56PI-NP-2-0	Supporting up to 512 positioning points	512 points	DC24V	2A max.	→P305
Positioner type meeting safety category		PCON-CG-56PI-NP-2-0					
Solenoid valve type		PCON-CY-56PI-NP-2-0	Same control actions as those applicable to solenoid valves	3 points	DC24V	2A max.	→P305
Pulse-train Input type (differential line driver specification)		PCON-PL-56PI-NP-2-0	Pulse-train Input type supporting a differential line driver	(-)			
Pulse-train Input type (open collector specification)		PCON-PO-56PI-NP-2-0	Pulse-train Input type supporting an open collector	(-)			
Serial communication type		PCON-SE-56PI-0-0	Dedicated serial communication type	64 points	DC24V	2A max.	→P335
Program control type		PSEL-C-1-56PI-NP-2-0	Programmable type capable of operating up to 2 axes	1500 points			

Appendix C Tests Pictures

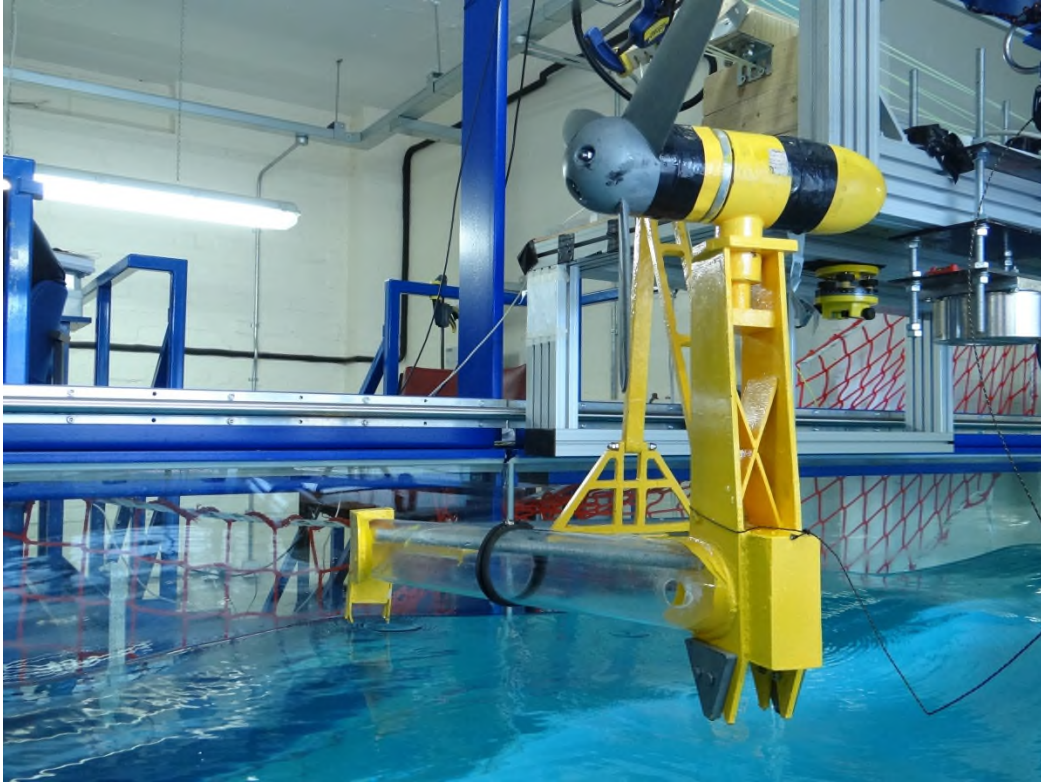
This appendix is regrouping a sample of pictures taken during the test operations.



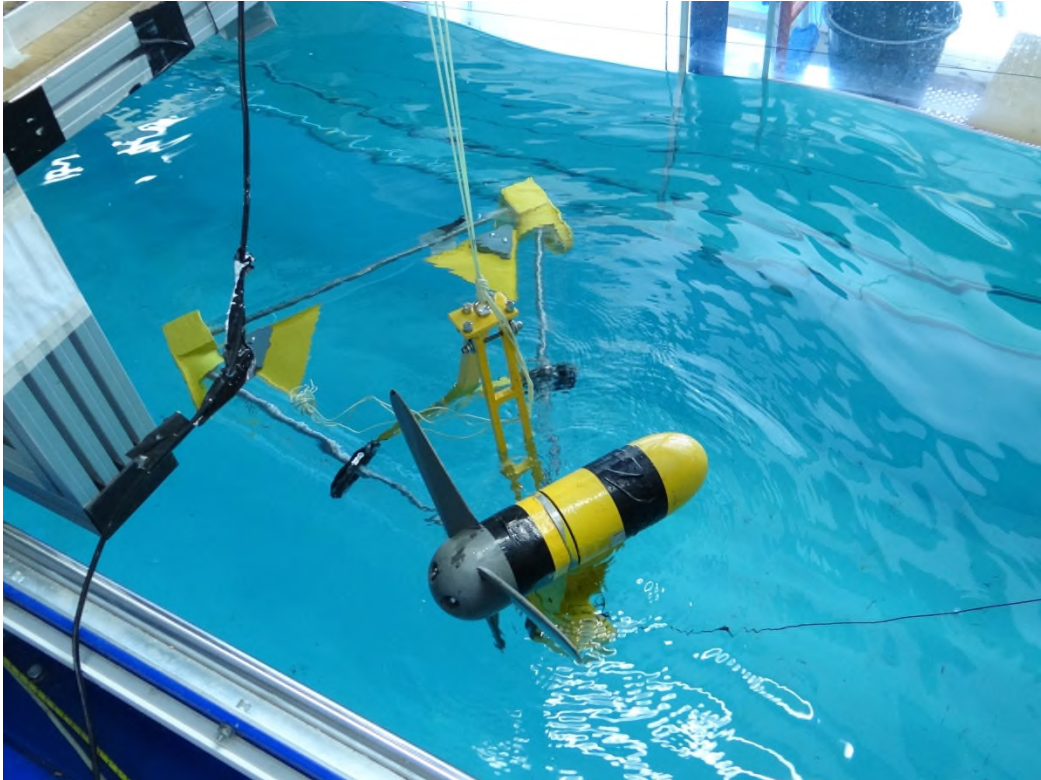
Figure_Apx C-1 Underwater Picture – On-going operation



Figure_Apx C-2 Underwater Picture – Landed



Figure_Apx C-3 Test operation - Deltastream lifted above the water



Figure_Apx C-4 Test operation - Deltastream entering in the water